Electric Drive Systems and Operation

Valery Vodovozov

Valery Vodovozov

Electric Drive Systems and Operation

Electric Drive Systems and Operation
© 2012 Valery Vodovozov & bookboon.com
ISBN 978-87-403-0166-3

Contents

Download free eBooks at bookboon.com

Preface

Be careful in driving

Charles Chaplin

An electric drive is the electromechanical system that converts electrical energy to mechanical motion. Being a part of automatic equipment, it acts together with the driven object, such as a machine tool, metallurgical, chemical, or flying apparatus, domestic or medical device. Electric drives area includes applications in computers and peripherals, motor starters, transportation (electric and hybrid electric vehicles, subway, etc.), home appliances, textile and paper mills, wind generation systems, air-conditioning and heat pumps, compressors and fans, rolling and cement mills, and robotics.

This book is intended primarily for the secondary-level and university-level learners of an electromechanical profile, including the bachelor and master students majored in electrical engineering and mechatronics. It will help also technicians and engineers of respective specialities.

Contemporary applications make high demands of modern drive technology with regard to dynamic performance, speed and positioning accuracy, control range, torque stability, and overload capacity. Control of electrical motors always was in the highlight of inventers and designers of mechanisms, machines, and transport equipment. As a rule, any mechanism is infinitely complex. Often, its behavior is vague, and its reaction on influences and disturbances is unforeseen. To a considerable degree, this concerns the electric drive. Nevertheless, a specialist should take into account the main laws and regularities of both the driving and the driven objects during maintenance design, and study his applications. To this aim, we pick out the traditional approach at which a complex system is divided in simple portions. Then, we examine the basic elements of the driving system, the typical models and features of its components, starting from the conditionally rigid and ideally linear details and finishing by the elastic distributed, non-linear, and non-stationary ones.

If you have completed the basics of electricity, electronics, mechanics, and computer science, you are welcome to these pages. The book will guide you in appreciation of applications built on the basis of electrical motors. In addition, you will know many electromechanical products and determine their important differences.

I believe in your success in learning electric drives.
I wish you many happy minutes, hours and years in your professional activities.

Author

1   Introduction

1.1   A science of electric drive

Disposition. Knowledge is developed and renewed, modified and changed, merges and falls to multiple branches, streams, and directions. Each particular science presents a realized and purposeful glance on the physical culture from a particular viewpoint and position. Take a look at Fig. 1.1.

Computer science   Power engineering   Mechanics

Information technology	Power technology	
Computer engineering	Power electronics	Electromechanics

Mechatronics

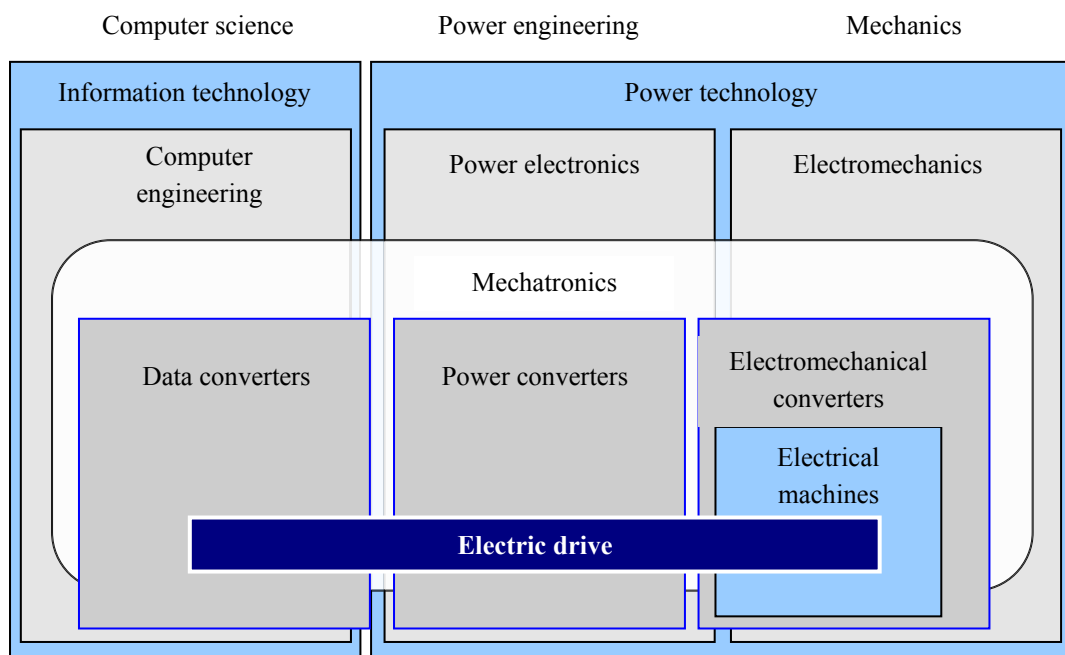| Data converters	Power converters	Electromechanical converters
		Electrical machines

Electric drive

Fig. 1.1 Electric drive in the frame of other sciences

It reflects the mutual penetration of the three fundamental directions of the natural thought, named computer science, power engineering, and mechanics. Computer science studies the nature of *data* acquisition, storage, processing, and transmitting, thus it serves as a basis of informational technology. Power engineering envelops the sphere of nature resources, such as output, conversion, transportation, and application of different kinds of energy. In this way, many electrical technologies are developed, particularly *electromechanics* related to the mechanisms that use electrical energy.

Further synthesis of energies of the mechanical motion and the intellect movement is a guarantee of progress and the source of new scientific directions. Thanks to this synthesis, the new research area, *mechatronics* was born which manages an intellectual control of the mechanical motion. The mechatronics states the *laws* of energy transformation upon data converting in *computer-mechanical systems*. The electric drive comprises the branch of mechatronics.

Definition and composition. An *electric drive* is the *electromechanical system* that converts electrical energy to mechanical energy of the *driven machine*. In Fig. 1.2 the functional diagram of the electric drive is presented.
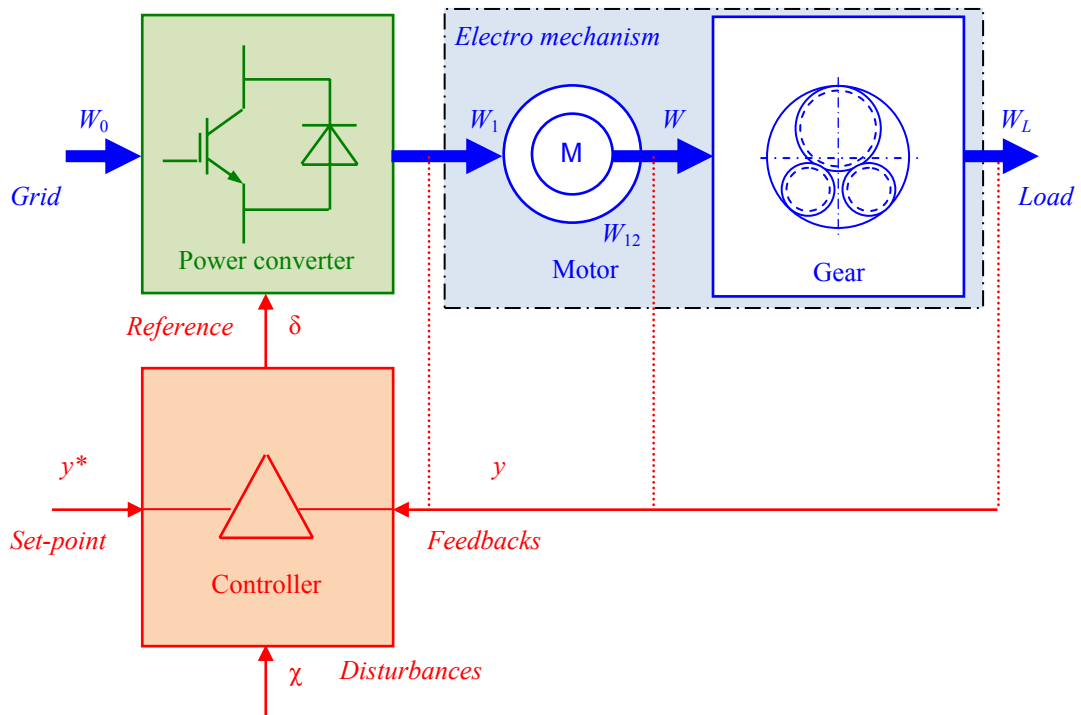
Fig. 1.2 Functional diagram of electric drive

It includes a motor M (or several ones), a mechanical transmission (gear, gearbox), an optional power converter, and a control system (controller). The power converter transforms electrical energy W_0 of the grid (mains) to motor supply energy W_1 in response to the set-point speed or path command. The motor is an electromechanical converter, which initially converts W_1 to electromagnetic energy W_{12} of the air gap between the stator and the rotor and then turns W_{12} to mechanical work W on the motor shaft. The gear transforms mechanical energy to the load work W_L in accordance with the requirements of the driven machine (actuator). The controller (regulator) compares the set-point y^* with outputs y and disturbances χ, and generates the references δ on its inputs. The part of electric drive, which involves the mechanical transmission and the motor rotor, is called a mechanical system.

The grid-operated constant-speed and the converter-fed adjustable electric drives are distinguished.

At present, the vast majority of applications exploits the *general purpose electric drives* of low and mean *accuracy* which constitute approximately 80 % of the word driving complexes. They are usually presented by the *mains-operated open-ended mechanisms* consisting of the motor, mechanical transmission, and a control system which provides commutation and protection operations only. They have neither the power converter nor the *feedbacks*.

The accurate variable-speed electric drives that comprise the rest drive area are the converter-operated close loop systems built on the microprocessor controllers. Their small group presents the high performance drives of the very broad speed range and positioning requirements.

Application. Developments in power electronics and microelectronics in the last decades resulted in an unprecedented growth of adjustable speed drives offering a wide range of advantages from process performance improvement to comfort and power savings. Nowadays electric drives can be found nearly everywhere, in heating, ventilation and air conditioning, compressors, washing machines, elevators, cranes, water pumping stations and wastewater processing plants, conveyors and monorails, centrifuges, agitators, and this list could continue on and on. Electric drives use approximately 70 % of generated electrical energy. It is more than 100000 billions kilowatt-hours per year. It was reported that currently 75 % of these operate at pump, fan, and compressor applications 97 % of which work at fixed speeds, where flow is controlled by mechanical methods. Only 3 to 5 % of these drives are operated at variable-speed control systems. Electric drive systems make up about one-third of overall automation equipment. The cost of the informational and electrical parts takes more than half of the overall drives value.

The leading companies in the world market of electric drive engineering are now as follows: American General Electric, Maxon Motors, Gould, Reliance Electric, LabVolt, Robicon, and Inland; Canadian Allen Bradley; German Telefunken, Siemens, Bosh, AED, Schneider Group, Sew Eurodrive, and Indramat; Danish Danfoss; Finnish Stromberg as a part of the ABB Brown Bowery, Int., Japanese Fanuc, Omron, Mitsubishi Electric, Hitachi; French CEM; Swiss Rockwell Automation, etc. They have the wide range of products and the broad service spectrum for solution of demanding automation tasks.

1.2 Electromechanical processes

Energy and power. The electric drive converts *electrical energy* of the supply grid to *mechanical energy* of the load. It can be recalled from the *energy conservation law* that conversion of *kinetic energy* W_d into *potential energy* W_L and backwards provides the energy balance. Particularly, on the motor shaft

$$W = W_d + W_L = \text{const.}$$

Along with the energy balance, the balance of *powers* is supported,

$$P = P_d + P_L.$$

A power is the differential work done in the particular time,

$$P = \frac{dW}{dt} = sW$$

where $s = \dfrac{d}{dt}$ is a differential operator. A *static power* $P_L = \dfrac{dW_L}{dt} = sW_L$ describes the cumulative potential energy needed to overcome the *counter-force* of the mechanism, such as friction, cutting, gravity, elastic force, etc. The time derivation of the kinetic energy stock describes the *dynamic power* $P_d = \dfrac{dW_d}{dt} = sW_d$.

The motion of the driven object is described by the *angular speed* ω (*angular frequency*) or by the *linear velocity v*. The angular speed of a rotating object determines how long it takes for an object to rotate a specified angular distance. An angular speed is calculated in rad/s.

In engineering practice it is often replaced by the *rotation frequency n*, measured in revolutions per minute (rpm), $n = \dfrac{60\omega}{2\pi}$. The angular speed is bounded up with the *angle* φ of the shaft turn as $\omega = \dfrac{d\varphi}{dt}$. Velocity, in turn, is the rate at which an object travels a specified distance *l*, $v = \dfrac{dl}{dt}$.

An object moves at the changing speed. An increase in the speed $\dfrac{d\omega}{dt} = s\omega, \dfrac{dv}{dt} = sv$ is called *acceleration*. Acceleration occurs only when there is a change in the force acting upon the object. An object can also change from a higher to a lower speed. This is known as *deceleration.*

Mechanical systems are subject to the law of inertia, which states that an object will tend to remain in its current state of rest or motion unless acted upon by an external force. This property of resistance to acceleration or deceleration is referred to as the *moment of inertia J*. At rotation,

$$W_d = \frac{J\omega^2}{2}, \; P_d = J\omega\frac{d\omega}{dt} + \frac{\omega^2}{2}\frac{dJ}{dt}.$$

Sometimes, a flywheel torque $GD^2 = 4J$ is used instead. For the motion of translation,

$$W_d = \frac{mv^2}{2}, \; P_d = mv\frac{dv}{dt} + \frac{v^2}{2}\frac{dm}{dt}$$

where *m* is a moving mass.

Mechanical torque. A *torque* is a twisting or turning force that causes an object to rotate. The *developed motoring torque* is defined as a *ratio* of the motor power *P* to the angular frequency ω whereas a *motoring force* is a ratio of the power *P* to the linear velocity *v*. In symbols,

$$T = \frac{dW}{d\varphi} = \frac{P}{\omega}, \; F = \frac{dW}{dl} = \frac{P}{v}.$$

Whenever a force causes motion, *work* is accomplished as the product of force times the distance applied. From these ratios, the *torque and force equilibrium equations* are as follows:

$$T = T_L + T_d = T_L + J\frac{d\omega}{dt} + \frac{\omega}{2}\frac{dJ}{dt}$$

$$F = F_L + F_d = F_L + m\frac{dv}{dt} + \frac{v}{2}\frac{dm}{dt}$$

Here, T_L and F_L are a static load torque (counter-torque) and a static resistive force (counter-force), and T_d and F_d are a dynamic torque and a dynamic force of the load. As well, T_L is known as a steady-state torque or an operational torque.

The torque equilibrium for *J* = const,

$$T = T_L + J\frac{d\omega}{dt} \tag{1.1}$$

is called a *major equation* of the *torque equilibrium* of an electric drive. As (1.1) shows, to move the driven mechanism with the constant speed, an electric drive has to develop the motoring torque equal to the counter-torque. To accelerate or decelerate the load, the drive has to develop an additional dynamic torque. The solution of this differential equation relative to the speed depends on the torque matter. As the torque is the fundamental variable for the speed and position adjustment, to control an electric drive, it is required to produce the necessary input impacts that change the motoring torque. The major equation explains the *operation principle* of many mechanisms.

Electromagnetic torque. Electromagnetism is the basic principle behind motor operation. In the sketch of Fig. 1.3, a motor as the source of the *electromagnetic torque* T_{12} and *magnetomotive force* (MMF) F_{12} has a couple of assemblies on the common axis, the stationary *stator* and revolving *rotor*. Being an electromechanical object, the motor consists of an *inductor* supplying the field and an *armature* inducing the current in the electrical conductors named *windings*. Depending on a design, the inductor may be placed on the stator or rotor and the same the armature is concerned. The inductor excites an electromagnetic *flux* Φ. In the case of a single *turn*, the flux feeds the magnetic field of density (*induction*) $B = \frac{\psi}{Q}$, where $Q = lr$ is the turn area that the flux crosses, ψ is an alternating *flux linkage*, which depends on the turn *position* in the inductor field, l is the turn length, and r is the turn radius. In accordance with the *Ampere's law*, in the turn supplied by the current I and placed into the magnetic field of induction B the MMF $F_{12} = BlI$ is generated. The strength of the MMF is proportional to the amount of current and its direction is perpendicular to the directions of both I and B. In turn, in accordance with the *Faraday's law*, if the short-circuiting turn crosses the magnetic field, a voltage is induced there known as an *electromotive force* (*EMF*) or an *induced voltage* which is a source of current I and, hence, the MMF.
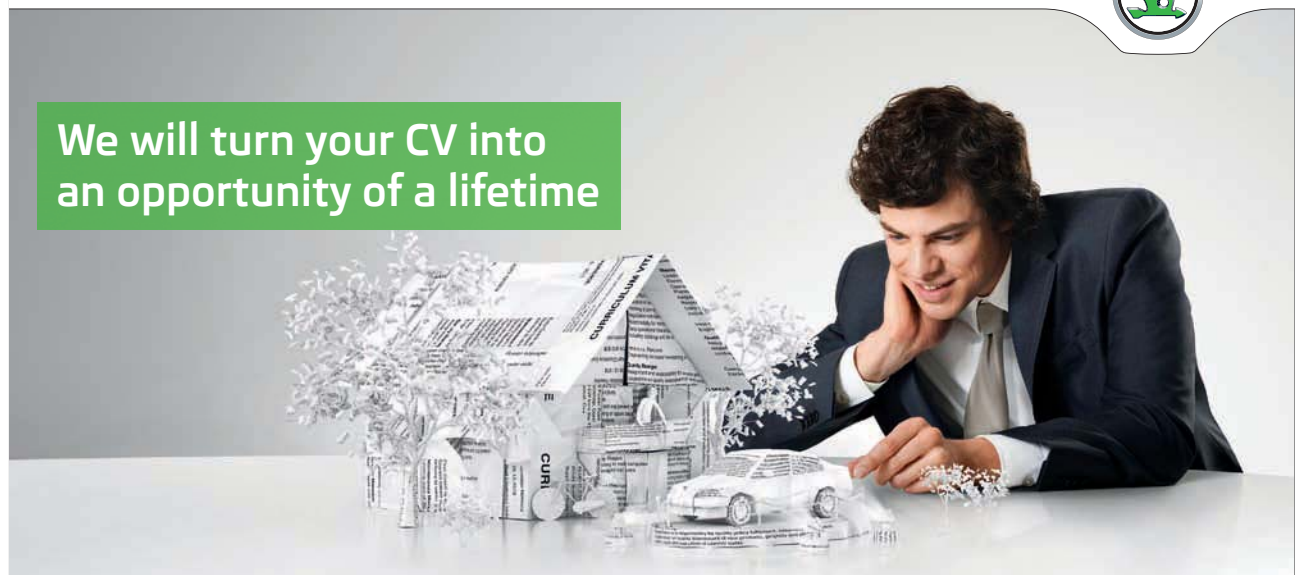
The sufficient turn affected by the MMF creates an electromagnetic torque in the air gap between the stator and the rotor,

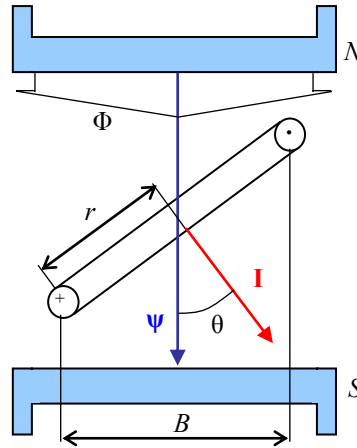$$T_{12} = BlIr \sin\theta = \psi I \ \sin\theta \tag{1.2}$$

Fig. 1.3 The sketch of a motor

where θ is an electrical angle between the flux ψ and the current I vectors called a *load angle*. Therefore, electromagnetic torque results from the interaction of the electrical current and the magnetic flux.

The torque of the electrical motor is produced by an *effective flux linkage* ψ_{12} in the air gap between the stator and rotor m-phase multi-turn windings turned around p pole pairs. Both the flux lincage and the current have two components: the *stator flux linkage* ψ_1 coupled with the *stator current* I_1, and the *rotor flux linkage* ψ_2 coupled with the rotor current I_2. Therefore, (1.2) can be resolved for the motor in different ways, like these vector equations:

$$T_{12} = mp\mathbf{\psi_{12}} \times I_2 = mp\mathbf{\psi_2} \times I_1 = mp\mathbf{\psi_1} \times \mathbf{\psi_2}, \text{ etc.} \tag{1.3}$$

The developed *mechanical torque* on the motor shaft differs from the electromagnetic torque due to the *friction* and windage motor *losses* δ_T known as a *no-load torque* as follows:

$$T = T_{12} - \delta_T.$$

Friction occurs when objects contact one another. It is one of the most significant causes of energy loss in a machine.

Control possibilities. For the torque to be produced, the magnetic fields of the stator and rotor must be stationary with respect to each other. To control the speed and torque, the mutual orientation and angular speed of the flux and current should by adjusted in accordance with (1.2).

Three types of electrical motors exist: *dc motors*, *synchronous motors*, and *induction* (*asynchronous*) *motors*. Their difference results from a method used to acquire the right load angle by rotation either the rotor with the flux speed or the flux with the rotor frequency.

Dependently on the stator and rotor supply method, all motors may be subdivided into the machines with the single-side and double-side *excitation*. Both have as minimum one ac fed winding. At the double-side excitation, the second winding may be both the ac *excitation winding* and the *dc excitation winding*, or by *permanent magnets* (PM).
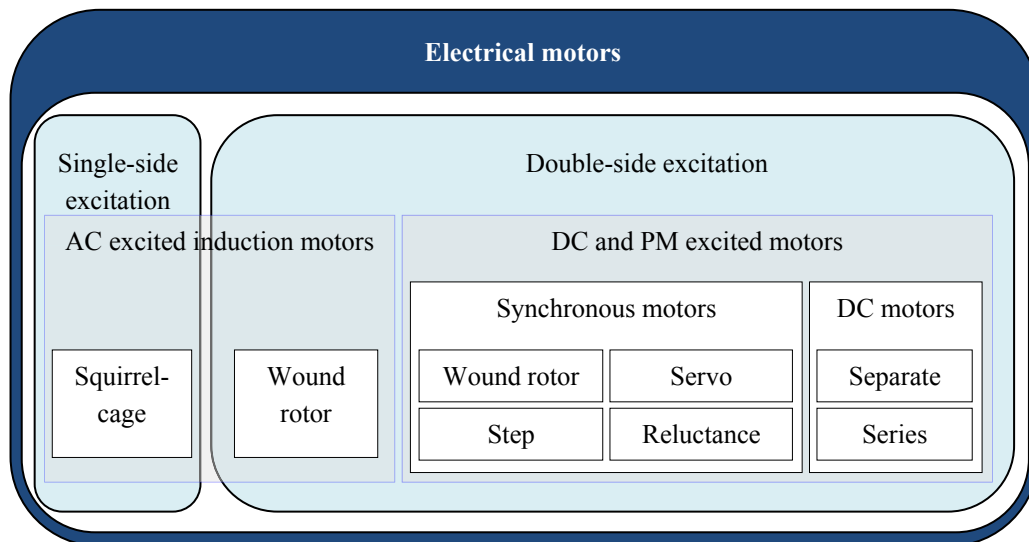
```
┌─────────────────────────────────────────────────────────────────────┐
│                         Electrical motors                             │
│  ┌──────────────┐  ┌───────────────────────────────────────────────┐ │
│  │ Single-side  │  │              Double-side excitation            │ │
│  │  excitation  │  │                                                │ │
│  │ AC excited induction motors │      DC and PM excited motors       │ │
│  │              │  │  ┌────────────────────────┐ ┌───────────────┐  │ │
│  │              │  │  │   Synchronous motors   │ │   DC motors   │  │ │
│  │ ┌──────────┐ ┌──────────┐ │Wound rotor│ Servo │ │   Separate    │  │ │
│  │ │ Squirrel-│ │  Wound   │ ├──────────┼───────┤ ├───────────────┤  │ │
│  │ │   cage   │ │  rotor   │ │   Step   │Reluctance│ │   Series     │  │ │
│  │ └──────────┘ └──────────┘ └──────────┴───────┘ └───────────────┘  │ │
│  └──────────────┘  └───────────────────────────────────────────────┘ │
└─────────────────────────────────────────────────────────────────────┘
```

Fig. 1.4 Motor classification

In the dc motor, the stator serves as an inductor whereas the ac in the rotor results from the mechanical *commutator* which fixes positioning the flux and the armature MMF. Using the appropriate commutator brushes disposition, the flux is oriented along the stator pole axes upon the orthogonal current vector. Hence, to control the torque, the armature current has to be adjusted. As both the load angle θ and the magnetic flux Φ are kept fixed, the dc motor torque follows the current and (1.2) is simplified as follows:

$$T \approx T_{12} = \psi I = k_T \Phi I, \qquad\qquad (1.4)$$

where k_T is called a dc *motor torque construction factor*.

Alternatively, in the synchronous motors, the dc voltage supplies the rotor whereas the stator is excited by the ac current. Here, the flux and the spatial angle of the torque require external control without which the angles between the stator and rotor fields change with the load yielding an unwanted oscillating dynamic *response*. In the synchronous *servomotors*, a built-in *rotor-position sensor* (*encoder*) provides the right angle between the field and current vectors similarly to a dc motor giving rise to (1.4).

However, in the induction motor voltage is induced across the rotor by merely moving it through the stator magnetic field. Because the stator windings are connected to an ac source, the current induced in the rotor continuously changes and the rotor becomes an electromagnet with alternating poles. Here, the flux and the spatial angle of the torque need in external control as well. As there is no autonomous channel to stabilize the flux linkage, the specific control systems are required to adjust the torque. While the rotating windings are supplied by ac, the load angle and the flux linkage change along with rotation.

As $\psi = LI$, where L is the winding *inductance*, the electromagnetic torque is expressed by the product of a flux-producing current component and a torque-producing component of the same current. Particularly, the torque control can be achieved by varying the torque-producing current, and to obtain the quick torque response the current needs in fast changing at the previously fixed field flux

To implement the torque, speed, and path control in the motor drives of any type, the power converters and electronic controllers have to supply the motor with the energy and control signals, whereas to conform these quantities to the load parameters different mechanical transmissions are to be connected to the motor shaft.

1.3   Efficiency of electric drive

Definition. The product of rms voltage U_0 and current I_0 of the supply lines gives the amount of work per unit time called *apparent power*, or *total power*, P_0, which can be equally well expressed in terms of the material *resistance* and measured in volt-amperes (VA):

$$P_0 = U_0 I_0 = I_0^2 R.$$

Power conversion is accompanied by losses,

$$\delta_\Sigma = P_0 - P_L$$

where P_L is the drive output. Losses are measured by *efficiency*

$$\eta_\Sigma = \frac{P_L}{P_0},$$

usually in percent. Total losses of an electric drive accumulate the sum of power converter losses δ_C, motor losses δ_M, and mechanical transmission losses δ_G, as drawn in Fig. 1.5 (a).
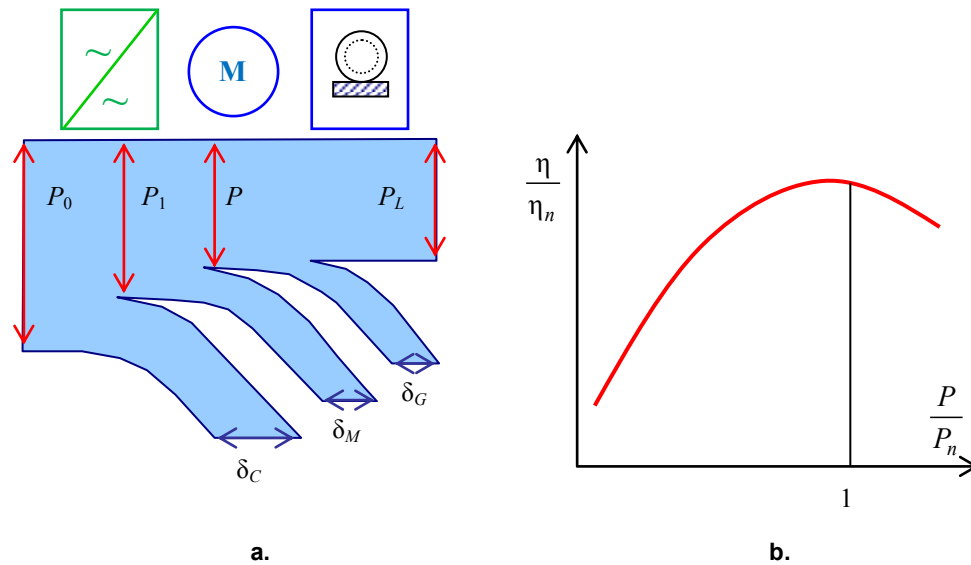

Fig. 1.5 Losses and efficiency of electric drive

Thus, efficiency of the electric drive may be expresses as follows:

$$\eta_\Sigma = \eta_C \, \eta_M \, \eta_G$$

Energy efficiency is a factor that manufacturers are greatly interested in improving.

Power converter efficiency. Efficiency of the power converter is usually 95 to 99 %. It is proportional to ohmic losses that depend on the *circuit* and operation conditions. Efficiency is reduced along with the speed reduction due to the voltage pulsating, discontinuous currents, and cooling problems.

The power converter supplies the motor by the *real power* (*effective power* or *average power*) P_1 having units of watts. The rest part of the apparent power is the *reactive power* P_{01}, having units of reactive volt-amperes (VAR). A *power factor* is a figure of merit that measures how effectively energy is transmitted between a source and load network. It is the ratio of the real power and apparent power. In the case of sinusoidal supply,

$$P_1 = P_0 \cos \varphi_0, \; P_{01} = P_0 \sin \varphi_0.$$

The power factor $\cos \varphi_0$ is determined here by the *phase displacement angle* φ_0 between the supply ac current and voltage. Being the load dependent, the power factor grows along with the load growth, but falls to 0.1…0.7 at idling.

These definitions are not adequate when considering the reactive power of converters. Most power converters produce a non-sinusoidal current waveform on the ac side whose fundamental component lags the voltage. In the case of such supply source and non-linear load, the power factor is expressed as a product of two terms, one resulting from the phase shift of the voltage and current fundamental components (effect of displacement, namely *displacement factor*) and the other resulting from the current harmonics (effect of distortion), namely the *distortion factor*. Only the fundamental frequency component of the current contributes to the active power. Due to harmonics, the apparent power is greater than the minimum amount necessary to transmit the average power.

Motor efficiency. The motor as the core of an electric drive converts the real power P_1 to the *mechanical power P*. Motor efficiency affects efficiency of the overall electromechanical transformation,

$$P = P_1 \eta_M$$

It is the fraction or percentage of energy supplied to the motor that is converted into mechanical energy at the motor shaft when the motor is continuously operating at full load with the rated voltage applied. The most usual values of η_M are in the *range* of 40 to 95 %. As Fig. 1.5 (b) Illustrates, actual efficiency alters with the motor utilization i.e. with the ratio of the *actual power P* to the rated power P_M given in the manufacturer's *datasheet*. Upon the partial loading the motors become less favorable. For larger motors efficiency is higher than for small motors.

Motor efficiency is a subject of increasing importance, especially for ac motors because they are widely applied and account for a significant percentage of energy used in industrial facilities.

Gear efficiency. The power loss in the mechanical transmission,

$$\delta_G = P - P_L$$

is mainly provoked by friction and is measured by transmission efficiency

$$\eta_G = \frac{P_L}{P} \; ,$$

usually 50 to 99 %. At braking, *reverse efficiency* factor is used instead:

$$\eta_{GR} = 2 - \frac{1}{\eta_G}$$

This term allows evaluating that part of the power, which passes to the motor from the load. When $\eta_{GR} > 0$, the torque becomes negative thus resulting in the adjustment problems of the active-loading mechanisms. To avoid such situations, mechanical *brakes* and self-braking transmissions are required.

At loading, transmission efficiency changes similarly to the motor efficiency. *Overall efficiency* of k sequentially connected transmissions is equal to

$$\eta_G = \eta_{G1}\eta_{G2}\ldots\eta_{Gk}$$

whereas overall efficiency of k transmissions connected in parallel is as follows

$$\eta_G = a_{G1}\eta_{G1} + a_{G2}\eta_{G2} + \ldots + a_{Gk}\eta_{Gk}$$

where a_{Gi} are the factors that show the part of the power carried by the i-th transmission section. Particularly to drive the load with k input shafts of P_{Li} powers and η_{Li} efficiencies, the required motor power is as follows:

$$P \geq \sum_k \frac{P_{Li}}{\eta_i}$$

Download free eBooks at bookboon.com

2   Common Properties of Electric Drives

2.1   Power topologies of electric drives

Classification. The grid-operated and converter-fed electric drives are known. The first group is the most popular and used in almost all applications. The main classes of converter-fed electric drives are shown in Fig. 2.1.
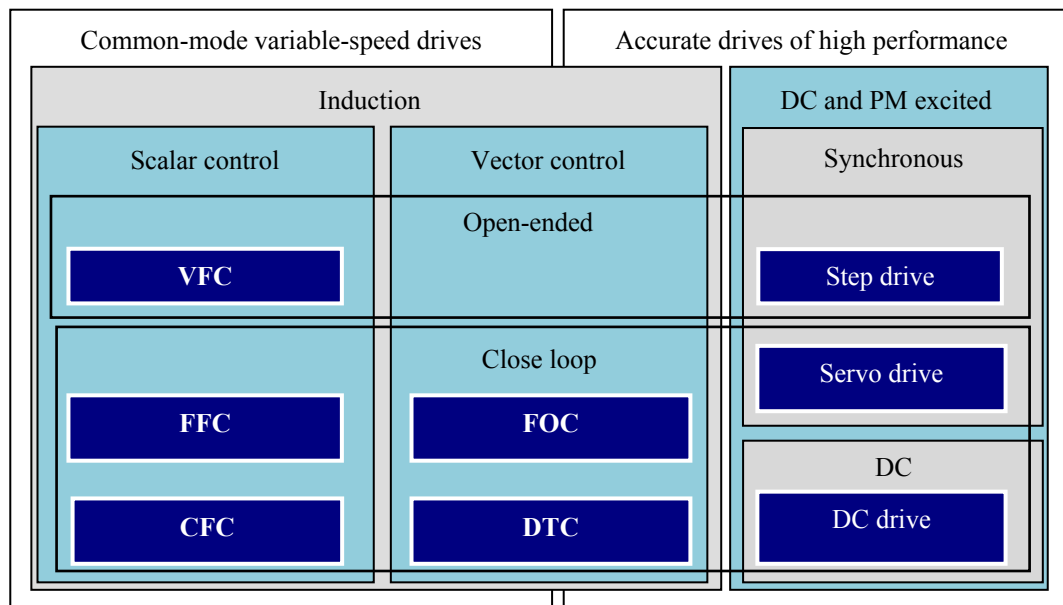

Fig. 2.1 Classes of converter-fed drives

Multiple classes of the converter-fed electric drives are manufactured. The approachable properties of the major classes are presented in Table 2.1.

Property	Induction electric drives				DC and PM excited drives	
	Open-ended scalar control (VFC)	Close loop scalar controls (FFC, CFC)	Field-oriented vector control (FOC)	Direct torque vector control (DTC)	Synchronous servo drive	DC drive
Speed range	40	100	1000	10000	40000	
Speed stability	90 %	98 %	99.5 %	99.9 %	99.9 %	
Run-up time	20 ms	5 ms	2 ms			

Property	Induction electric drives				DC and PM excited drives	
	Open-ended scalar control (VFC)	Close loop scalar controls (FFC, CFC)	Field-oriented vector control (FOC)	Direct torque vector control (DTC)	Synchronous servo drive	DC drive
Run-up torque, % of rated torque	100 %	200 %	300 %		400 %	800 %
Comparative cost	100 %	200 %	300 %			
Comparative mass and size	70 %				40 %	100 %
Application areas	Pumps, fans	Conveyers	Hoists	Lifts	Machine-tools, devices, robots	

Table 2.1 Properties of converter-fed electric drives

The least expensive and complex are the induction drives whereas the most accurate are the dc and PM excited electric drives.

In the field of the converter-fed ac drives two directions are emphasized, the common-mode variable-speed induction drives of the low and mean speed range ($D = 10...100$) and the high performance accurate drives, the speed range of which approaches tenths of thousands. The last ones are known as the servo drives.

To adjust the ac motors, the frequency converters are included between the mains and the motor. Along with the frequency, the voltage, current, slip, or EMF are usually changed. The frequency control, the slip control, and the mutual voltage-frequency, current-frequency, and flux-frequency controls are called the *scalar controls* because they use the rms (static) motor description to distinguish them from the *vector controls*, such as the field-oriented control and the direct torque control, which requires the *intellectual* approach with the motor model in the control loop.

Power converters. Power converters are supplied from the single-phase or three-phase mains. To decrease the non-sinusoidal current with high harmonics they generate, the converters are often connected to the mains through the *chokes*, *EMC filters*, *isolating transformers* or *auto transformers* which limit supply sags and spikes and improve power factor.

Based on the principle of electrical motor operation, some prevailing directions to influence on the motor mechanical energy may be distinguished. In the completely adjustable electric drive the control of the magnitude, frequency, shape, and phase of the motor current, voltage, flux, torque, and speed should be processed. To this aim, the following power converters are used in electric drives:

- *ac/dc converters* known as *rectifiers* that convert the input ac voltage U_0 to dc with controlled or uncontrolled output voltage U_1 and current I_1 (Fig. 2.2 (a));

- *dc/ac converters* called *inverters* that produce the output ac voltage of controllable magnitude and frequency from the input dc voltage (Fig. 2.2 (b));
- *ac/ac converters* called *frequency converters* and *changers* that establish ac frequency, phase, magnitude, and shape (Fig. 2.2 (c))
- *dc/dc converters* called *choppers* that change dc voltage and current levels using the switching mode of semiconductor devices (Fig. 2.2 (d))
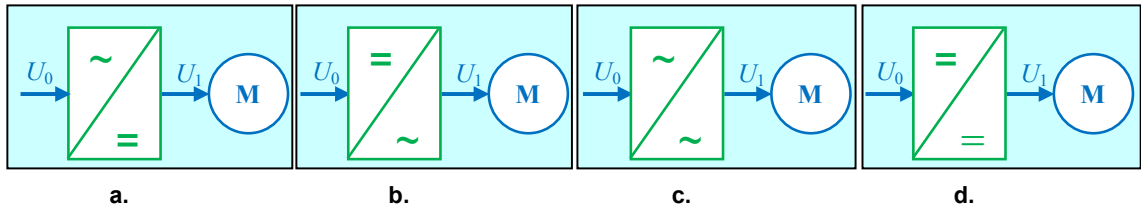

Fig. 2.2 Classes of power converters

Supply topologies. The supply topology of the squirrel-cage and wound-rotor induction motor drives is shown in Fig. 2.3 (a). Here, the stator circuit is fed by the ac/ac converter. The ac/ac power converter is driven by the mains voltage U_0 of the *power* leads (often through the *mains transformers*). Energy from the converter of the demanded frequency, magnitude, phase, and shape (U_1) supplies the motor stator. The frequency and magnitude of the stator voltage or current are adjusted by the control system, which sets the demanded drive characteristics by online calculations or using information from sensors.

Practically the same supply topology the PMSM has (Fig. 2.3 (b)). To adjust the frequency and voltage by the stator converter, the built-in motor encoder senses the shaft position here.
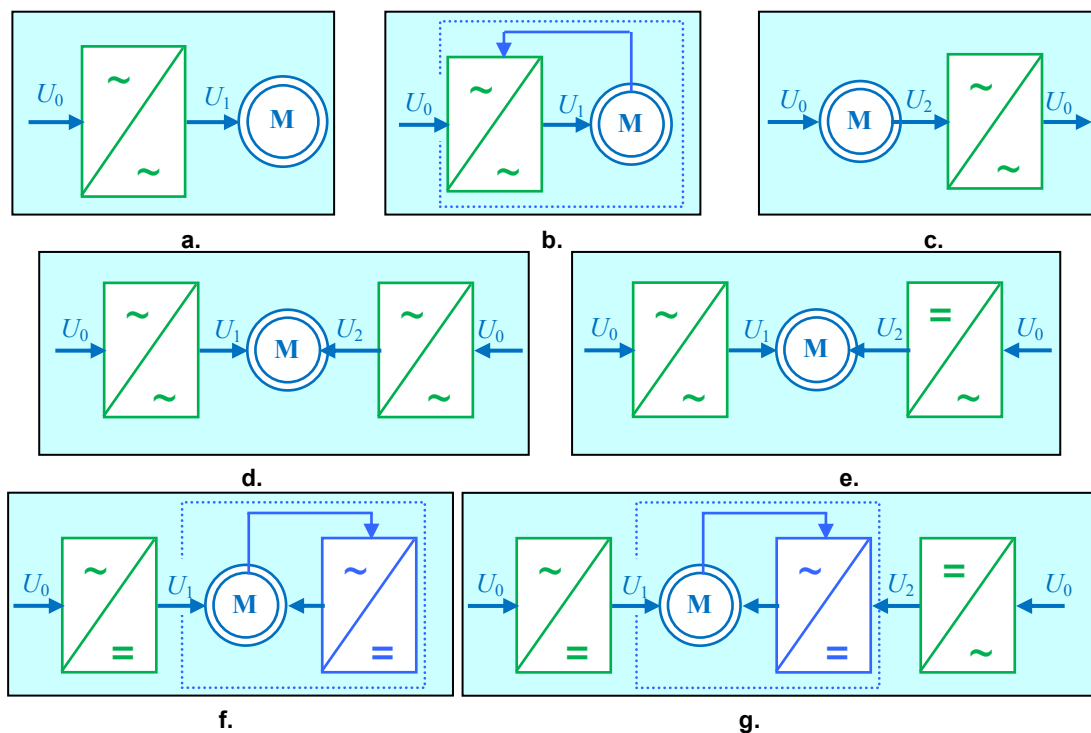
Download free eBooks at bookboon.com

Fig. 2.3 Power topologies of converter-fed electric drives

To excite the rotor circuit of the wound rotor machine, so-called *rectifying cascades* are sometimes applied (Fig. 2.3 (c)). In such topology the *naturally-commutated* (*direct*) *inverters* are used which regenerate the slip energy to the mains thus introducing an additional EMF to the rotor. Another method is based on the *double fed converters*, operated in both the motoring and the generator modes.

Figure 2.3 (d) presents the topology of the completely controlled electric drive in which both the stator and the rotor circuitry of the motor are excited by the separate stator- and rotor-feeding ac/ac converters. This organization can be applied in the variable-speed wound rotor induction drive. Energy from the converter of the demanded frequency, magnitude, phase, and shape supplies the motor rotor (U_2) and stator (U_1) circuits.

The power topology of the wound rotor field excited synchronous motor drives is shown in Fig. 2.3 (e). To adjust the speed and voltage the ac/ac stator converter is used. The rotor circuit is excited through the separate rectifier.

The voltage and the flux are adjusted in the dc electric drive as well. Here, the mechanical commutator plays the inverter functions whereas an excitation is provided by the PM (Fig. 2.3 (f)) or by the separate excitation circuit (Fig. 2.3 (g)).

2.2 Control topologies of electric drives

Control system. A drive system solves the problem of the most accurate implementation of the demanded impacts by the driven machine which is the control object of the electric drive. For simple applications where speed and path accuracy is not required, an open-ended control may be sufficient. An open-ended drive is one in which the signal goes from the controller to the actuator only. There is no signal returning from the load to inform the controller that the motion has occurred.

However, the object of management is usually unstable, non-linear and encumbrance-affected therefore the set-points are executed with errors. Applications that require the control over a variety of complex motion profiles use the closed loop technique. These may involve the control of either velocity or position, high resolution and accuracy, very slow or very high speeds; high torques in a small package size, etc. Because of additional components such as the feedback device, complexity is considered by some to be a weakness of the closed loop approach. These additional components do add to initial cost.

Behaviour of the electric drive is described (Fig. 2.4) by some *control variables y* (the speed, torque, flux, or machine position), disturbances χ (moments of inertia, counter-torques, and encumbrances), set-points y^*, intermediate variables y' (voltages and currents). The control errors δ are just usual here like in any automatic system. Commonly the set-points are time-changing therefore for their reproduction the *adjustable* and *automatic control systems* are used. In some cases an electric drive plays a role of the *stabilizing system* with the time-constant set-points.

Variable data pass across the direct channels and feedbacks. They are processed by the controllers (regulators) – information converters that generate the references using the error signals δ with the help of filters – information converters that select the useful particle of the sensor signals *y, y'*. The set-points are generated by different set-point devices. The feedback is the property of the *dynamic electric drive* operated in the close loop system. In a servo drive the feedback loops the position, path, flux, torque, current, etc.

Feedback and feedforward loops. The feedback looping of the control object (Fig. 2.4 (a)) weakens an impact of the external variables χ on the system performing accuracy therefore as a rule the feedbacks loop the unstable and inertial units. Such system consists of objects (O), regulators (Reg) and loops with summers and fork nodes. The *negative feedback* provides *boosting* before the set-point approaching. Such boosting evidently appears in the linear area of the system operation, comes down upon the influence of the non-linear factors, and disappears at saturation. The *positive feedback* brings down the system quick action.

Stability of the close loop system is of the first importance. Yet, stability is the mandatory, but insufficient, condition of the satisfactory management. The sufficient condition requires compensating of disturbances. The regulators, which design does not meet these rules should be considered as improper.

In the control topology two ways are combined commonly – the *deflection control* by looping the components with feedbacks, and the *load-responsive control* by arrangement the *feedforward* loops.

Cascading. *Multi-loop* (*cascade*) *systems* with *outer* and *inner* loops change significantly the properties of the components they envelop. They provide stability of the unstable loop, decrease its lag effect, or encourage its integrating or differentiate properties. Unlike the *single-loop systems* shown in Fig. 2.4 (a), in the inner loops of the cascade systems (Fig. 2.4 (b)) the additional impacts is produced. The inner loops promote effective compensation of the system disturbance because they feel disturbances faster as compared with the major outer loop. Particularly, the *predictive control* with a feedforward brings the reference closer to the control object thus specifying the value of *y* by the signal of the error δ (Fig. 2.4 (c)). The so-called *compound systems* (Fig. 2.4 (d)) provide an indirect measurement and compensation of the disturbances and errors. The equipment to measure and derive the signals in these systems forms an *observer*, that is the regulator of the *state controller* class The systems with observers are applied when variables are untraceable for the direct measurement and the reference presents the calculated function.
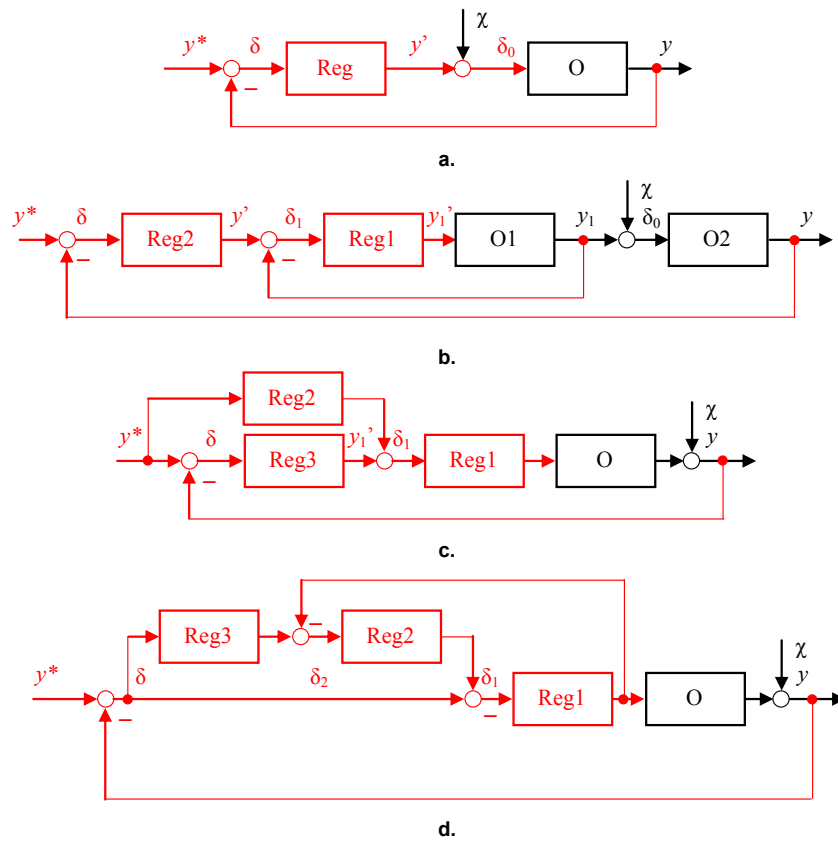
Fig. 2.4 Control topologies of electric drives

3   Characteristics of Electric Drives

3.1   Dynamic characteristics

Definition. In order for the driven machine to produce good, accurate speeds and parts, it must operate in two distinct modes: transient and steady state. The first mode of operation, the transient state, occurs when the input command changes. This causes the load to accelerate and decelerate i.e. change the speed. During this time period, there is an associated time required for the load to reach a final speed or position (rise time), a time for the load to settle, and a certain acceptable overshoot. The second mode of operation, steady state, occurs when the load has reached the final speed, i. e. continuous operation. During this time, there is an associated tracking accuracy typically called a steady state error. The machine must be capable of operating in these modes to handle the variety of operations required for prescribed performance.

Demands in the dynamic properties of a drive arise as a result of even faster machining processes, increases in automation *cycles*, and associated production efficiency. *Dynamic characteristics*, called also the *time responses*, reflect an electric drive behavior in *transients*, such as *start-up* (*starting*), *braking*, set-point *switching*, load applying and fault. Any transient is the assembly of a pair of motions - a free motion with the disturbed equilibrium and a motion forced by the applied impact.

A dynamic *diagram* (*trace*) shows the changing in time of the output control variables y like linear and angular speeds (v, ω) and *paths* (l, φ), torques (T), currents (I), fluxes (ψ), and powers (P). They reflect the system respond to the set-points $y^\star$ and disturbances χ upon the counter-torque T_L, voltage U, and parameters oscillations.

Step response. The system dynamic quality is usually evaluated by the deterministic transients. The most typical of them are the steps (*step responses*). In some applications the trapezoidal and more complex inputs are used to test the drive dynamics. Fig. 3.1 shows conventional transients excited by the step arising of the reference or the disturbance at the zero instant. Basing on these curves, a system may be evaluated using such quality factors as the response property, quick action, overshoot, oscillation, stability, and the steady-state mode.
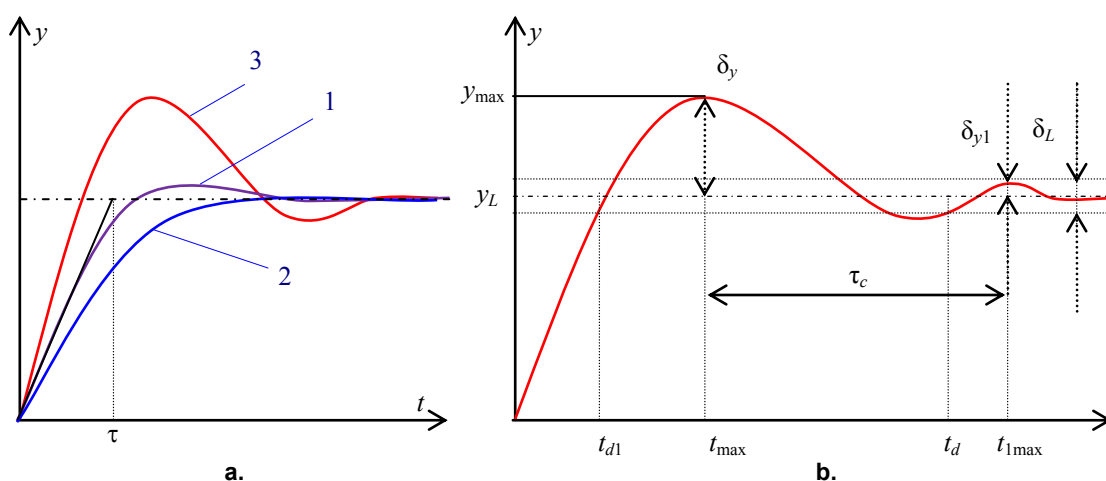

Fig. 3.1 Examples of step responses

The *response properties* are subdivided into *oscillation-free monotonous*, oscillation-free *exponential*, and *oscillating processes* plotted by the traces 1, 2, and 3 in Fig. 3.1 (a).

Quick action. The *quick action* known also as the *speed of response* or the *transient response* is measured by the *first-matching time* t_{d1} and the overall *startup time* t_d. In Fig. 3.1 (b), t_{d1} and t_d are the minimum and the maximum time intervals, after the expiry of which the following inequality is met:

$$\left| \frac{y - y_L}{y_L} \right| \leq \delta_L$$

where y and y_L are the current and the steady-state outputs and δ_L is the permissible *accuracy range* (*tolerance*) known also as the *irregularity factor*. Normally, $\delta_L \leq 0.05$, i.e. the transients are considered as completed when y differs from y_L no more than 5 %. In the case of oscillation-free exponential modes of operation, $t_d = t_{d1} = 3\tau$, where τ is the system *time constant*.

Time constants. The time constants describe the rate of the heating, mechanical, and electrical processes in electric drive. Every time constant is the ratio of energy stored during the transient (power consumption) and the returned power (power conductivity):

$$\tau = \frac{W}{P} \, .$$

Particularly, the *thermal time constant* $\tau_{\tau\circ} = \dfrac{C}{A}$ is the ratio of the motor heat *capacity* C to its heat emission A. A *mechanical time constant*

$$\tau_T = \frac{J\omega_M}{T_d} \tag{3.1}$$

describes the speed-up rate of the driven mechanism. It defines the time required to run the motor of the moment of inertia J and the maximum possible starting torque T_d to the *rated speed* ω_M neglecting electromagnetic loss. At the rated speed the motor develops the rated power at rated voltage and frequency. Is serves as an indication of how fast the output shaft will turn the connected equipment.

An *electromagnetic time constant*

$$\tau_e = \frac{L}{R} \tag{3.2}$$

is the important index of the electrical process rate in the drive of inductance L and resistance R.

To raise efficiency of the drives operated at the intensive start-up and braking modes and to increase the accuracy of the servo systems, the electric drives require the smallest values of t_d and t_{d1}.

In the systems of high speed and torque stability, the *transient errors* caused by the load disturbance (T_L), by the reference change (y^*), or by the braking influence restrict the quick action. An increase of the speed of response is limited also by the motor overload capacity, the current rate of the power converter, and permissible mechanical accelerations. On the other hand, in the percussion-type machines (punches, presses, pile-drivers, etc.) the speed of response is lowered forethought.

Overshoot. An *overshoot* is the ratio of the difference between maximum and the steady-state values of the output signal to its steady-state value:

$$\gamma = \frac{\delta_y}{y_L} = \frac{y_{\max} - y_L}{y_L} \, .$$

Typically, the overshoot is to be less than 0.15 to 0.50. In the machine-tool systems it is restricted by 0.10, whereas in some drives it is prohibited. As well, the oscillation magnitude $y_{\max}$ is limited by the commutation, durability conditions, etc. At last, the oscillation-free exponential processes have never overshoot.

Oscillation and attenuation. *Oscillation* is described by the number of alternations (unidirectional transitions) of the output value y through the steady value y_L per the transient time t_d. Usually, 3 to 5 oscillations are permissible. An interval between the neighbor amplitudes $\tau_c = t_{1\max} - t_{\max} = \sqrt{\tau_T \tau_e}$ is called a period of *free oscillations* or *self-oscillation*. A *self-oscillation angular frequency* $\omega_c = \dfrac{2\pi}{\tau_c}$ describes the system *bandwidth* and the value $f_c = \dfrac{1}{\omega_c}$ is known as the free oscillation frequency. It is assumed that the system senses the oscillations, which frequency is less than f_c. The rate of the oscillation attenuation is measured by the *damping factor*, known also as an *attenuation factor*:

$$\xi = \frac{\delta_y - \delta_{y1}}{\delta_y} = \frac{1}{2} \sqrt{\frac{\tau_T}{\tau_e}} \tag{3.3}$$

where δ_y and δ_{y1} are the magnitudes of the first and second oscillations. It is preferable to have $0.7 \le \xi \le 1.0$.

Damping indicates the rate of system *stability*. In the *stable system* the first overshoot has the highest magnitude, that is $\delta_y = \delta_{y1}$. When the magnitude has no damping and raises with time, we say about an *unstable system* with *sustained oscillation*.

Steady-state mode. Gradually, the free component in the transient is damped, and the system works in the steady mode of the *forced oscillation*. The features of the *steady-state mode* are described by the steady or periodic processes dependently on the applied influences. To evaluate the first, the static characteristics are used, and in the last case the dynamic traces are popular.

In electrical converters, the steady processes are accompanied by *ripples*, which are distinguished as the harmonic and sub-harmonic ones. In motors, the steady-state mode is accompanied by *pulsations*. The pulsation caused by the converter ripples should not destroy the motor dynamics. In mechanical system, the steady state is described by the *load diagrams* that reflect the periodic load time-changing, and by the *travel diagrams* that illustrate the speed-time trajectories of a machine.

3.2   Static characteristics

Definition. The static characteristics describe the system in the steady-state modes while the counter-forces and counter-torques are considered as constant or weakly changed ones. These characteristics may be discussed as the particular cases of the transients supposing the smallest input deviation in the referred time interval. Usually, the static curve represents the trace of the control variable y (I, T, F, ω, v, φ, l, etc.) forced by some main disturbance χ (U, T_L, F_L, etc.) upon the fixed set-point y^*. The influence of other disturbances is displayed as the *drift*, which distorts the diagram shape.

External characteristics (*output characteristics*) and *control characteristics* describe the operation of power converters in the steady-state mode. Examples are: $U_1(I)$, $U_1(\chi)$. The main static characteristics of motors are an *electromechanical characteristic* (a *speed-current characteristic* $\omega(I)$) and a *mechanical characteristic* (a *speed-torque characteristic* $\omega(T)$). The typical static *characteristics of the load* are the counter-force and counter-torque diagrams as the functions of speeds and paths, $T_L(\omega)$, $F_L(l)$, etc.

Universal diagram. As a rule, the static characteristics are represented in the *universal diagrams* that combine the motor and the load curves, and, sometimes, the power converter curves. In their intersection the *operating point* of an electric drive is placed. For example, Fig. 3.2 (a) illustrates the speed-torque characteristic curves of the motor $\omega(T)$ and the mechanism $T_L(\omega)$.
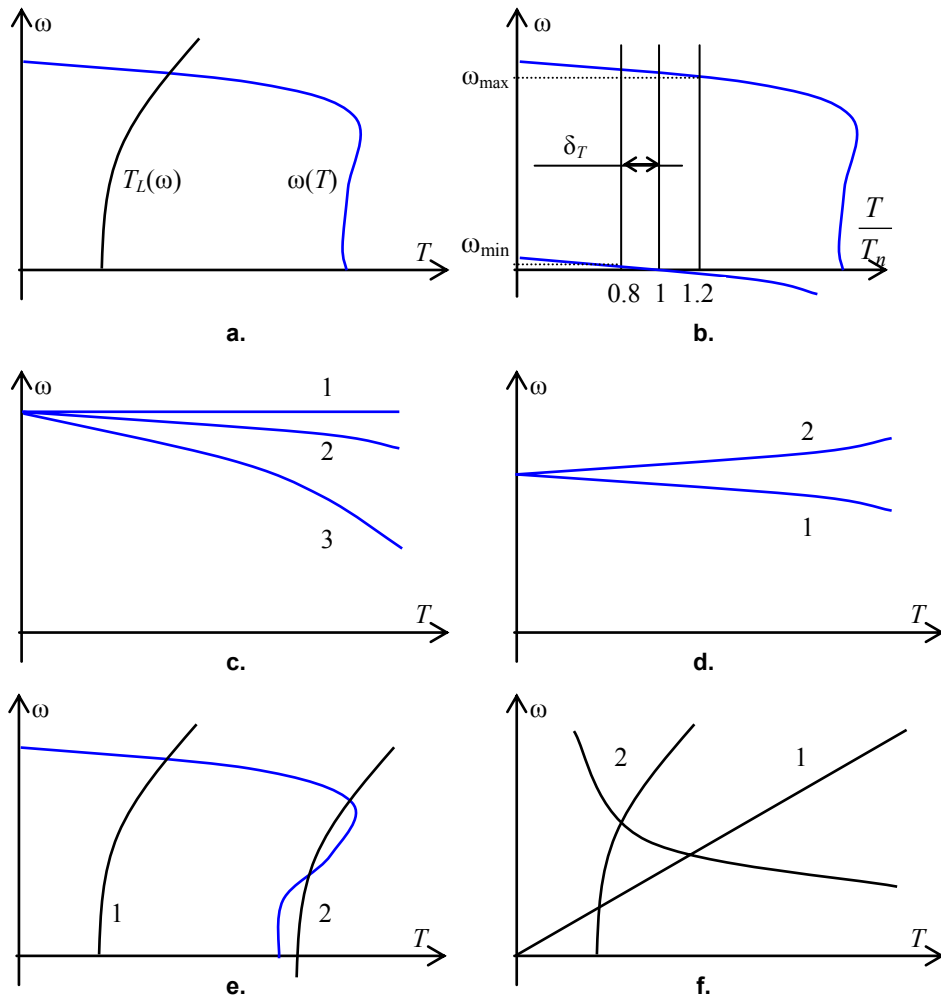
Fig. 3.2 Examples of speed-torque characteristics

At start-up, the motor runs from the zero speed and follows its speed-torque characteristic until reaching the stable operating point $T = T_L$ where the load characteristic and the motor characteristic intersect. This stable operating point will be reached if the load torque is smaller than the motor maximum torque.

To evaluate the system on the basis of the static characteristic, the following quality indexes are used: an overload capacity λ, a speed range D, rigidity β, linearity, and the steady-state errors.

Overload capacity. An *overload capacity* is the ratio of the *inrush value* of a disturbance χ_{max} to its rated value χ_n:

$$\lambda = \frac{\chi_{max}}{\chi_n}$$

In power converters, the overload capacity is restricted by their heat dissipation features. Typically, for the semiconductor devices it is relatively small, but for the magnetic devices and electrical machines it is enough significant. The overload capacity of motors presents the ratio of their maximum and rated torques, $\lambda = \dfrac{T_{max}}{T_M}$, and is indicated in the datasheets.

Speed range. A *speed range* (*speed ratio*) is the ratio of the control variable inrush value $y_{max} = \omega_{max}$ to its minimum possible value $y_{min} = \omega_{min}$

$$D = \frac{y_{max}}{y_{min}} = \frac{\omega_{max}}{\omega_{min}},$$

which is true in the full range of the disturbance drift. Particularly, to measure the speed adjustment range, the drift of the load torque δ_T should be limited by the permissible values $T_{L\,min}$ and $T_{L\,max}$ or by the constant range $\pm 0.2 T_L$. An example is given in Fig. 3.2 (b). Usually, the speed adjustment range of the simple electromechanical systems is equal 2 to 5. The close loop automotive electric drives implement ranges that are of 1 to 3 orders more. The full speed adjustment range of the *auxiliary electric drive* of the precision milling machine, lathe, or turned lathe reaches 10^2 to 10^5. The theoretical speed range of the feed drive for the contour machining using the computer numerical control is infinite. In practice, the minimum auxiliary value is restricted by the sensitivity to the supply voltage and frequency deviations. Their permissible ranges are -15 to +10 % and 2 % accordingly. The speed range of the machine-tool *main electric drive* riches typically 200, 500, or 1000.

Rigidity. The *rigidity* factor

$$\beta = \frac{d\chi}{dy},$$

shows an alteration of the control variable y upon the main disturbance χ, thus indicating the motor possibility to perceive the load. Rigidity of the motor speed-torque characteristics $\omega(T)$,

$$\beta = \frac{dT}{d\omega}$$

and the motor speed-current characteristics $I(T)$,

$$\beta_I = \frac{dI}{d\omega}$$

are of tenths and hundreds. Such characteristics are called the *rigid curves* or *flat characteristics* in distinct from the *soft*, or *drooping*, *characteristics* that depend on the disturbances. Examples of absolutely rigid (1), rigid (2), and soft (3) characteristics are given in Fig. 3.2 (c). Absolutely rigid are the synchronous motor characteristics, whereas the characteristics of the series dc motor are mostly soft. Rigidity relates to the speed range as follows:

$$D = \frac{2\beta\omega_0 - T_{L\,max} - T_{L\,min}}{T_{L\,max} - T_{L\,min}}$$

where ω_0 is the *idle speed* at $T_L = 0$.

Rigidity of the power converter characteristics practically never exceeds 100. On the other hand, rigidity of mechanical systems changes within the broad bounds. Rigidity of the machine counter-torque characteristic

$$\beta_L = \frac{dT_L}{d\omega} \tag{3.4}$$

is called a *viscous friction factor* or the *inner friction factor*. The ratio of motor rigidity β to the mechanism rigidity β_L treats the condition of the drive stability. We call the system as stable when an adjusted variable decreases while the disturbance increases. In a stable system, an adjusted variable decreases while the disturbance increases (curve 1 in Fig. 3.2 (d)) whereas it increases in a non-stable system (curve 2 in Fig. 3.2 (d)). Consequently, the stability condition is $\beta < \beta_L$ that is the closer is the angle between $\omega(T)$ and $\omega(T_L)$ to 90˚, the higher is the stability of the process. In other words, if, after the speed rising, the load trace T_L is placed to the right of the motor trace T, the motor will not develop the torque to return the speed to the previous state. Therefore, this drive system has the necessary stability. And vice versa, if, after the speed rising, the trace of the counter-torque T_L is placed to the left of the trace of the motor torque T, the developed *wasted torque* will accelerate the motor. Examples of the stable (1) and unstable (2) systems are given in Fig. 3.2 (e).

Linearity and steady-state errors. From the *linearity* point of view, the systems with constant rigidity are called *linear systems*, whereas any variability of rigidity is the feature of a *non-linear system*. Characteristics examples of the linear (1) and non-linear (2) systems are given in Fig. 3.2 (f).

The *steady-state errors* describe the deviation of the system motion from the constant or smoothly changed reference upon the constant or smoothly changed disturbances.

Usually, the external characteristics of power converters are evaluated by the same features as the motor and the load static characteristics. As the control curves are concerned, normally they are not restricted by overloading capabilities, rigidity, or the steady-state errors, though the control range and linearity are their important properties.

Correlation of dynamic and static characteristics. Earlier the time constants of the electric drive were introduced. To associate the mechanical time constant τ_T from (3.1) with the moments of inertia and the load torque, introduce the following equation:

$$\tau_T = \frac{J\omega}{T} = \frac{J_M + J_L}{T_{\max} - T_L}\omega = \frac{J_M \omega \gamma_J \lambda_T}{T_{\max}(\lambda_T - 1)} \tag{3.5}$$

Here $\gamma_J = \dfrac{J_M + J_L}{J_M}$ is the load *inertia ratio* and $\lambda_T = \dfrac{T_{\max}}{T_L}$ is called a motor *overtorque*. Usually $T_L \cong T_M$, therefore the motor overtorque λ_T is defined by its overload capacity λ. The equation is used to calculate the systems at the alternate load. It shows that the less is the machine inertia and load, the higher is the quick action. Any increasing of these items decreases the speed of response. The load inertia ratio changes within the broad range in the rolling mills, sluices, and machine-tools to 20 and more in the paper machines and excavators.

3.3   Load characteristics

Passive and active loads. The electrical motor is the reversible electrical machine capable to perform in the motoring and generator modes dependently of the load features. The load forces and counter-torques which are independent on the sign of the motion speed are called *reactive* or *passive forces* and *torques*. They are typical for the machine-tools and conveyers where the weight and cutting forces prevent the motion and change their sign along with the change of the machine direction (Fig. 3.3 (a)). In the *hoists* and weights, the *active forces* and *torques* are presented. Their sources are gravity and deformation therefore they keep direction when the load direction changes. These forces may both prevent and contribute to the motion. The hoists usually require some specific control methods for the vertical motion.
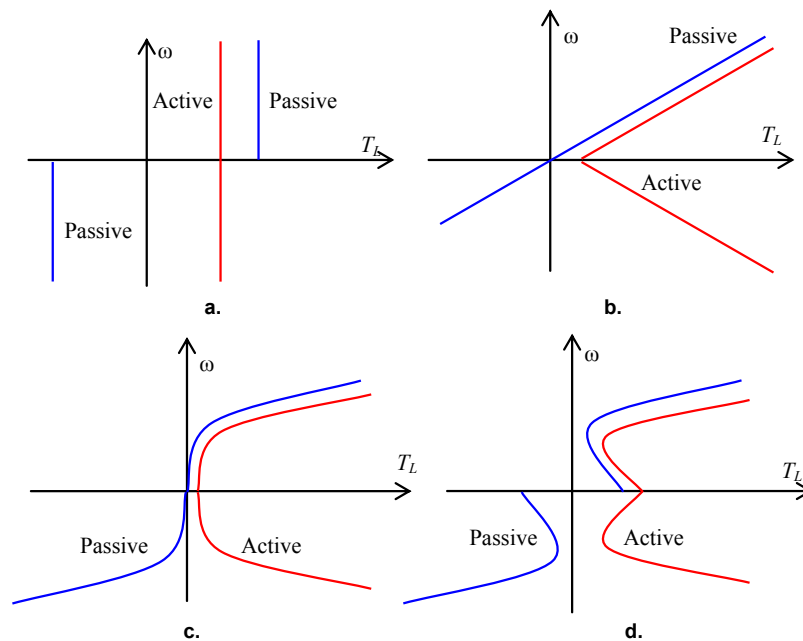

Fig. 3.3 Active and passive torques

Motoring and regeneration. Figures 3.4 (a) present possible variants of applying of the work forces to the motor shaft for the *four-quadrant operation*. The first and the third quadrants illustrate the *motoring mode* of the drive performance. The second quadrant shows the *generator mode* of *regeneration* where energy of the load motion returns to the motor. The forth quadrant displays the generator mode of the *counter-motion*. In the motoring mode, the motor torque contributes to the mechanism motion whereas in the generator modes, the motor develops the torque, which prevents the mechanism motion.
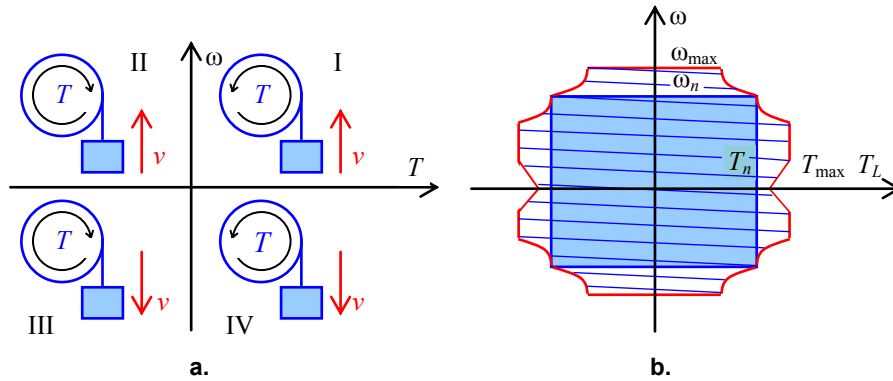

Fig. 3.4 Modes of drive operation and restrictions of the speed-torque characteristics

The *reversing drive* operates within four quadrants with a *clockwise/counterclockwise* (*CW/CCW*) *rotation* of the motor and an *excursion motion* of the load. In the other cases the direction change of the load is prohibited or impermissible thus the *non-reversing drive* is required. The specific *means for prevention of reverse* rotation are developed in some of cases.

Load profiles. The four most popular load profile types are as follows:

- torque independent of speed (constant torque)
- torque proportional to the square of the shaft speed (variable torque)
- torque linearly proportional to speed (linear torque)
- torque inversely proportional to speed (inverse torque)

Fig. 3.3 (a) shows the active and reactive load torque diagrams (T_L = const) of some machine-tools, conveyers, and traction equipment. The load can be considered to be constant if the torque remains the same over the operating speed range. Typical constant torque loads are lathes, axial and centrifugal pumps and ventilators, screw and centrifugal compressors, and agitators.

Extruders, draw benches, paper and printing machines, conveyers, and lifts have the linear torque, whereas the rolling mills, winders, wire drawers, and some lifts have the inverse torque. The loading generators usually have the linear static characteristics plotted in Fig. 3.3 (b)):

$$T_L = k_0 + k_1 \omega$$

Other applications have a variable torque characteristic that is their torque increases with the speed. Centrifugal pump characteristic is described by the quadratic *pump and fan characteristic* (Fig. 3.3 (c)) like this one:

$$T_L = k\omega^2$$

As the torque of pumps and fans, stirrers and mixers is proportional to the square of the speed, their power is proportional to the cube of the speed. This means that at reduced speeds there is a great reduction in power and therefore energy saving. Because the power is greatly reduced, the voltage applied to the drive can also be reduced and additional energy saving is thus achieved.

The vacuum cleaner motion is described by a cubical low, and some extruders, mixers, and robots have more complex model of operation. (Fig. 3.3 (d)), for example,

$$T_L = k_0 + k_1\omega + k_2\omega^2 + \ldots$$

Restrictions of speed-torque characteristics. Figure 3.4 (b) shows the typical limitations of the modes of the electric drive operation. In the nominal operation points the rated torque T_n is developed within the rated speed range ω_n. At the torques equal and below the rated value, an electric drive power varies proportionally to the speed, $P = T\omega$. This area provides the ability of the drive *constant torque operation*. To exceed the rated speed, the torque should be decreased to save the constant output power in the *high speed operation mode* beyond the rated speed. This area provides the ability of the drive *constant power operation*. The drive *override* ω_{max} is restricted by the mechanical durability and, as a rule, cannot exceed the double rated speed. In the range of the low speeds due to the cooling deterioration, the load *derating* is recommended up to 15…30 %. This motor derating is essentially independent of the drive type, thus the constant torque ability is declined.

The maximum torque of the dc and servomotor is limited, among other factors, by the load capacity of the permanent magnets. The rms torque must be smaller than the torque at zero speed. If a motor is too heavily loaded and the current increases to an excessive value, the magnets will become demagnetized and the motor will "lose the torque". To avoid demagnetization, the currents of the motor and power converter must be agreed. Additionally, if the thermal limiting rate is exceeded, this also will result in demagnetization of the magnets or damage of the winding insulation.

Torque restriction in the upper speed range depends on the supply voltage and the voltage drop in the cables. Due to the counter-EMF (voltage induced in the motor) the maximum current can no longer be injected. This results in a reduced torque.

The permissible torque T_{max} is restricted by the motor inrush current. All motors work continuously within the *rated current* (*full-load current*) range. Their short-time *run-up* locked-rotor currents overcome the rated value 2 to 10 times. Mechanical systems, such as *bearings*, shafts, and gearboxes have the limited overload capacity as well. Typically, within the speed range from ω_M to $0.5\omega_M$ the 1.5-times overload is possible up to 60 seconds and the 2 to 3-times *short-term overload* in 0.2 to 3.0 seconds. Within the speed range from $0.5\omega_M$ to $0.25\omega_M$, the 3 to 4-times *overload limit* is possible in milliseconds, and in the case of very low speeds, the 4 to 6-times *overload electronic trip* may occur.

4 Universal Model of Electrical Machine

4.1 Park's machine

Orthogonal reference frames. To describe any rotational machine, R. H. Park have introduced the orthogonal reference frames, which interpret a multiphase multi-pole system as an equivalent double-phase bipolar ($p = 1$) machine. The aim of the Park's transformation is to simplify the analysis of multi-phase circuits by reduction of many ac quantities to the pair of dc variables. Simplified calculations can be carried out on these imaginary dc quantities resulting, if required, in the following inverse transformation to recover the actual multi-phase ac results.

An elementary Park's machine has two identical stator coils ($m_1 = 2$) located such that their axes are shifted by 90°, and two rotor coils ($m_2 = 2$) disposed in the similar way. The air gap between the stator and the rotor is assumed to be constant and independent of the rotor position. In the winding diagram shown in Fig. 4.1 (a), three orthogonal winding systems are represented. The lengthwise and the transversal stator windings $w_{1\alpha}, w_{1\beta}$ are placed along the axes which are denoted as an orthogonal stator reference frame (α, β). The orthogonal reference frame for the rotor windings, w_{2d}, w_{2q}, is denoted as (d, q). The lengthwise axis d is superposed with the positive direction of the rotor MMF. Any arbitrary frame of references is denoted as (x, y). Normally, the stator frame is fixed in space whereas the rotor frame and other arbitrary frames can rotate in space with some angular frequencies. The counter-clockwise rotation is considered as positive and clockwise rotation as negative. Angles are counted in the positive direction of the rotor rotation. The positive directions of the β, q and y axes are selected in advance with α, d and x.
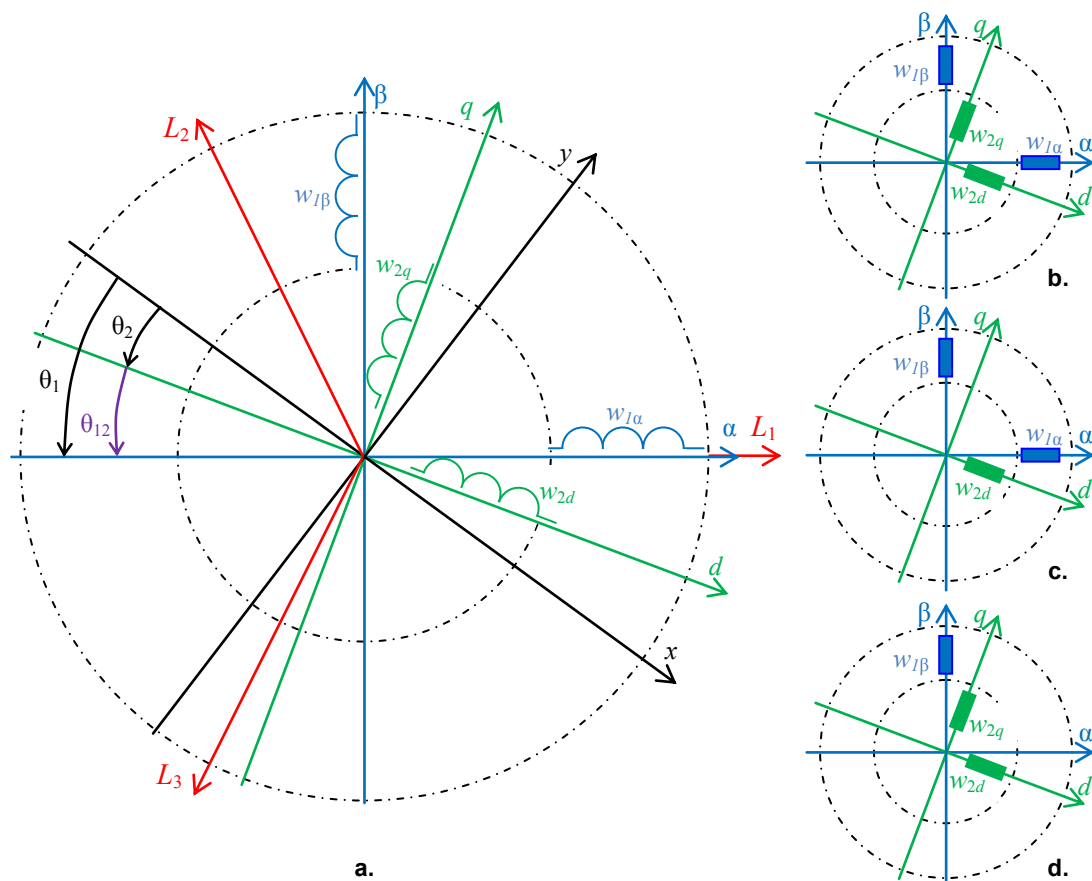
Fig. 4.1 Park's model of a motor

Park's notation. Below, the Park's notation is introduced which is used throughout the text:

L_1, L_2, L_3 – a natural *reference frame* of the actual balanced three-phase machine;

(α, β) – an orthogonal stator reference frame of the Park's model;

(d, q) – an orthogonal rotor reference frame of the Park's model;

(x, y) – an orthogonal arbitrary reference frame rotated at some angular frequency ω_k ;

θ_1, f_1 – a phase and a frequency of the stator *voltage*;

$\omega_1 = s\theta_1 = 2\pi f_1$ – an *angular frequency of the stator field* and *stator EMF E_1* rotated in the stator reference frame (α, β) and called also a synchronous speed of the unipolar motor field;

θ_2, f_2 – a phase and a frequency of the *rotor EMF E_2* called also an induced voltage;

$\omega_2 = s\theta_2 = 2\pi f_2$ – an *angular frequency of the* rotor EMF and of the corresponding vector of the rotor current in the rotor reference frame (d, q) called also a *slip speed*;

θ_{12}, f_{12} – a phase and a frequency of the rotor EMF relative to the stator voltage;

$\omega_{12} = s\theta_{12} = 2\pi f_{12}$ – an *angular frequency of the rotor EMF relative to the stator.*

Frequency equilibrium. As the stator windings match the reference frame (α, β) and the rotor windings match the reference frame (d, q), hence

$$\omega_1 = \omega_2 + \omega_{12}, \tag{4.1}$$

$$\omega_1 = \frac{E_1}{\psi_1}, \quad \omega_2 = \frac{E_2}{\psi_2}.$$

Here, the stator frequency ω_1 is the frequency of the voltage and current in the stator circuit whereas the slip frequency determines the induced voltage and current in the rotor circuit. In the induction machines both the stator and the rotor are excited by ac (Fig. 4.1 (b)). In the synchronous machines the rotor is excited by dc, that is $\omega_2 = 0$ and $\omega_1 = \omega_{12}$ (Fig. 4.1 (c)). In the dc machines the stator is excited by dc, that is $\omega_1 = 0$, therefore $\omega_2 = -\omega_{12}$ (Fig. 4.1 (d)).

Electrical equilibrium. The model of the Park's machine in the arbitrary reference frame (x, y) rotated with the frequency ω_k depicts the electrical equilibrium of the stator and rotor winding voltages by the following Kirhchoff's equations:

$$
\begin{aligned}
U_{1x} &= R_1 I_{1x} + s\psi_{1x} - \omega_k \psi_{1y}, \\
U_{1y} &= R_1 I_{1y} + s\psi_{1y} + \omega_k \psi_{1x}, \\
U_{2x} &= R_2 I_{2x} + s\psi_{2x} - \left(\omega_k - \omega_1 + \omega_2\right)\psi_{2y}, \\
U_{2y} &= R_2 I_{2y} + s\psi_{2y} + \left(\omega_k - \omega_1 + \omega_2\right)\psi_{2x}.
\end{aligned}
\tag{4.2}
$$

Thanks to the system orthogonality,

$$U_1 = \sqrt{U_{1x}^2 + U_{1y}^2}, \quad U_2 = \sqrt{U_{2x}^2 + U_{2y}^2},$$

$$I_1 = \sqrt{I_{1x}^2 + I_{1y}^2}, \quad I_2 = \sqrt{I_{2x}^2 + I_{2y}^2}.$$

As follows from (4.2), the supply voltages are distributed between three components. The first component ($R_i I_i$) describes the ohmic voltage drop in the stator and rotor windings caused by the Joule's power loss. The second one, the flux linkage derivation ($s\psi_i$), is caused by the voltage drop in the winding leakage reactance. It is called a *transformer EMF*, or a *self-induction EMF*. The mutual motion of the windings results in a *back*, or *rotation EMF*, known also as the *counter-EMF*, $E_i = \psi_j \omega$. In (4.2) rotation EMF exists in both the stator and the rotor.

Flux equilibrium. In the orthogonal reference frame (x, y) the flux linkage results from two components. As the phase winding resistances R_1, R_2 are symmetrically distributed along the rotor circle, the following equations unify the motor fluxes, inductances, and currents:

$$
\begin{aligned}
\psi_{1x} &= L_1 I_{1x} + L_{12} I_{2x}, \\
\psi_{1y} &= L_1 I_{1y} + L_{12} I_{2y}, \\
\psi_{2x} &= L_2 I_{2x} + L_{12} I_{1x}, \\
\psi_{2y} &= L_2 I_{2y} + L_{12} I_{1y},
\end{aligned}
\tag{4.3}
$$

$$\psi_1 = \sqrt{\psi_{1x}^2 + \psi_{1y}^2}, \ \ \psi_2 = \sqrt{\psi_{2x}^2 + \psi_{2y}^2}$$

where L_1, L_2 are the *stator* and *rotor inductances* and L_{12} is the *mutual inductance*. Inductances are defined by the magnetic conductivity and the number of turns. Introducing of *electromagnetic link factors* and a *leakage factor*

$$k_1 = \frac{L_{12}}{L_1}, \ \ k_2 = \frac{L_{12}}{L_2}, \ \ \sigma = 1 - \frac{L_{12}^2}{L_1 L_2} = 1 - k_1 k_2 \qquad (4.4)$$

yields the reverse expressions of the currents through the flux linkages:

$$I_{1x} = \frac{1}{\sigma L_1}\left(\psi_{1x} - \frac{\psi_{2x}}{k_2}\right)$$

$$I_{1y} = \frac{1}{\sigma L_1}\left(\psi_{1y} - \frac{\psi_{2y}}{k_2}\right)$$

$$I_{2x} = \frac{1}{\sigma L_2}\left(\psi_{2x} - \frac{\psi_{1x}}{k_1}\right)$$

$$I_{2y} = \frac{1}{\sigma L_2}\left(\psi_{2y} - \frac{\psi_{1y}}{k_1}\right)$$

Electromechanical equilibrium. Unlike the ideal Park's machine, in the real $2p$-pole machine the angular frequency ω_0 of the stator magnetic field (a motor *synchronous speed* or an *ideal no-load speed*), the motor shaft angle φ and frequency ω called simply a *motor speed* are as follows:

$$\omega_0 = \frac{\omega_1}{p}, \quad \varphi = \frac{\theta_1 - \theta_2}{p} = \frac{\theta_{12}}{p}, \quad \omega = \frac{\omega_1 - \omega_2}{p} = \frac{\omega_{12}}{p} \tag{4.5}$$

Thus, (4.5) determines the relationship between the electrical and mechanical angles and speeds through the number of the machine pole pairs p.

Recall the vector product (1.2) of the current and the flux linkage that originates the motor electromagnetic torque T_{12}. Assuming $T \approx T_{12}$ and taking into account (1.3) and (4.3), the motoring torque can be presented by the following equations:

$$
\begin{aligned}
T &= m_1 p L_{12}\left(I_{1y}I_{2x} - I_{1x}I_{2y}\right), \\
T &= m_1 p \frac{k_1}{\sigma L_2}\left(\psi_{1y}\psi_{2x} - \psi_{1x}\psi_{2y}\right), \\
T &= m_1 p k_1 \left(\psi_{1y}I_{2x} - \psi_{1x}I_{2y}\right), \\
T &= m_1 p k_2 \left(\psi_{2x}I_{1y} - \psi_{2y}I_{1x}\right), \\
\frac{d\omega}{dt} &\approx \frac{1}{J}\left(T - T_L\right).
\end{aligned}
\tag{4.6}
$$

Thus, the motor torque is defined by the values of the following variables: the stator flux linkage ψ_1, the rotor flux linkage ψ_2, the effective flux linkage ψ_{12}, the stator current I_1, the rotor current I_2 as well as their phase displacements. The torque does not depend of the reference frame selected for calculation, whether (x, y), (d, q) or (α, β). The last expression in (4.6) is the major equation (1.1) of the torque equilibrium which determines the motor speed ω through the motor torque T, the counter-torque T_L, and the moment of inertia J.

4.2   Coordinate transformation

Transformation of (L_1, L_2, L_3) to (α, β). This transformation can be thought of in geometric terms as the projection of the three phase quantities onto two stationary axes, the α axis and the β axis. To proceed from the balanced natural three-phase current system I_{L1}, I_{L2}, I_{L3} where $I_{L1} + I_{L2} + I_{L3} = 0$ to the orthogonal reference frame (α, β), the following equations are applied:

$$
\begin{aligned}
I_{1\alpha} &= \frac{2}{3}\left(I_{L1} - \frac{1}{2}\left(I_{L2} + I_{L3}\right)\right) = I_{L1} \\
I_{1\beta} &= \frac{1}{\sqrt{3}}\left(I_{L2} - I_{L3}\right)
\end{aligned}
\tag{4.7}
$$

Transformation of (L_1, L_2, L_3) to (d, q). This transformation is conceptually similar to the previous transformation. It can be thought of as the projection of the three separate sinusoidal phase quantities onto two axes rotating with the same angular frequency as the sinusoidal phase quantities. The two axes are called a direct, or d, axis and a quadrature, or q, axis respectively. To convert the natural frame (L_1, L_2, L_3) to the orthogonal frame (d, q), the following equation system is used:

$$I_{2d} = \frac{2}{3}\left(I_{2L1}\cos\theta_2 + I_{2L2}\cos\left(\theta_2 - \frac{2\pi}{3}\right) + I_{2L3}\cos\left(\theta_2 + \frac{2\pi}{3}\right)\right)$$

$$I_{2q} = -\frac{2}{3}\left(I_{2L1}\sin\theta_2 + I_{2L2}\sin\left(\theta_2 - \frac{2\pi}{3}\right) + I_{2L3}\sin\left(\theta_2 + \frac{2\pi}{3}\right)\right)$$

Transformation of (α, β) and (d, q) to (L_1, L_2, L_3). The reverse conversion formulae are as follows:

$$I_{L1} = I_{1\alpha}$$

$$I_{L2} = -\frac{1}{2}\left(I_{1\alpha} - \sqrt{3}I_{1\beta}\right)$$

$$I_{L3} = -\frac{1}{2}\left(I_{1\alpha} + \sqrt{3}I_{1\beta}\right)$$

(4.8)

$$I_{2L1} = I_{2d}\cos\theta_2 - I_{2q}\sin\theta_2$$

$$I_{2L2} = I_{2d}\cos\left(\theta_2 - \frac{2\pi}{3}\right) - I_{2q}\sin\left(\theta_2 - \frac{2\pi}{3}\right)$$

$$I_{2L3} = I_{2d}\cos\left(\theta_2 + \frac{2\pi}{3}\right) - I_{2q}\sin\left(\theta_2 + \frac{2\pi}{3}\right)$$

Transition between (α, β) and (d, q). The mutual transformation formulae are as follows:

$$I_{2d} = I_{1\alpha}\cos\theta_{12} + I_{1\beta}\sin\theta_{12}$$

$$I_{2q} = -I_{1\alpha}\sin\theta_{12} + I_{1\beta}\cos\theta_{12}$$

$$I_{1\alpha} = I_{2d}\cos\theta_{12} - I_{2q}\sin\theta_{12}$$

$$I_{1\beta} = I_{2d}\sin\theta_{12} + I_{2q}\cos\theta_{12}$$

Transition between (α, β) and (x, y). The same concerns the mutual relationship between (x, y) and (α, β) frames,

$$I_{1x} = I_{1\alpha}\cos\theta_1 + I_{1\beta}\sin\theta_1$$

$$I_{1y} = -I_{1\alpha}\sin\theta_1 + I_{1\beta}\cos\theta_1$$

$$I_{1\alpha} = I_{1x}\cos\theta_1 - I_{1y}\sin\theta_1$$

$$I_{1\beta} = I_{1x}\sin\theta_1 + I_{1y}\cos\theta_1$$

(4.9)

Voltage transformation. The transformations of voltages and flux linkages are similar to those of the current formulae, for example:

$$U_{1\alpha} = U_{L1} - \frac{1}{2}\left(U_{L2} + U_{L3}\right)$$

$$U_{1\beta} = \frac{\sqrt{3}}{2}\left(U_{L2} - U_{L3}\right)$$

<div align="right">(4.10)</div>

4.3   DC motor

Design. A dc motor is the example of the electrical machine in which solely the dc signals provide direct torque and speed control. When comparing the dc motor with an ac machine, the former represents the best control plant because the main flux and the armature current distribution here are fixed in space and can be directly and independently controlled while with an ac machine these quantities are strongly interacting and move with respect to the stator, the rotor, and each other. To implement the same control in other types of machines, their control systems convert the ac variables to the dc ones using electrical or mechanical Park's transformations. This is the reason why the dc motor properties serve as the sample of the reachable control possibilities for all kinds of drives.

Mathematical model. The dc motor has two separate sources that interact to develop the torque. These are the stator field and the rotor circuit. To build the dc motor model in the fixed frame (α, β) shown above in Fig. 4.1 (d), the β axis is placed along the pole axis, which commutates during the motor operation therefore the sole stator winding is fixed along β. The α axis is superposed with the brush axis and with an equivalent (substitution) rotor winding. The following designations are used in the dc machines:

$$L_1 = L_\Phi, R_1 = R_\Phi, I_{1\beta} = I_\Phi, U_{1\beta} = U_\Phi,$$
$$L_2 = L_a, R_2 = R_a, I_{2\alpha} = I_a, U_{2\alpha} = U_a.$$

Here, an index Φ depicts the parameters of the excitation circuit for the effective flux linkage whereas a indicates the armature torque-producing parameters. The excitation current I_Φ establishes the permanent flux $\psi_1 = \Phi$. The parameters of the dc motors are as follows: $L_{12} \ll L_1$, $L_{12} \ll L_2$, thus the stator flux linkage ψ_1 is the dc *motor constant* considered as

$$\psi_1 = k_T\Phi = k_\omega\Phi = pL_{12}I_\Phi = \frac{U_M - R_M I_M}{\omega_M}, \tag{4.11}$$

where U_M, R_M, I_M are the rated dc motor armature data, ω_M is the rated angular frequency.

Torque and voltage equations. As well as in other types of motors, the current vector consists of two components. But in the dc motor, both the current components are structurally disconnected and can be adjusted independently. The load-dependent armature current I_a creates the EMF and the torque. Because of the permanent excitation and the commutator action, the developed torque is given by (4.6),

$$T = pL_{12}I_\Phi I_a.$$

In (4.2) $\omega_k = \omega_1 = 0$ and $\omega_2 = \omega_{12}$, which yields in the following *scalar model* of the motor:

$$
\begin{aligned}
&U_\Phi = R_\Phi I_\Phi, \, sI_\Phi = 0,\\
&U_a = R_a I_a + L_a sI_a + k_\omega\Phi\omega,\\
&T_{12} = k_\omega\Phi I_a,\\
&T \approx T_{12} = T_L + Js\omega.
\end{aligned}
\tag{4.12}
$$

As (4.12) implies, the armature voltage U_a is distributed between the armature voltage drop $R_a I_a$, the self-induction EMF $s\psi_2 = L_a sI_a$, and the back EMF described by the Faraday's law as $E_a = k_\omega\Phi\omega$.

Vector diagram and motor characteristics. The *vector diagram* (*phasor diagram*) of the motor drawn in Fig. 4.2 (a) interprets geometrically the above mentioned components in the particular time instant using the *space vectors* of the rotor variables fixed along the brush axis (α) and the stator flux axis (β).
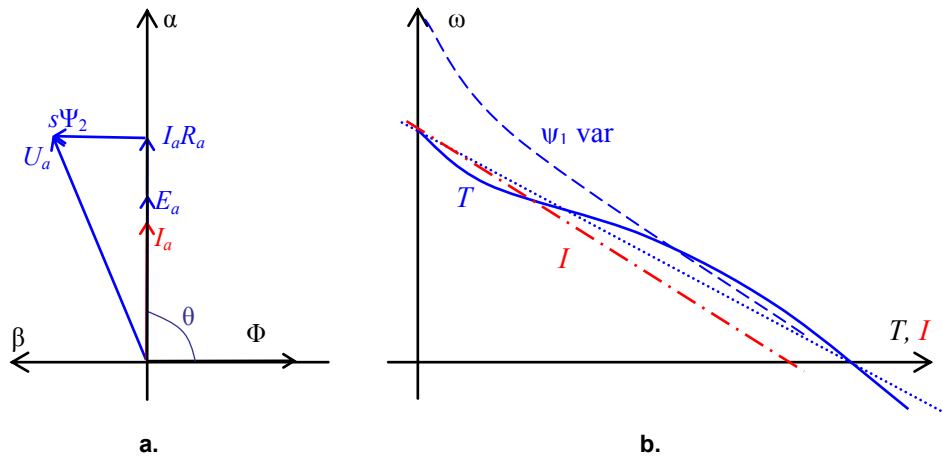
Fig. 4.2 Vector diagram and speed-torque and speed-current characteristics of a dc motor

To build the motor characteristics, convert (4.12) as follows:

$$U_a = \frac{R_a T_L}{k_\omega \Phi} + \frac{R_2 J}{k_\omega \Phi} s\omega + \frac{L_2}{k_\omega \Phi} s T_s + \frac{L_2 J}{k_\omega \Phi} s^2 \omega + k_\omega \Phi \omega \qquad (4.13)$$

Divide (4.13) by $k_\omega \Phi$ and apply the superposition,

$$\frac{R_a J}{(k_\omega \Phi)^2} = \frac{R_a J\omega}{k_\omega \Phi R_a I_d} = \frac{J\omega_0}{T_d} = \tau_T$$

$$\frac{R_a}{L_a} = \tau_e \qquad (4.14)$$

$$\frac{U_a}{k_\omega \Phi} = \omega_0$$

Here, τ_T is the mechanical time constant of the motor drive given in (3.1), τ_e is the electromagnetic time constant given in (3.2), I_d and T_d are the run-up current and torque, and ω_0 is the no-load angular frequency. Using (4.14), replace (4.13) by the following second-order differential equation:

$$\tau_T \tau_e s^2 \omega + \tau_T s\omega + \omega = \omega_0 - \frac{\tau_T T_s}{J} - \frac{\tau_T \tau_e}{J} s T_L \qquad (4.15)$$

To find the ratio of the armature current and voltage, time the second equation of (4.12) by s,

$$L_a s^2 I_a + R_a s I_a + k_\omega \Phi s\omega = s U_a .$$

Replace $s\omega$ by $T_{12} - \dfrac{T_L}{J} = \dfrac{k_\omega \Phi I_a - T_L}{J}$ and divide all the components by $\dfrac{(k_\omega \Phi)^2}{J}$,

$$\tau_T \tau_e s^2 I_a + \tau_T s I_a + I_a = \frac{T_L}{k_\omega \Phi} + \frac{\tau_T}{R_a} s U_a \,. \tag{4.16}$$

In the steady-state mode of operation, $s = 0$, the speed-torque characteristics can be obtained as the particular case of (4.15) as follows:

$$\omega = \frac{U_a}{k_\omega \Phi} - \frac{R_a T_L}{(k_\omega \Phi)^2} = \omega_0 - \frac{\tau_T T_L}{J} \tag{4.17}$$

The characteristics of (4.17) built in Fig. 4.2 (b) are slightly twisted due to the instability of Φ called an *armature reaction.* This reaction is usually compensated by additional construction means. In the case of the overall compensation the static traces became linear as the dotted line in Fig. 4.2 (b) shows. Using the armature current instead of the torque, the speed-current curves may be built in the same way (the dash-dot line in Fig. 4.2 (b)):

$$\omega = \frac{U_a}{k_\omega \Phi} - \frac{R_a I_a}{k_\omega \Phi} = \omega_0 - \frac{R_a I_a}{k_\omega \Phi} \,. \tag{4.18}$$

In accordance with the speed-torque and speed-current characteristics of the dc motors described by (4.17) and (4.18), the speed of the dc motor drops at loading being at full load about 90 to 95 % of the no-load speed ω_0. The voltage drop across the armature resistance and the armature reaction are responsible for this.

5   Synchronous Motor Drives

5.1   Field-excited synchronous motor drive

Design. An ac machine whose rotor is supplied from the dc source or by the PM is referred to as a synchronous motor. In the synchronous motor, when the stator and the rotor are energized, a rotating magnetic field is established in the rotor that interacts with the stator rotating magnetic field. The term synchronous means that the rotor rotation is synchronized with the stator magnetic field, and the rotor speed is the same as the motor synchronous speed.

To run the wound rotor synchronous motor, the ac power is first applied to the stator, and the synchronous motor starts like a squirrel cage machine. As the stator is energized, the ac current I_1 flows across the stator windings and an MMF revolves at the angular frequency ω_1 which initialises the rotor current I_2. After the motor has accelerated, the dc power is applied to the rotor coils. The synchronous motors with a PM do not need a dc power source to magnetize the rotor therefore their stator and rotor are excited simultaneously.

A heavy permanent rotor magnetic field locks the rotor in step with the rotating stator magnetic field. In this way, the rotor turns at the permanent synchronous speed (4.5)

$$\omega_0 = \frac{2\pi f_1}{p} = \frac{\omega_1}{p} = \frac{\omega_{12}}{p} \ ,$$

where f_1 is the frequency of the applied voltage and p is the stator pole pair number.

As the rotor is excited by dc, the slip speed $\omega_2 = 0$ and the slip (6.1) is absent. Thanks to the spatial arrangement of the stator coils and the chronological sequence of the supply current, this current generates a rotating permanent magnetic flux Φ in the air gap superposed with the axis of the rotor winding. The flux Φ produced by the rotor winding or by the PM intersects the stator windings and generates the back EMF, which makes the synchronous motor significantly different from the induction motor.

Vector diagram and replacement circuit. The synchronous motor design is usually described by the Park's model in the rotational rotor-linked reference frame (d, q) at $\omega_k = \omega_{12}$ shown above in Fig. 4.1 (c) where the stator and the rotor rotating fields run synchronously with the angular frequency $\omega = \omega_0$ or $\omega_1 = \omega_{12}$, as (4.1) implies. Voltages, currents and flux linkages of the model can be resolved on the orthogonal components (d, q).
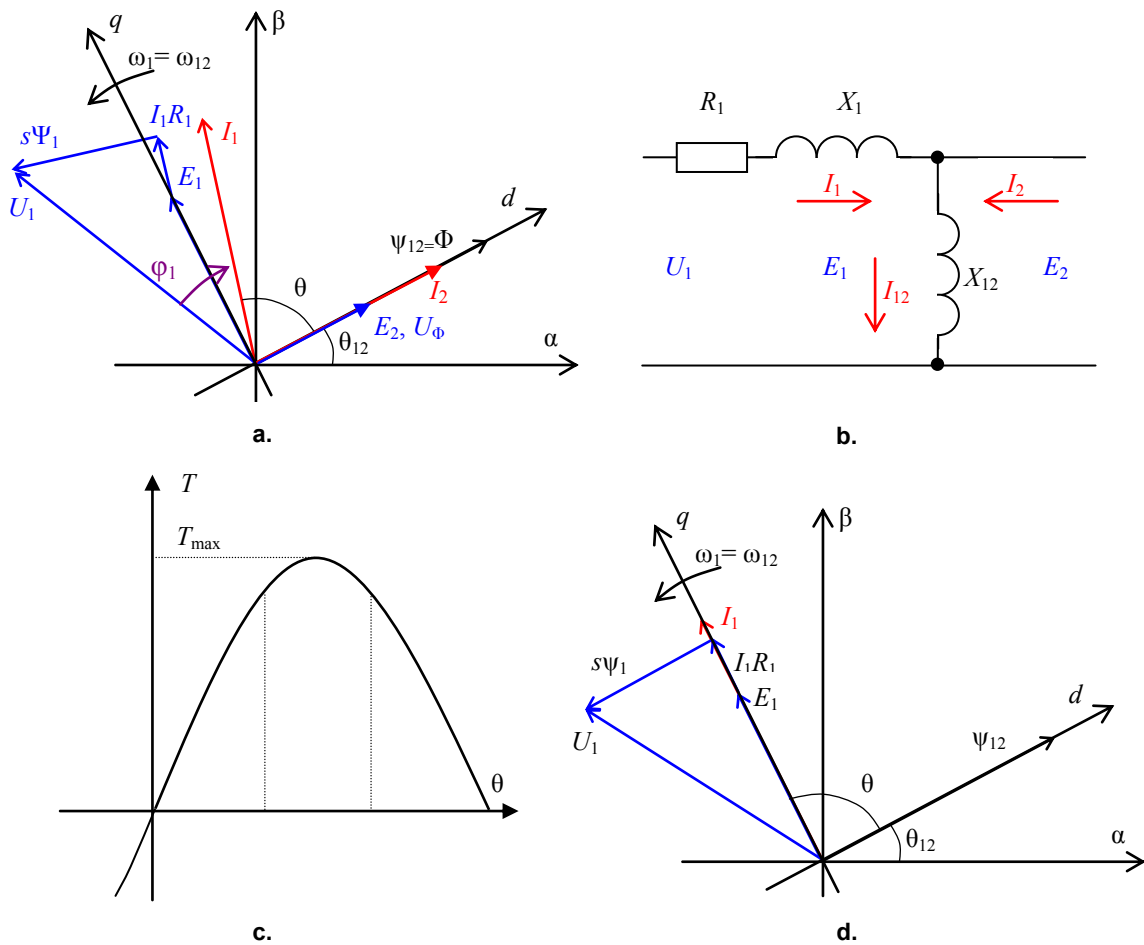
Fig. 5.1 Vector, replacement, and angle diagrams of synchronous motor

In Fig. 5.1 (a), the vector diagram of the synchronous motor is presented, in which the reference frame (x, y) shown in Fig. 4.1 (c) is superposed with the rotor frame (d, q) and $\psi_1 = \psi_{12} = \Phi = \text{const}$. The d axis superposes with the axis of the rotor poles and excitation winding w_Φ whereas the q axis is perpendicular. Herein, the voltage and the permanent flux linkage of the rotor excitation flows along the d axis only, thus $U_{2d} = U_\Phi$.

The stator current I_1 has two components responsible for developing MMF E_2 and E_1 along the d and q rotor axes, that is the flux-producing current I_{1d} and the torque-producing current I_{1q}. In the stator reference frame (α, β) these representations are the sinusoidal quantities of the stator frequency. The components of the supply voltages in (4.2) are described as follows:

$$U_{1d} = R_1 I_{1d} + s\psi_{1d} - \omega_{12}\psi_{1q},$$
$$U_{1q} = R_1 I_{1q} + s\psi_{1q} + \omega_{12}\psi_{1d},$$
$$U_\Phi = R_\Phi I_\Phi + s\psi_\Phi$$

To analyze the steady-state processes in respect to the rms values, the balanced three-phase system is treated on a per-phase basis wherefore the full phase reactances X are examined instead of inductances. Herewith, $X_1 = \omega_1 L_{1\sigma}$ is the stator phase *leakage reactance*, $X_2 = \omega_1 L_{2\sigma}$ – the rotor phase leakage reactance, referred to the stator, and $X_{12} = m_1 \omega_1 L_{12}$ – the *exciting reactance*. The T-shape *replacement circuit* for this model is presented in Fig. 5.1 (b). Here, the left-hand loop describes the steady state of the stator phase, the right-hand loop – the state of the rotor phase, whereas the *magnetizing current* $I_{12} = I_1 + I_2$ serves as the source of the rotation EMF $E_1 = -E_2$.

The rotor current $I_2 = I_\Phi$ of the synchronous machine is defined by the excitation flux Φ only and does not depend on the load and the stator current I_1. The rotor EMF E_2 is determined by the rotation speed $\omega = \omega_0$ which, according to (4.5), is proportional to the supply frequency ($\omega_1 = \dfrac{d\theta_1}{dt} = 2\pi f_1$).

Power control. The power consumed by the motor will be given by

$$P_1 = m_1 I_1 U_1 \cos\varphi_1$$

where φ_1 is the phase angle between the phase voltage and current. An important property of the dc excited synchronous motor is the possibility to control the consumed reactive power by affecting the excitation current. By increasing I_Φ, the flux can be regulated in the rotor, thus reaching the disappearance of the current reactive component. Further rise of excitation will cause the stator demagnetizing. Eo ipso, energy losses in the supply grid are minimized. Assuming negligible power loss in the rotor resistance, the mechanical power may be considered the same as the consumed power.

Angle diagram. The torque in (4.6) is produced here independently of the rotor current as follows:

$$T = m_1 p(\psi_{1d} I_{1q} - \psi_{1q} I_{1d})$$.

Neglecting the voltage drop across the stator resistance, the developed motor torque can be found from the vector diagram as

$$T = \frac{m_1 p \psi_1 U_1}{\omega_1 L_1} \sin\theta \approx m_1 p I_1 \psi_{12} \sin\theta \qquad (5.1)$$
.

As (5.1) shows, the torque is proportional to the sine of the load angle, the effective flux, and the stator current remaining independent of the speed.

While the motor is unloaded, the stator MMF superposes the induced rotor MMF and the load angle θ is zero. If the load torque is applied to the shaft, the machine will momentary slow down causing the rotor rotating field ψ_2 to lag in relation to the stator rotating field, thus producing the *rotor displacement angle* θ_{12}. Accordingly, the load angle θ shown in Fig. 1.3 and Fig. 5.1 appears between the rotor field and the stator current. The load angle will adjust to match the applied load torque, and the machine continues to spin at the synchronous speed.

The greater the load angle, the more the torque increases in (1.2) and (5.1), as shown in the *angle diagram* of Fig. 5.1 (c). The stator pole leading the rotor pole "pulls" the rotor and the lagging stator pole "pushes" it, producing the described effect. When θ reaches 90° electrical, i.e. the rotor poles dispose precisely between the stator poles, the force acting on the rotor reaches its maximum and the stator current will be in phase with the back EMF, as Fig. 5.1 (d) shows. The amplitude of the stator current now fully determines the torque. If the load angle θ further rises causing the motor overloading, the torque will fall again, and the motor will reach an unstable operating position, thus it can stall and come to a standstill.

To develop the maximal torque at all speeds the motor is to be driven by the inverter capable to keep the voltage-frequency ratio constant. Nevertheless, the maximal torque that the motor can develop diminishes at low speed because of the voltage drop across the stator resistance. This obstacle can be avoided by boosting the input voltage. At the same time, the synchronous motor dynamics is complicated also due to the problems of the torque *swinging*.
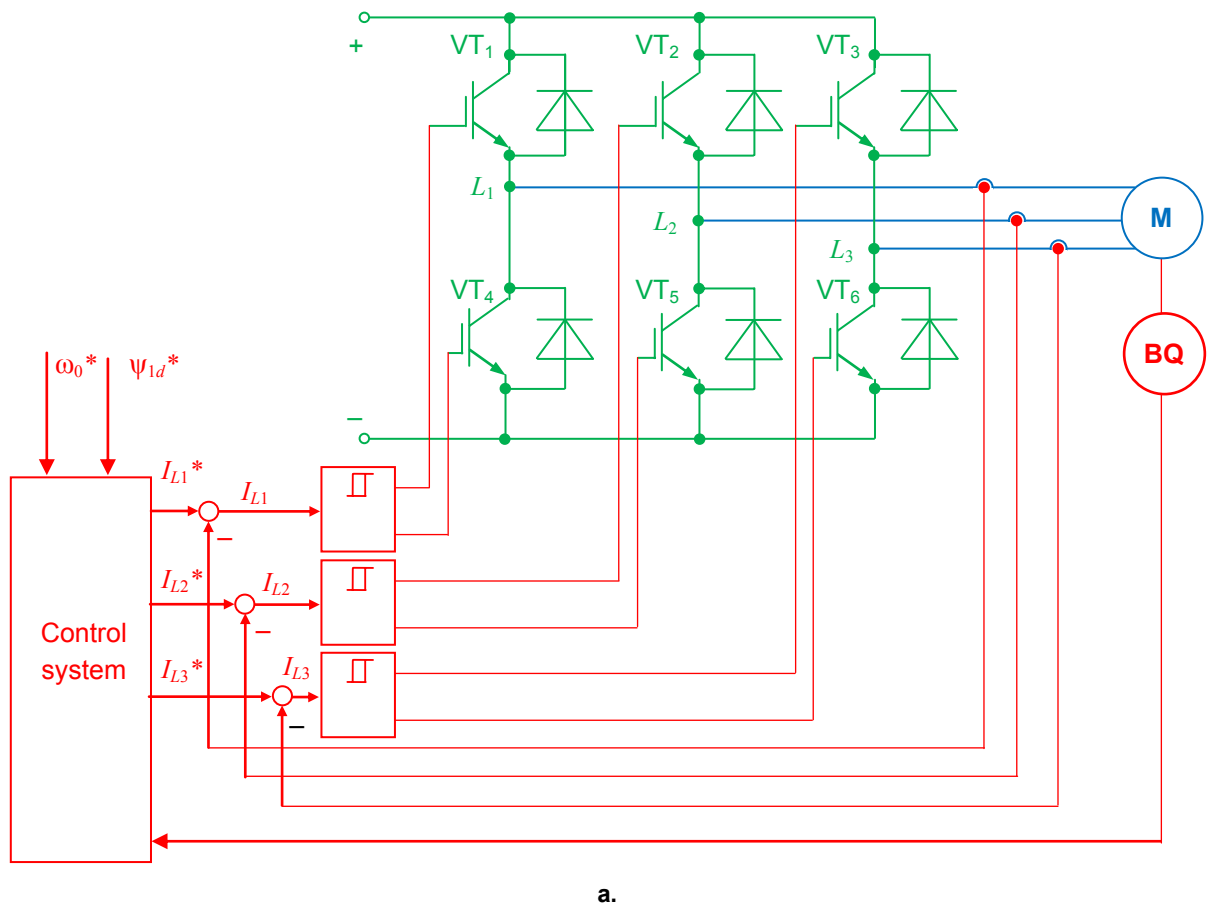
5.2   Synchronous servo drive

Benefits of servomotors. Since the synchronous motor spins at the synchronous speed at all loads, an open-ended speed control scheme may suffice for some applications, such as fans, compressors, etc.

Unlike the common-mode FESM, the PMSM have numerous advantages, like best efficiency and compact design due to the use of rare-earth magnetic system. They are widely used in high performance variable-speed close loop servo drives. To provide these benefits, the servo drive is composed by the PMSM with the built-in position encoder, external inverter and controller that jointly support the load angle $\theta = \dfrac{\pi}{2}$ between the stator current vector and the rotor flux linkage vector similarly to the dc motor as shown before in Fig. 5.1 (d).

Following (5.1), an electromagnetic torque of the synchronous motor is defined as the product of the effective flux and the orthogonal component of the stator current. Thanks to $\theta = \dfrac{\pi}{2}$, the demanded motor torque will be produced at the minimal stator current. Such motor model can be presented by the following equation system:

$$\psi_{1d} = L_{12d} I_{\Phi}, \ \ \psi_{1q} = L_{1q} I_{1q}, \ \ \psi_{\Phi} = L_{\Phi} I_{\Phi},$$
$$U_{1d} = s L_{12d} I_{\Phi} - \omega_1 L_{1q} I_{1q},$$
$$U_{1q} = \left(R_1 + s L_{1q} \right) I_{1q} + \omega_1 L_{12d} I_{\Phi},$$
$$T = m_1 p \psi_{1d} I_{1q}.$$

Circuit diagram of servo drive. The operation principle of the servo drive is expanded by the functional circuit and diagrams in Fig. 5.2.
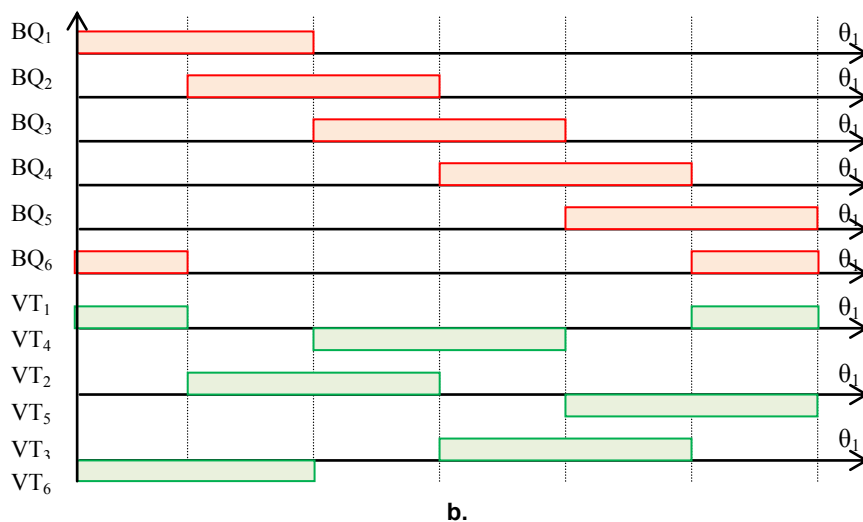

a.

b.

Fig. 5.2 Functional circuit and performance diagrams of synchronous servo drive

The stator supply of the servomotor is similar to that of the induction machine, therefore the uniform power converters are designed often for both kinds of ac motors. The dc supplied typical three-phase VSI includes the power switches VT_1... VT_6 and the freewheeling diodes which sinusoidal signals initialize the motor phase currents of the required frequency. The negative feedbacks of the momentary stator currents are arranged. The set-points I_{L1}^*, I_{L2}^*, I_{L3}^* are compared with the actual currents I_{L1}, I_{L2}, I_{L3} measured by the current sensors. Their differences enter the hysteresis current regulators, the outputs of which may obtain just two logical states, 1 or 0. The active state (1) switches the corresponding forward transistor on and the reverse transistor off, whereas at the passive state (0) switches the forward transistor off and the reverse transistor on. While the forward transistor is off, the phase current falls. Since the current riches the minimum permissible level, the hysteresis current regulator will change its state and switches the forward transistor on while the reverse transistor becomes off. As a result, the phase current starts to grow. Since the current riches up the maximum possible level, the hysteresis regulator changes the state again and switches the forward transistor off while the reverse transistor is on, causing the phase current to decrease. Using this *sliding control* mode, the cycle repeats and the phase current follows the reference signal with a delay dependent on the hysteresis width.

The aim of the control system is to derive the current torque of the motor. This means the stator field must always lead by 90˚ when the drive is motoring and lag by 90˚ when it is regenerating. Herewith, the stator field is to be forward shifted in the motoring mode or backward shifted in the regeneration mode with respect to the rotor position. To be able to drive a servomotor with a maximum possible torque and to hold the load angle θ near 90˚ electrical, the control system adds 90˚ to or subtracts 90˚ from the value of the position angle, according to the direction of rotation and the direction of torque and calculates the associated torque. To this aim, the rotor of the motor M is coupled with the rotor position encoder BQ fitted on the motor shaft in such a way that the starting lag angle between the stator and the rotor MMF is 120˚ and the ending lag angle is 60˚. Therefore, the rotor position encoder senses the rotor displacement angle.

To "rotate" the stator field by assigning its magnitude and direction, the corresponding position of the stator rotating field is determined for each rotor position as following. The rotor position encoder generates the signals $BQ_1...BQ_6$ as the timing diagram in Fig. 5.2 (b) shows.

These signals arrange a three-phase system of rectangle pulses within the period 2π. The sequence order of these pulses depends on the required rotational direction. To determine the rotation angle precisely, a "home" pulse (*z-phase pulse*), that is the pulse generated once per the encoder turn, provides the zero crossing presented as a reference point. Further, continuously measured rotor position θ is used as the torque feedback signal shown in the circuit diagram in Fig. 5.2 (a).

Switching algorithm. The switching algorithm may be different, for example the traditional six-step scheme is popular, in which case the transition occurs every 60° of the shaft turn, or the more sophisticated SVM algorithms can be used. At that, the torque rises from $\theta = 60°$ to $\theta = 90°$ and then drops until $\theta = 120°$. Then, the switching occurs and the process repeats. As a result, the average load angle is

$$\theta = \frac{120° + 60°}{2} = 90°$$

and the average torque value on the angle diagram of Fig. 5.1 (c) is given by

$$T = \int_{\frac{2\pi}{3}}^{\frac{\pi}{3}} T_{max} \sin \theta \, d\theta = \frac{3}{\pi} T_{max}$$

.

The torque and the speed have a pulsing character the frequency of which depends on the rotor speed of rotation.

To provide the current flow in the stator according to the torque requirements, the control signals are then multiplied by the signal of the speed regulator. Thus, using the high resolution signals from the encoder the sine-shape motor currents are generated by electronic arrangement. This results in a very smooth, precise running of the motor and in a high quality control.

Operating speeds of up to 50000 rpm are possible. In the case of multi-pole motors the electronic components can limit the speed, since more commutation cycles must be run through per motor revolution. The maximum speed is selected with service life considerations of the ball bearings at the maximum permissible residual unbalance of the rotor. Together with the electronic components, the servomotor achieves service life of several tens of thousands of hours.
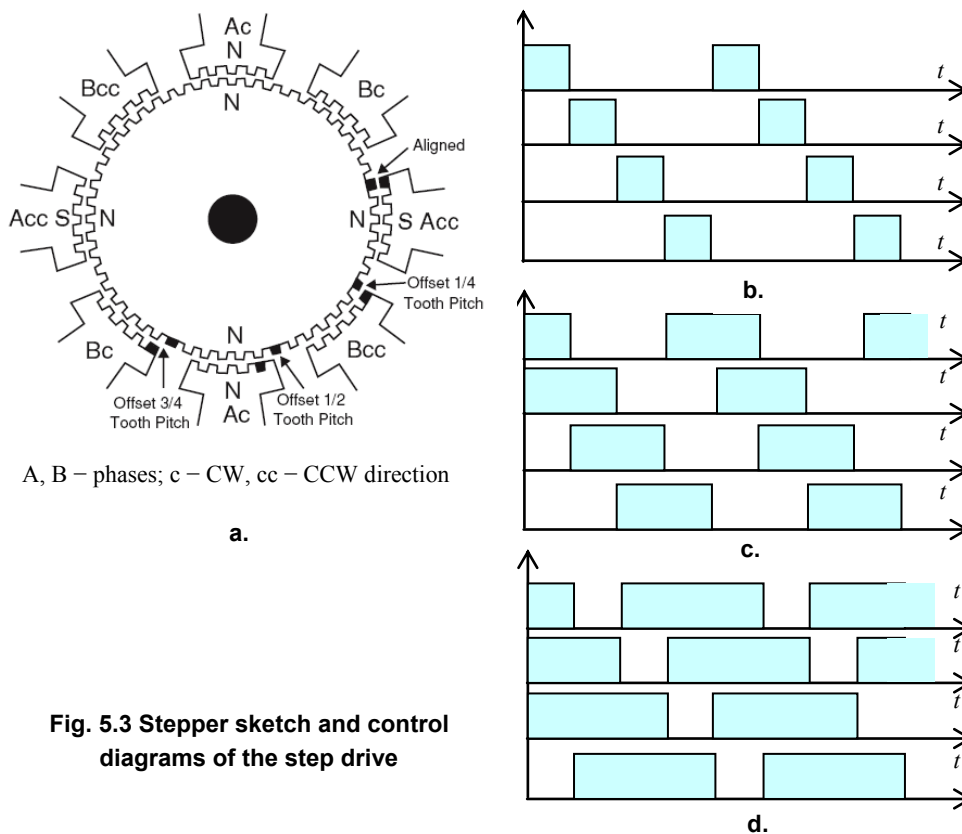
5.3 Step motor drive

Application area. A step motor, or *stepper*, is the synchronous small power machine destined for the tracing and positioning. This electromechanical actuator converts digital inputs to analog motion through the controller electronics. There are various types of step motors such as solenoid activated, variable reluctance, PM and synchronous inductor. Step motor normal operation consists of discrete angular motions of uniform magnitude rather than continuous motion. It is particularly well suited to applications where the controller signals appear as pulse trains. One pulse causes the motor to increment one angle of motion. The normal steppers have an accuracy of 3 to 5 % of the step value without error accumulation. Most step motors are used in an open-ended system configuration, which can result in oscillations. To overcome this, either complex circuits or feedback is employed thus resulting in a close loop system.

As compared with other electric drives, the step drive is possessed the structural simplicity, the broad speed range, and the small static error within the single step. Because of the sensorless, gearless, and brushless construction, this drive is of high reliability. Other advantages concern the possibility of the very low speed development upon the loads directly connected to the motor shaft because, unlike the collector motors, the step motors produce the maximum torque at the low speeds and do not operate at overspeeds. Its energy consumption does not depend on the load.

At the same time, the stepper open-ended system speed of response is limited because of possible stability lost in transients. Such drive has high sensitivity to oscillations of the moment of inertia and the static torque. It undergoes the resonance and can lose the position control without the feedback. Its application area is limited by the small power systems of mean accuracy, usually about one kilowatt.

Commutation. The stepper rotor rotates in the strong concordance with the number of the set-point pulses and stops at overtorque. The sketch of the stepper design is shown in Fig. 5.3 (a). Its toothed rotor of the variable magnetic resistance is manufactured from the soft electrotechnical steel without magnetization. The stator pole endings are also toothed. The ratio between the step and the teeth numbers are selected in the way that the small shift occurs between the stator teeth and the non-excited pole teeth. As the voltage is applied to the winding, the rotor seeks the closed flux position and its teeth stops opposite the current-flowing poles. Therefore, to rotate the rotor the motor phases must be switched alternately.

A, B − phases; c − CW, cc − CCW direction

a.

Fig. 5.3 Stepper sketch and control diagrams of the step drive

The 2-, 3- and 4-phase steppers are supplied from the pulse controller which includes the pulse commutator and the winding power amplifiers. The resulting rotor angle corresponds to the number of commutations of the stator winding whereas the rotation direction is defined by the commutation order, and the angular speed depends on the switching frequency. Thanks to the commutator, each control pulse dislocates the corresponding pole thus exiting the synchronisation torque which rotates the rotor to the position of the maximum flux linkage.

The pulse commutator can operate at different algorithms, such as alternate, pair, or synchronous switching. The alternate switching (Fig. 5.3 (b)) produces the minimum consumed power. At pair commutation (Fig. 5.3 (c)) as the regular pulse comes, one of the windings is switched off but the adjacent winding is switched on. This is the most popular mode which provides higher efficiency, better damps the transients, and has the simpler control architecture. The synchronous tapping of the three adjacent windings (Fig. 5.3 (d)) provides an effective stepper operation at the inertial load thanks to the improved stability in the resonant frequency band.

Performance indexes. The stepper performance is designated by the main indexes. The important static indexes are a *step* $h = \dfrac{2\pi}{m_1}$ that is the field rotation at the sole pulse where $m_1 \le 2p$ is the commutation number per the rotor turn and discreteness measured by the *positioning angle* $\varphi_L = \dfrac{2\pi}{m_1 z}$,, where z is the rotor teeth number. The stepper dynamic performance is described by *acceleration performance* $f_{\max}$ that is the maximum permissible frequency change at which the loaded motor keeps its stability. Usually $f_{\max} = 2$ to 20 kHz.

6   Squirrel-Cage Induction Motor Drive

6.1   Models of induction motor

Passport data. AC motors are used worldwide in many applications. There are many types of AC motors, but this chapter focuses on induction motors, the most common type of motor used in industrial applications. The motors of this type may be part of a pump or fan or connected to some other form of mechanical equipment such as winders, conveyors, or mixers.

The specific data of a *squirrel-cage motor* are the frame size, rated power, cyclic duration factor, rated speed, current and voltage, power factor, enclosure, mass, and thermal class. This information is given on the motor *rating plate* and is relates to an ambient temperature of 40˚C and an installation altitude of at most 1000 meters above sea level.

As given by (4.5), the synchronous speed of ac motors depends on the pole numbers and for f_1 = 50 Hz the speeds are listed in Table 6.1.

Speed	Pole pair number, p						
	1	2	3	4	6	8	12
n_0, rpm	3000	1500	1000	750	500	375	250
ω_0, rad/s	314	157	105	78	52	35	26

Table 6.1 Synchronous speeds of ac motors

The squirrel-cage motors with one fixed speed are generally designed as 4-pole machines as the 2-pole motors produce excessive noise and reduce the service life of the gear unit. The motors with higher pole number of the same power are of a larger volume and, due to unfavorable efficiency and power factor as well as the higher price, are not as economical.

Slip. At any given point in time, the magnetic field for the induction motor stator windings is exerting forces of attraction and repulsion against the rotor bars. This causes the rotor to rotate, but not exactly at the synchronous speed. After (4.5), the rated speeds of the synchronous motor n_M, ω_M at the rated power P_M in the motoring mode are always less than the synchronous speeds n_0, ω_0. The difference between the synchronous and actual speeds is called a *slip*, which is defined as

$$S = \frac{\omega_0 - \omega}{\omega_0} = \frac{\omega_2}{p\omega_0} \tag{6.1}$$

Thus, the slip is expressed through the slip speed as a fraction of the synchronous speed, often presented in percent. The slip is zero at the synchronous speed and unity at zero speed. With small drive systems, less that of 0.5 kW output power, the rated slip is approximately of 10 %, while the larger drives have the slip of 2…5 %.

Reflection of rotor data to stator. As a rule, the rotor variables are reflected to the stator axes. For this purpose, recalculation is made resulting in the reflected (referred) EMF E_2, currents I_2, inductances L_2, and resistances R_2 of the rotor windings,

$$E_2 = k_E E_{2M} \; ; \; I_2 = k_I I_{2M} \; ; \; R_2 = k_Z R_{2M} \; ; \; L_2 = k_Z L_{2M}$$

Therefore, the electromagnetic power, losses, and consumed power in the reflected and in the source machines are equal. In these formulae, $k_E = \dfrac{k_{w1} w_1}{k_{w2} w_2}$ is the *EMF reflecting factor*; $k_I = \dfrac{m_2}{m_1 k_E}$ − current reflecting factor; $k_Z = \dfrac{m_1 k_E^2}{m_2}$ − impedance reflecting factor; k_{w1}, k_{w2} − stator and rotor winding factors. An index M relays to the motor rated data. The reflected values are usually presented in the vendors' datasheets.

Dynamic model. The dynamic model of the stator-supplied induction motor without rotor supply is normally presented in the stator reference frame (α, β) rotated with the angular frequency ω₁ (Fig. 4.1 (b)). To build this model, replace (*x, y*) with (α, β), ω_k with ω₁, and $U_{2x,y}$ with zero in (4.2):

$$\begin{aligned}
U_{1\alpha} &= R_1 I_{1\alpha} + s\psi_{1\alpha} - \omega_1 \psi_{1\beta}, \\
U_{1\beta} &= R_1 I_{1\beta} + s\psi_{1\beta} + \omega_1 \psi_{1\alpha}, \\
0 &= R_2 I_{2\alpha} + s\psi_{2\alpha} - \omega_2 \psi_{2\beta}, \\
0 &= R_2 I_{2\beta} + s\psi_{2\beta} + \omega_2 \psi_{2\alpha}.
\end{aligned} \qquad (6.2)$$

Example. An example of the computer simulation is given in Fig. 6.1 for the following data: $L_1 = 6.24$ mH, $L_2 = 10.7$ mH, $L_{12} = 189$ mH, $R_1 = 1.66$ Ω, $R_2 = 1.27$ Ω, $p = 2$, $m_1 = 3$, $J = 0.108$ kgm². The equation system has been solved here by the fourth-order Runge-Kutta's method with a step of 100 μs. The stator mains supply was modelled by the symmetrical orthogonal system of harmonic voltages:

$$U_{1\alpha} = U_{1\max} \cos(\omega_1 t)$$
$$U_{1\beta} = U_{1\max} \sin(\omega_1 t)$$

where $U_{1\max}$ is an amplitude of the stator phase voltage and t is a time. By changing the parameters and inputs in simulation, the electrical motor transients may be displayed and optimized.
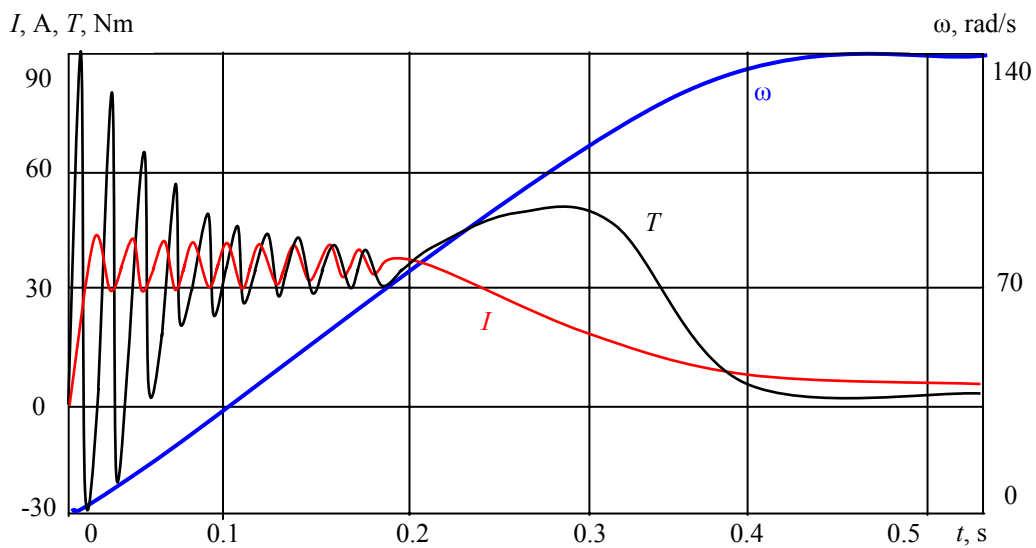

Fig. 6.1. Transients of induction motor

Scalar model. To analyze the steady-state processes in respect to the rms values, the balanced multiphase system is treated on a per-phase basis wherefore the variable flux linkages are excluded from (6.2), and the full phase reactances X are examined instead of inductances. Herewith, $X_1 = \omega_1 L_{1\sigma}$ is the stator phase leakage reactance, $X_2 = \omega_1 L_{2\sigma}$ – the rotor phase leakage reactance, referred to the stator, and $X_{12} = m_1 \omega_1 L_{12}$ – the exciting reactance. Upon these assumptions, the scalar model of the separate motor phase is as following:

$$U_1 = R_1 I_1 + X_1 I_1 + X_{12} I_{12},$$
$$0 = \frac{R_2}{S} I_2 + X_2 I_2 + X_{12} I_{12}. \tag{6.3}$$

Replacement circuit. The T-shape replacement circuit for this model is presented in Fig. 6.2 (a).
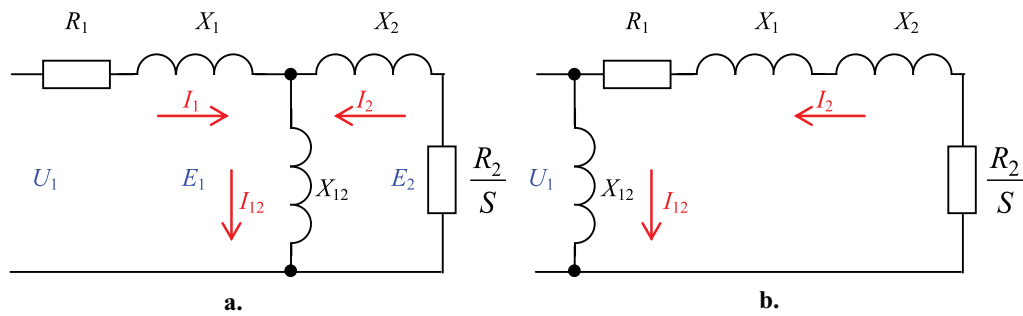
Fig. 6.2. Replacement circuits for the single phase of induction motor

Here, the left-hand loop describes the steady state of the stator phase, the right-hand loop – the state of the rotor phase, whereas the magnetizing current $I_{12} = I_1 + I_2$ serves as the source of the rotation EMF $E_1 = -E_2$. The effective flux linkage in the air gap is as follows:

$$\psi_{12} = L_{12}I_{12} = \frac{2X_{12}I_{12}}{m_1\omega_1} \qquad (6.4)$$

The brunch $\dfrac{R_2}{S}$ displays the motor active resistance resulted from the slip. While this component is presented in the equivalent circuit, it is a fictional resistor which does not truly represent the electrical behavior of the motor. Such model is suitable for the motor analysing at the fixed rotor, which active resistance emits an *air-gap power*.

Space vectors and vector diagram. The vector diagram of the motor phase drawn in Fig. 6.3 geometrically interprets the above mentioned components in the particular time instant. Here, the space vectors of a separate phase present the geometric sums of the phase vectors. Their magnitudes are of 1.5 times the phase rms values and the angles display the phase shifts in this time.
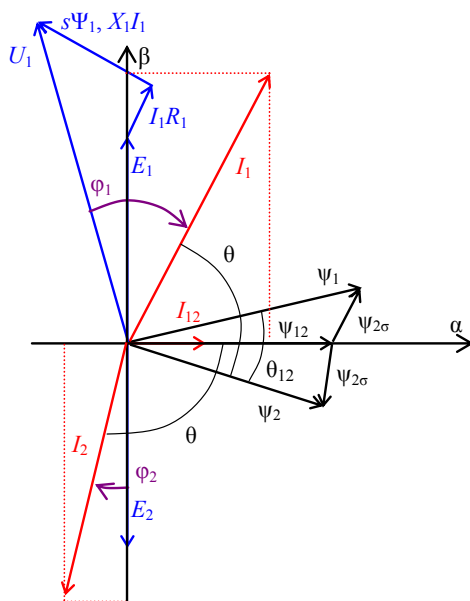
Fig. 6.3. Vector diagram of induction motor

In the diagram the following vectors are shown:

$I_{12} = I_1 + I_2$ – the vector of the magnetizing current;

$\psi_{12} = \psi_1 - \psi_{1\sigma} = \psi_2 - \psi_{2\sigma}$ – the vector of the effective flux linkage created by the magnetizing current in the air gap;

$\psi_{1\sigma} = L_{1\sigma}I_1,\ \ \psi_{2\sigma} = L_{2\sigma}I_2$ – the vectors of the flux leakages at the phase leakage inductances $L_{1\sigma} = L_1 - L_{12}$ and $L_{2\sigma} = L_2 - L_{12}$;

$\cos\varphi_1 = \dfrac{R_1}{Z_1}$ – the power factor which defines the mutual disposition of U_1 and I_1 for the complex stator reactance Z_1;

θ – the load angle;

θ_{12} – the angle between the stator and rotor fluxes.

Here, an applied voltage U_1 excites both the stator current I_1 and the rotor current I_2. Each current has two components. Their *real* (*active*, β) *components* are defined by the load. These components participate in the *torque T* and *EMF E_1* and E_2 *producing*. Vector E_1 of the stator EMF follows U_1. Vector E_2 of the rotor EMF has the opposite direction and the rotor current I_2 follows E_2. The *imaginary* (*reactive*, α) *component* of the magnetization current $I_{12} = I_1 + I_2$ creates an effective flux linkage ψ_{12} in phase with I_{12} along the α direction. This reactive *flux-producing component* enlarges the full current and heats the induction motor, especially at low speeds. The stator and rotor flux linkages ψ_1 and ψ_2 differ from ψ_{12} by the *leakage* flows $\psi_{1\sigma} = L_{1\sigma}I_1$ and $\psi_{2\sigma} = L_{2\sigma}I_2$. The induced EMF in the stator phase E_1 leads the flux vector by 90°. The rotor current I_2 lags the EMF by the phase angle φ_2. The stator phase current I_1 is the vector sum of I_2 and I_{12}. All the rotor quantities shown in the vector diagram are referred to the stator.

The vectors rotate in time and the *vector model* describes this rotation. In transients, the vector magnitudes and their mutual disposition change. Actually, the stator of the induction motor plays the role of both the armature and the inductor. As both the current components intercommunicate, the change of one of them changes another component.

6.2   Performance characteristics

Speed-current characteristic. To simplify the steady-state analysis, consider the effective flux linkage in (6.4) as the stabilized value at the fixed magnetizing current,

$$\psi_{12} = \Phi = \text{const},\ I_{12} = \text{const}.$$

In this case, the T-shape circuit diagram may be replaced by the L-shape circuit shown in Fig. 6.2 (b). Here, the magnetizing current I_{12} does not depend on the slip. Now

$$I_2 = \frac{U_1}{\sqrt{\left(R_1 + \dfrac{R_2}{S}\right)^2 + X_b^2}},\ \ I_1 = I_{12} - I_2 \tag{6.5}$$

where $X_b = X_1 + X_2$ is the *short circuit reactance* of the machine.

Because of (6.1), the relationships between the slip S and the currents I_1, I_1 represent the static electromechanical characteristics $\omega(I_1)$, $\omega(I_2)$ (speed-current curves) of induction drive. The diagrams in Fig. 6.4 (a) depict:

   ω_L – the *steady-state speed* of the motor referred to the load operating torque T_L and *operating current* I_L;

I_d – run-up current;

ω_0 – synchronous speed.
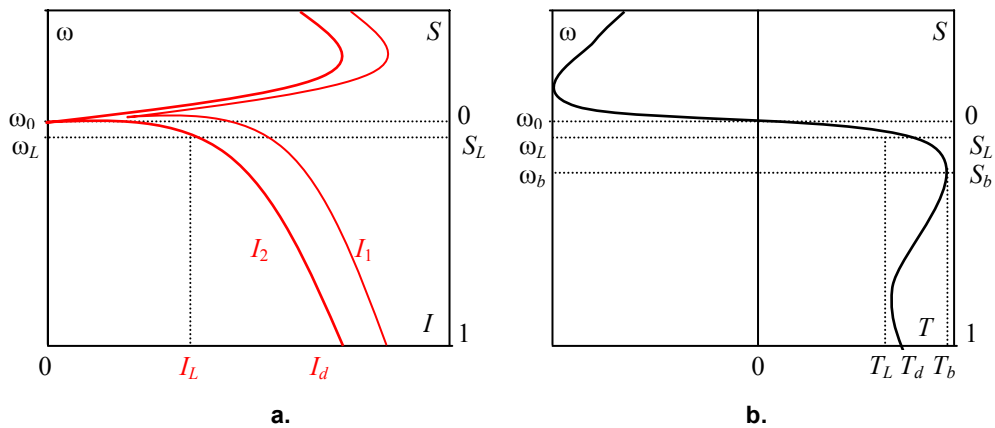

a.　　　　　　　　　　　　　　　　　**b.**

Fig. 6.4 Electromechanical and mechanical characteristics

While $I_{12} \approx \mathrm{const}$, the curve $\omega(I_1)$ is very similar with the graph $\omega(I_2)$. This is not true at no-loading and running modes.

Idle and running modes. At no-loading,

$$S = 0, \ \omega = \frac{\omega_1}{p}, \ E_2 = 0, \ \omega_2 = 0, \ I_2 = 0$$

the machine consumes energy of the magnetizing current $I_{12} = I_1$ from the mains only. In this mode of operation the rotor windings do not cross the force lines of the magnetic field, that is $U_1 = E_1$. In the replacement circuit this mode is presented by the broken rotor loop.

The negative slip is possible also. It means that the machine is spinning at the speed higher than the synchronous speed implying the generator mode of operation.

At running

$$S = 1, \ \omega = 0, \ \omega_1 = \omega_2, \ \varphi_2 \to \max, \ I_2 \to \max, \ I_1 \to \max, \ I_{12} \to \min.$$

The run-up current, also referred to as the *starting current* or the *locked rotor current* is as follows:

$$I_d = \frac{U_1}{\sqrt{(R_1 + R_2)^2 + X_b^2}}.$$

This current given in the vendors' datasheets will supply the motor when the rated voltage is initially applied to the rotor at rest.

Usually, it is of 4…8 times higher than the rated current supplied the motor with the rated voltage U_M, frequency f_1, and load T_M. Knowledge of the current requirements for a motor is critical for the proper application of overcurrent protection devices.

Electromagnetic power. Analyze now the motor *electromagnetic power*. In the motoring mode (Fig. 6.4 (a)), the electromagnetic power P_2 results from the motor supply power P_1, with the deduction of slight *stator copper losses* $\delta_1 = m_1 I_1^2 R_1$ and core losses $\delta_{12} = \dfrac{m_1 E_{12}^2}{R_{12}}$. Since the reactances do not consume any average power, the total power absorbed by the rotor is as follows:

$$P_2 = \frac{m_1 I_2^2 R_2}{S}.$$

A part of P_2 dissipates as *rotor copper losses* $\delta_M = P_2 S = m_1 I_2^2 R_2$ which are considered as major motor losses, and the remainder is transmitted as the developed *real power* $P = P_2(1 - S)$. Thereby, the consumed motor power is as follows:

$$P_1 = m_1 U_1 I_1 \cos\varphi_1 = \delta_M + \delta_1 + \delta_{12} + P$$

where $m_1 U_1 I_1$ is the *apparent power*.

Motor efficiency may be calculated as follows:

$$\eta_M = \frac{P}{P_1} \approx 1 - S.$$

Download free eBooks at bookboon.com

Speed-torque characteristic. Proceed from the electromagnetic power to the electromagnetic torque,

$$T_{12} = \frac{P_2}{\omega_0} \approx \frac{m_1 I_2^2 R_2}{\omega_0 S} \qquad (6.6)$$

Using the speed-current characteristic (6.4), express of the static mechanical (speed-torque) characteristic, which sets the following relation of the squared voltage, slip, and torque in the induction motor:

$$T_{12} = \frac{m_1 U_1^2 R_2}{\omega_0 S \left[\left(R_1 + \dfrac{R_2}{S} \right)^2 + X_b^2 \right]} = \frac{m_1 U_1^2}{\omega_0 S} \sin \theta . \qquad (6.7)$$

Taking into account (4.6), the developed torque may also be found from the vector diagram as a product of the effective flux linkage Ψ_{12} and the projection of the rotor current vector on the rotor EMF axis:

$$T = m_1 p \psi_{12} I_2 \sin \theta . \qquad (6.8)$$

Because the motor torque varies with speed, the speed-torque relationship is usually shown in a speed-torque curve which shows the motor torque as a fraction or percentage of the full-load torque over the motor full speed range. The speed-torque diagram plotted in Fig. 6.4 (b) depicts the following:

> T_d – *run-up torque* at $S = 1$;
> T_b – *breakdown torque*, called also a *pull-out torque*;
> S_b – *breakdown slip*;
> ω_b – *breakdown speed*.

The run-up torque, also referred to as the *starting torque* or the *locked rotor torque*, is the torque the motor develops each time it starts at the rated voltage and frequency. When the voltage is initially applied to the motor stator there is an instant before the rotor turns. At this instant, the motor develops a starting torque T_d. As the motor picks up the speed, the torque decreases slightly until the *pull-up* value this is slightly lower than the starting torque, but greater than the full-load torque. As the speed continues to increase, the torque will increase to a maximum value of the full-load torque. This maximum value of torque is referred to as the breakdown torque T_b. Then the torque drops rapidly as the speed grows beyond the breakdown torque until it reaches the full-load level T_L at a speed ω_L slightly less than 100 % of synchronous speed ω_0. The full-load torque is developed with the motor operating at the rated voltage U_M, frequency f_1, and load T_M.

The run-up and breakdown torques are approximately equal to $T_d = (1...2.2) \cdot T_M$, $T_b = (1,7...3.7) \cdot T_M$ where T_M is the motor *rated torque*.

The torque is zero at zero slip, that is, at the synchronous speed, and increases approximately linearly with slip until the maximum torque is reached. Once the torque reaches its breakdown value, it decreases with the increase in slip despite an increase of the rotor current due to reduction of the air gap flux.

This is true for both the motoring and the generating modes of operation. When the motor overcomes the breakdown, it stalls and the overload protection must immediately disconnect the supply to prevent damage due to overheating.

Motors are designed with speed-torque characteristics that match the requirements of common applications. Various motor designs have different characteristics.

$$T_b = \frac{m_1 U_1^2}{2\omega_0 \left(\sqrt{R_1^2 + X_b^2} + R_1 \right)} \,.$$
(6.9)

Kloss' formula. The correlation between the electromagnetic and breakdown torques yields the following equation of the mechanical characteristic:

$$T = \frac{2T_b(1+\varepsilon)}{\dfrac{S}{S_b} + \dfrac{S_b}{S} + 2\varepsilon} \,,$$
(6.10)

known as a *Kloss' formula*. At running, while $1 < S < S_b$, T_{12} exceeds this value by $\delta T_d = (T_d - T)S$ where the run-up torque T_d is calculated using (6.7) at $S = 1$.

In the small motors, $R_1 \approx R_2$ thus $\varepsilon \approx S_b$. For the large induction machines with $R_1 << X_b$ ignoring of R_1 results in the simplified Kloss' formula

$$T \approx \frac{2T_b}{\dfrac{S}{S_b} + \dfrac{S_b}{S}} \,,$$

in which

$$\varepsilon = 0 \,, \quad T_b = \frac{m_1 U_1^2}{2\omega_0 X_b} \,, \quad S_b = \frac{R_2}{X_b} \quad .$$
(6.11)

All the above discussed simplified models are suitable for approximate electric drive analysing and engineering calculation.

6.3 Braking modes

Classification. When slowing down, the electrical motor enters the generator mode and its power flow is reversed. As soon as the supply of an induction motor is switched off, the friction forces T_L cause the *freewheel stop*, or *coasting*. As follows from (1.1), coasting without motor torque is a slow process:

$$dt = J \frac{d\omega}{T_L} \,.$$

To speed-up braking, different braking modes were developed including mechanical braking, counter-force braking (counter-current or reversing), dynamic braking called also a dc injection braking, and regenerative braking.

Mechanical braking. For many applications where relatively fast positioning is required, the motor is equipped with a mechanical brake (YB in Fig. 6.6 (a)). The brake is manufactured on the basis of the electromagnet which presses the rotated motor or mechanism shaft by the chocks. Switching of the brake is usually very fast. Thanks to mechanical braking, the mechanism stops even if the motor continuous its rotation. This is important, particularly, for the active loaded hoists, lifts, traction, and conveyer systems. The drawbacks of mechanical braking are the requirements on the permanent maintenance and improvement of the chocks, difficulty in modernisation, and heat emission at braking. Therefore, in many cases the brake is applied not for stop but for holding the mechanism fixedly.
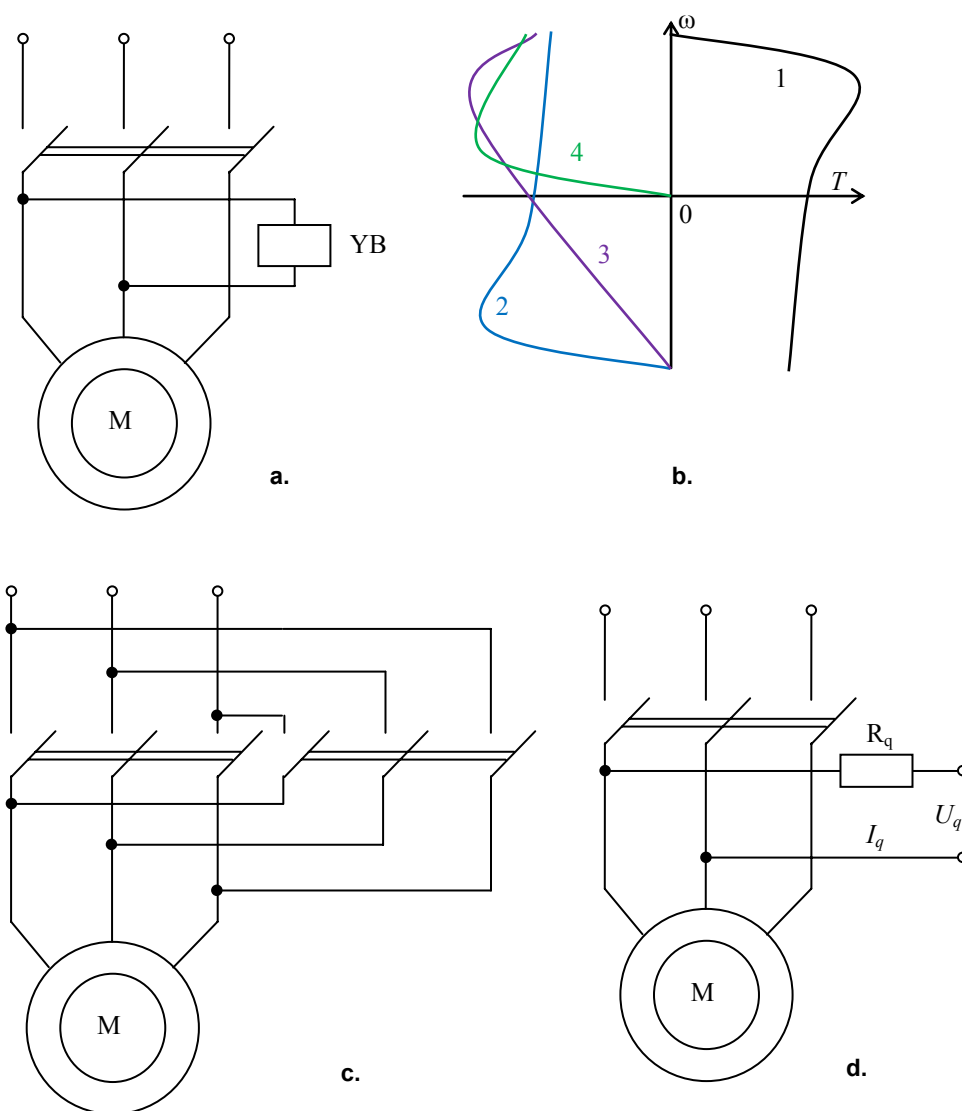

Fig. 6.6 Braking modes

Besides the applications, in which the mechanical brake is used as working brake, the *brake motors* are also used, if safety is the decisive factor. For example in hoisting applications, where the motor is brought to a standstill electrically in a specific position, the "holding brake" engages in order to secure the position. Similar safety requirements apply on the mains interruption failure where the mechanical brakes on the motors guarantee emergency stops. When the supply voltage is applied, the brakes release electrically. When switching off the supply voltage, the brakes engage automatically by spring force. In addition, the brake can be released mechanically. For mechanical release, a releasing level or a screw for fixing the brake is supplied.

Regenerative braking. Being the reversible machine, the induction motor turns its direction upon the change of the magnetic field polarity (phase order). As a convertible device, an induction machine can be employed both in the motoring and in the braking generator modes. In the regenerative braking mode, (II quadrant of the speed-torque characteristic in Fig. 3.4 and Fig. 6.4) it works at the negative slip.

Herewith the rotor turns in the same direction with the stator field but its speed exceeds the rotation speed of the magnetic field. To jump to this mode, an *active load* must be applied to the motor shaft. The regenerative mode is broadly used in the hoist electrical motors which speed, at the load lowering, can overcome the field rotation speed due to potential energy. The regenerative breakdown torque overcomes the motoring breakdown torque though the breakdown slip value remains the same.

Download free eBooks at bookboon.com

Counter-force braking. More often, a counter-force braking is applied called also a counter-current braking or a *plugging* in which the motor jumps to the IV quadrant of the speed-torque characteristic in Fig. 3.4 and Fig. 6.4 upon the significant increase of the loading torque or at reverse. Herewith, the direction of the rotor rotation is opposite to the stator field direction though, like in the motoring mode, the machine generates the counter-torque for the load. The slip exceeds 1, the current is above the run-up value, and energy is dissipated as heat. In the particular case, at $S = 1$, the induction machine keeps the transformer *locked-rotor mode*. This braking method is known also as a *counter-feed braking* or *reversing* because the polarity inversion of the running motor constitutes high mechanical and thermal loading of the machine and the connected transmission units. It is the generator mode in which the direction of the motor shaft rotation is opposite to the demanded one. To jump to this mode, the stator phases must be commutated from line 1 to line 2 in Fig. 6.6 (b) resulting in change of the torque sign and the power return to the mains (Fig. 6.6 (c)). The same effect may be obtained in the hoists when the pulled-over weight reverses the speed thus directing both the net and the motor energies to the load. Similarly to the starting, the optimal breakdown slip value may be found for this mode to provide the fastest braking. The optimal line 3 in Fig. 6.6 (b) is described as follows:

$$t_{q\,\min} = \tau_T \left(\frac{3}{4S_b} + \frac{S_b}{3} \right), \; S_{b\,\text{opt}} = \sqrt{\frac{3}{2\ln 2}} = 1.47.$$

This is the suitable mode for the wound rotor motors. As this condition cannot be met in the common-mode squirrel-cage induction motors, their counter-current braking is not time-optimal.

The counter-current braking is cheap and fast. Nevertheless, the significant drawback of this mode is high energy losses, $W \geq \frac{3J\omega_0^2}{2}$, 2...3 times overcoming the starting loss. Therefore, the counter-current braking is considered as one of the heavy modes of induction drive. Additionally, it is unreliable because since the stop point is missed, the motor runs in the reverse direction, causing the mechanism damage. At the same time, the braking torque, current and rate are heavy adjustable.

The dynamics of the motor disconnection and the following switching on the voltage of reverse phase consecution major depends on the motor commutation ability and the damping rate of the air gap magnetic field. The shorter is the commutation time, the higher are the shock currents and torques. Additional problems appear at re-switching that causes the reactive power to generate the motor fields and the active power to run the inertial masses. This obstacle limits the number of commutations per hour permissible for induction motor.

DC injection braking. To proceed to another braking method, connect the pair of the motor phases through the *brake resistor* afterwards the motor disconnection from the mains. This dynamic braking results in mechanical energy dissipation in the resistor and in other winding and steel resistances (line 4 in Fig. 6.6 (b)).

More popular is a dc injection braking mode implemented in the following way. To avoid the drop of the magnetic field at the motor disconnection, it is excited by the external dc source I_q in braking (Fig. 6.6 (d)). The dc source generates the permanent magnetic field in the stator which creates an EMF in the windings of the rotated rotor causing the braking current. Interaction of the permanent stator flux and the rotor current produces the braking torque. The motor operates as the reversible synchronous generator in which the stator serves as the field winding and the rotor is the ac EMF-producing winding. The stator resistance R_1 is usually low therefore the source voltage does not overcome 10...12 VDC. It is difficult to obtain the symmetrical stator winding connection to the dc source thus one of the typical circuits shown in Fig. 6.7 is used, usually the first or the third one.
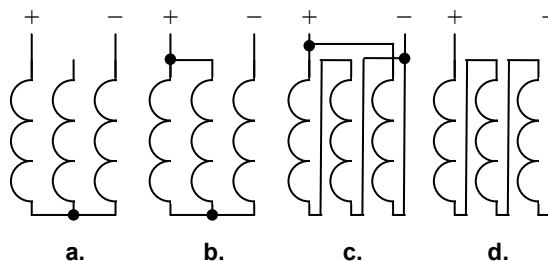

Fig. 6.7 Stator connection to dc source

The circuit characteristics are given in Table 6.2.

Circuit	I_1	I_q	R_q	U_q
a.	$\sqrt{\dfrac{2}{3}}I_q$	$\sqrt{\dfrac{3}{2}}I_1$	$2R_1$	$2\sqrt{\dfrac{3}{2}}I_1R_1$
b.	$\dfrac{\sqrt{2}}{2}I_q$	$\sqrt{2}I_1$	$\dfrac{3}{2}R_1$	$\dfrac{3}{\sqrt{2}}I_1R_1$
c.	$\dfrac{\sqrt{2}}{3}I_q$	$\dfrac{3}{\sqrt{2}}I_1$	$\dfrac{2}{3}R_1$	$\sqrt{2}I_1R_1$
d.	$\dfrac{2\sqrt{2}}{3}I_q$	$\dfrac{3}{2\sqrt{2}}I_1$	$3R_1$	$\dfrac{3}{2}\dfrac{3}{\sqrt{2}}I_1R_1$

Table 6.2 Dependences of the dc injection braking for different stator connection circuits

The replacement circuit of the dc injection braking mode shown in Fig. 6.8 (a) differs from Fig. 6.2 by the slip value which is replaced by the relative speed $S_q = \dfrac{\omega}{\omega_0}$. Here, the stator current I_1, is an MMF-equivalent of the dc field current I_q injected to the stator at braking. The rotor current

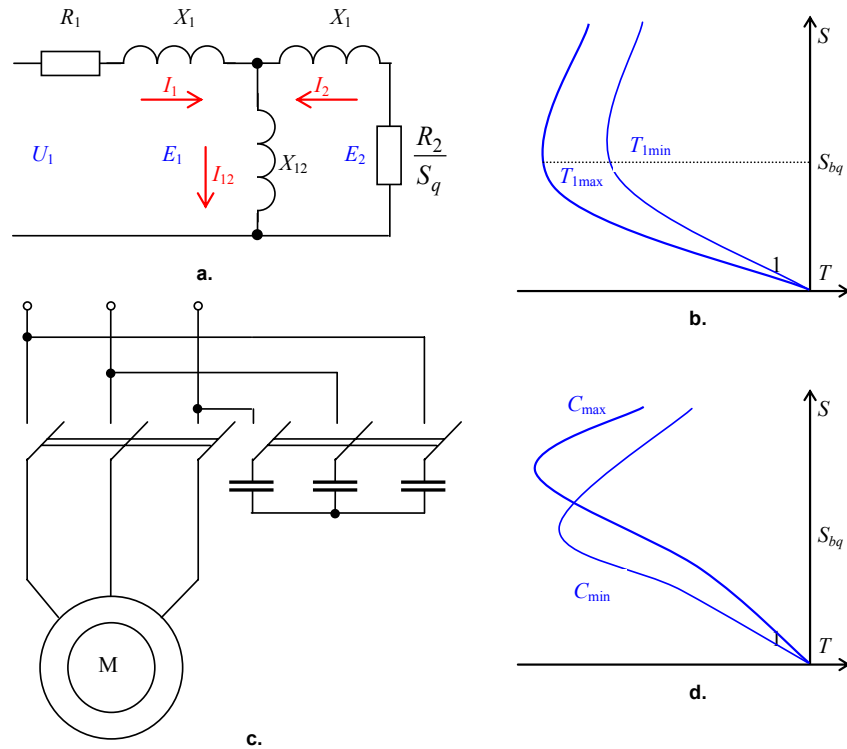$$I_2 = \frac{E_2}{\sqrt{\left(\dfrac{R_2}{S_q}\right)^2 + X_2^2}}.$$

Fig. 6.8 DC injection and capacitor braking

EMF and the rotor reactance are the frequency functions,

$$E_2 = 4.4 \ f_2 \Phi k_2 w_2, \ X_2 = 2\pi f_2 L_2, \ \omega = \frac{2\pi f_2}{p}.$$

At high speeds, while $X_2 \gg R_2$,

$$I_2 \approx \frac{4.4 \ f_2 \Phi k_2 w_2}{2\pi f_2 L_2} = \text{const}.$$

At low speeds, when $X_2 \ll R_2$, the stator current is proportional to the speed,

$$I_2 \approx \frac{4.4 \ f_2 \Phi k_2 w_2}{R_2'}.$$

Convert this equation by counting $E_2 = X_{12} I_{12}, I_{12} = I_1 - I_2$,

$$I_2 = \frac{X_{12} I_1}{\sqrt{\left(\dfrac{R_2}{S_q}\right)^2 + (X_2 + X_{12})^2}}.$$

By substitution of I_2 to the torque expression, obtain the following mechanical characteristic:

$$T = \frac{m_1 I_1^2 R_2}{\omega_0 S_q} \approx \frac{2 T_{bq}}{\dfrac{S_{bq}}{S_q} + \dfrac{S_q}{S_{bq}}}$$

where $T_{bq} = \dfrac{m_1 I_1^2 X_{12}^2}{2\omega_0 (X_{12} + X_2)}, S_{bq} = \dfrac{R_2}{X_{12} + X_2}$. Mechanical characteristics of the electric drive in the dc injection braking mode are shown in Fig. 6.8 (b). The most effective this braking is at the increased rotor resistance, at $S_{bq} = 0.41$. Unlike the counter-feed braking, there is no danger of self-reversing in this mode. It is easy in maintenance, tuning, servicing, and the braking rate control. Nevertheless, the dc source increases the drive mass and weight, whereas the braking effect fails as the speed drops. Besides, as the motor overheating is possible, it is prohibited more than 4…6 stops per hour in some machines.

In power converters from Siemens this method is combined with regeneration resulting in so-called *compound braking* for small power systems with low motor efficiency.

Capacitor braking. An additional dc source for dc braking can be replaced with the capacitor battery (Fig. 6.8 (c)). Since the capacitors are connected, the resonance arises along with intensive self-exciting and EMF growing. As the accompany current demagnetizes the motor, an initially intensive braking gradually fails (Fig. 6.8 (d)). This mode of the *capacitor braking* is considered as more reliable than the dc injection braking. Nevertheless, it can be employed only if the rotor moment of inertia overreaches the mechanism inertia. Additionally, it is difficult to control the braking torque here, and the limited capacity prevents its use in applications above 5…15 kW. Therefore, in practice, for example in ALTIVAR, the combined capacitor-dc braking systems are used where the braking starts in the capacitor mode and completes at the dc supply. This approach increases efficiency and lowers losses.

In adjustable converter-fed drives, the programmable *controlled stop* is applied. The braking program sets the slow coasting, fast stop with mechanical braking, or smooth deceleration at multiple laws. The reduced adjustable frequency produces regeneration in the second quadrant of the mechanical characteristic with energy reimbursement to the supply network.

7   Special Types of Induction Motor Drives

7.1   Pole-changing

Pole-changing motor. A *pole-changing motor* called also a *multispeed motor* or a *change-speed motor* is the proper solution of the cheap variable speed drive systems. These motors are frequently used as travel and hoist drives where the high speed is used as rapid traverse whereas the low speed is applied for positioning.

Using the known equation (4.5) $\omega_0 = \dfrac{2\pi f_1}{p}$ the speed ω may be controlled by adjustment of the pole pair number *p*. The pole-changing motors are manufactured with consequent poles, of two-, three- and four speeds. In order to switch the pole pairs in the ratio of 1:2, the winding of each phase is divided by two sections (Fig. 7.1 (a), star and delta connections, $p = 4$). By changing the current direction in a section, the pole number changes. Usually two-speed motors have one such winding, three-speed machines have two windings one of which allows switching, and four-speed motors have two switching windings. As the pole-changing motors have the squirrel-cage construction, the poles are commutated in the stator.
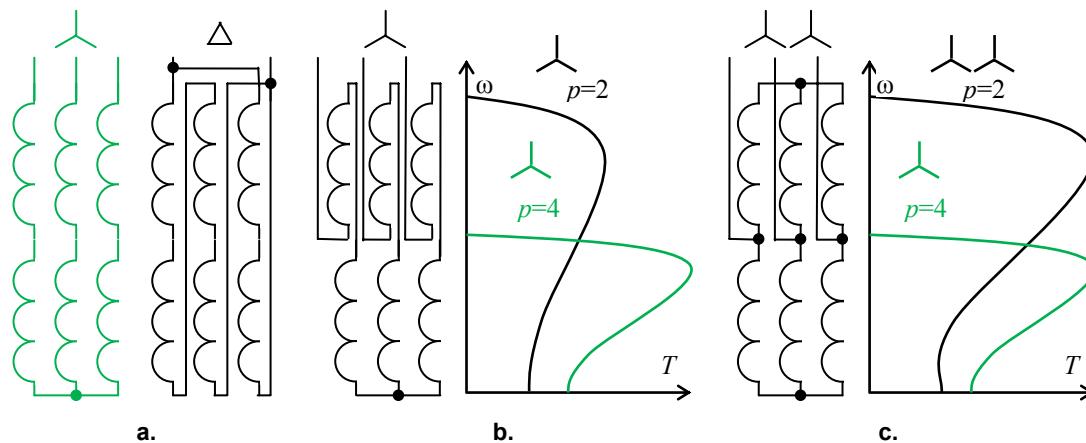
Fig. 7.1 Commutation of pole-changing motor

Connection diagrams. Fig. 7.1 (b, c) illustrates pole pair commutation by the change of the *connection diagram*. By the series connection of two sections, four pole pairs are obtained (Fig. 7.1 (a), star connection, $p = 4$). As soon as the current direction is changed in the upper sections (star connection, $p = 2$), the pole number decreases twofold thus causing the increase of the synchronous speed and the drop of the breakdown torque (6.9), $T_b \approx \dfrac{m_1 U_1^2}{2\omega_0 X_b}$, at the constant machine power.

In the case of parallel section connection, the same two pole pairs are obtained (double star connection, $p = 2$). Herewith, the torque T_b seems to be halved. But, thanks to doubling of the number of stator windings, the consumed power twofold increases and the torque holds its value.

Complicated structures, significant mass and size, commutations in power circuits, and the step character of the speed control are the drawbacks of these machines that restrict their application area.

Braking methods. For the pole-changing motors the same braking methods are used as for the common-mode squirrel-cage motors. Besides, in electric drives built on these motors the regenerative braking is often applied to return energy to the mains. The most effective instant for regeneration is the pole number increasing because the braking torque promotes fast transition to the lowering speed. Nevertheless, for at all, this mode does not provide the overall motor stop. Therefore many companies, to decrease the torque inrush at pole commutation, use electronic soft-switching devices which disconnect a phase before commutation and connect it again after switching.

Example. In Fig. 7.2 the circuit diagram of the hoist mechanism with a pole-changing motor is presented. The circuit includes the normally pressed break YB, the linear *contactor* KM1, two direction contactors KM2 and KM3, the speed commutation contactor KM4, the *time delay relay* KT, two *stroke-end switches* SQ1 and SQ2, two direction buttons SB1 and SB2, and two speed commutation buttons SB11 and SB21. The low speed motor winding is supplied through the contacts KM1…KM4 as soon as one of the buttons SB1 or SB2 is pressed. Contactor KM4 is supplied through SB11 or SB21. At staring it changes the low speed by the high speed upon the control of the relay KT.
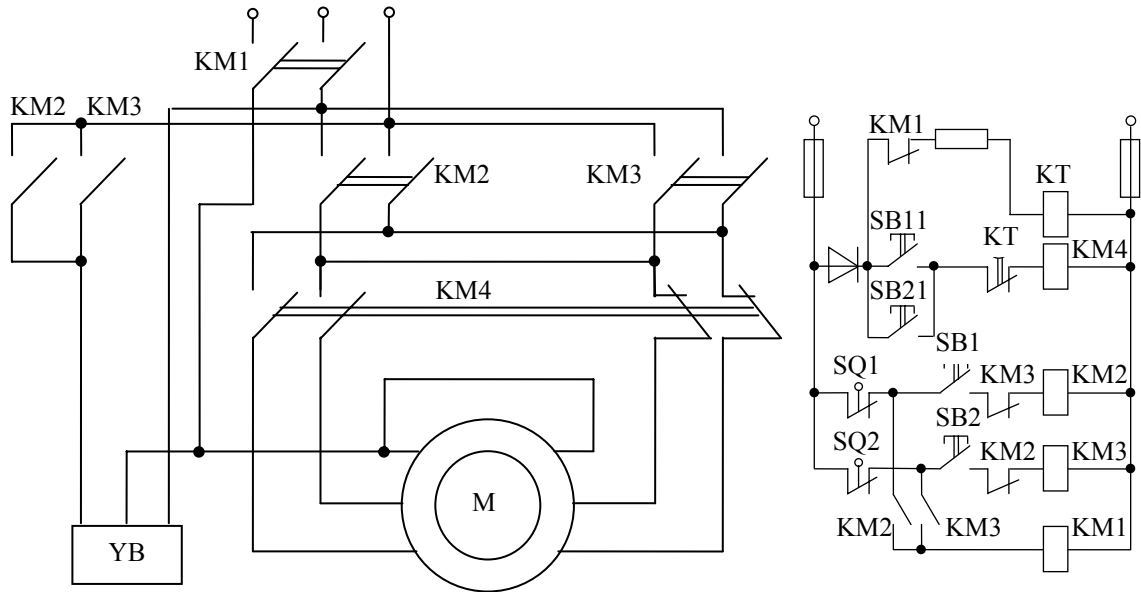
Fig. 7.2. Hoist electric drive with pole-changing motor

7.2   Wound rotor induction motor drive

Rheostat control. The description to this point has been centered on the squirrel cage induction motors. Another type of the three-phase induction motor is the wound rotor machine. A major difference between the wound rotor motor and the squirrel cage motor is that the conductors of the wound rotor consist of wound coils instead of bars. These coils are connected through slip rings and brushes to external variable resistors or rheostats. The rotating magnetic field induces a voltage in the rotor windings. These machines are more expensive and bulky and less economical as compared with the squirrel-cage motors.

As soon as an increase of the rotor resistance R_2 results in the increase of the breakdown slip without T_b and ω_0 change as (6.11) shows, addition of resistors to the rotor circuit may be used to adjust the normal operating speed called a *rheostat control* or a *secondary speed control*. An increase of the rotor resistance causes less current to flow in the rotor windings, thus decreasing the rotor speed. A decrease of the resistance causes more current to flow, thus increasing the rotor speed. The speed lowering from some level ω_L to the new level ω_{Li} is accompanied by the transition to the new slip:

$$S_{Li} = \frac{\omega_0 - \omega_{Li}}{\omega_0}.$$

To perform the rheostat control, an additional resistance R_{2i} is introduced to each rotor phase as shown in Fig. 7.3 (a).

Speed-torque characteristics. Every mechanical characteristic, both the natural and the rheostat (Fig. 7.3 (b)) is described by the equation

$$T_s \approx \frac{2T_b}{\dfrac{S_L}{S_b} + \dfrac{S_b}{S_L}} = \frac{2T_b}{\dfrac{S_{Li}}{S_{bi}} + \dfrac{S_{bi}}{S_{Li}}},$$

which yields

$$\frac{S_L}{S_b} + \frac{S_b}{S_L} = \frac{S_{Li}}{S_{bi}} + \frac{S_{bi}}{S_{Li}}.$$
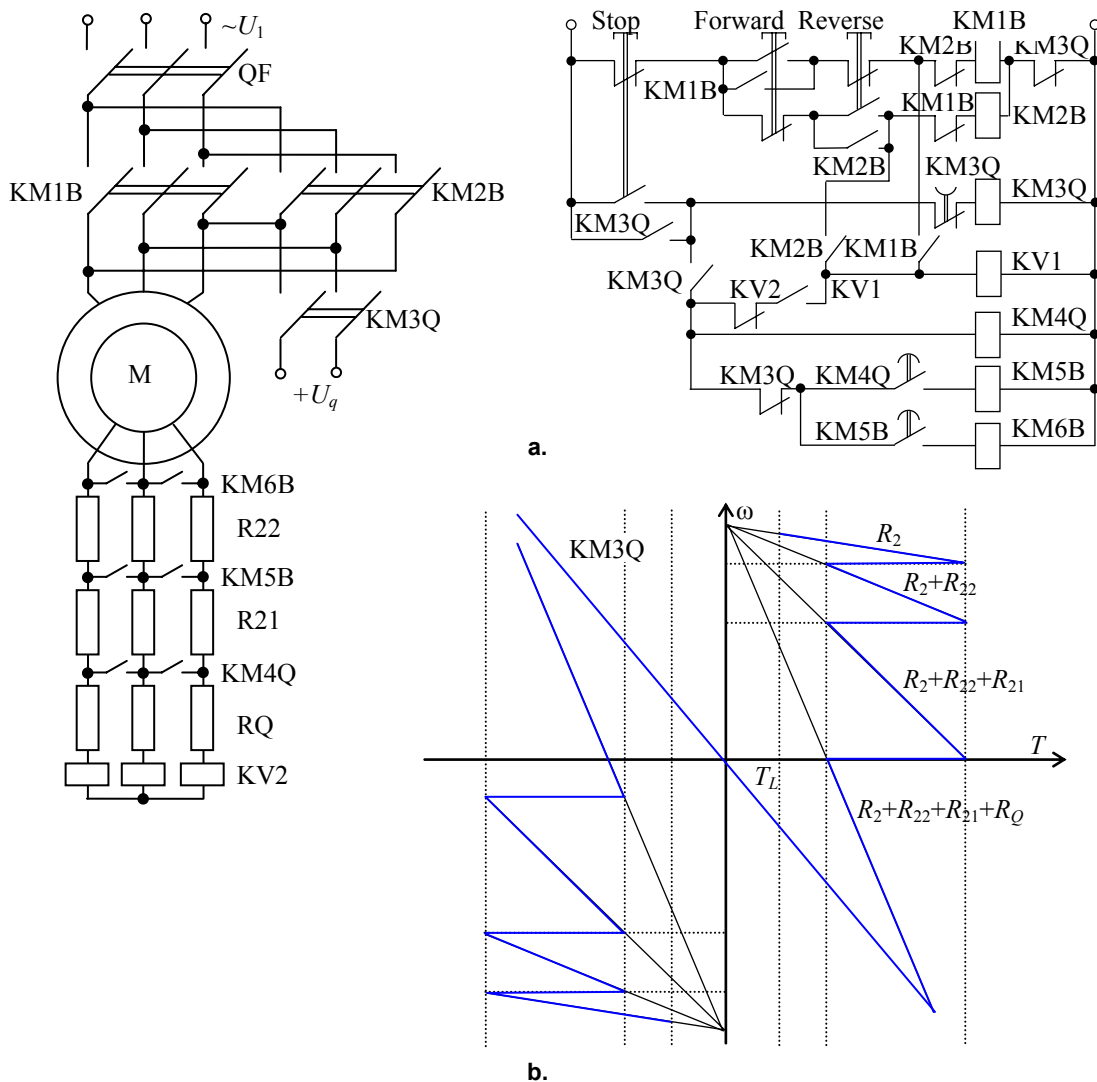
Fig. 7.3 Wound rotor induction motor drive

From similarity of triangles, the quasi-linear parts of the curves are described as $\dfrac{S_L}{S_b} = \dfrac{S_{Li}}{S_{bi}}$. Replace S_b by $\dfrac{R_2}{X_b}$ and S_{bi} by $\dfrac{R_2 + R_{2i}}{X_b}$, and find

$$\frac{S_L X_b}{R_2} = \frac{s_{Li} X_b}{R_2 + R_{2i}} ,$$

where $R_{2i} = R_{21} + R_{22} + ...$ Therefore,

$$R_{2i} = R_2 \frac{S_{Li}}{S_L} - R_2 = R_2 \frac{S_{Li} - S_L}{S_L} .$$

Meaning the rotor resistance, the new breakdown slip is as following:

$$S_{bi} = \frac{R_2 + R_{2i}}{\sqrt{R_1^2 + X_b^2}},$$

and the artificial mechanical characteristic (6.10) is as follows:

$$T = \frac{2T_b(1+\varepsilon)}{\dfrac{S}{S_{bi}} + \dfrac{S_{bi}}{S} + 2\varepsilon}.$$

The drawbacks of the rheostat speed adjustment first of all concern of wasteful power dissipation in a rotor circuit and the stepped control character. In addition, unstable operation at low speeds restricts the speed range by 2…4.

Starting and braking. For the *rheostat starting* of the wound rotor induction motor drives the specific *accelerating resistors* are required. They restrict the run-up current, increase the run-up torque, protect the driven machine against blows in transmissions at starting and protect the motor from overheating in the repeated starting and braking modes.

Both the counter-force and the dc injection braking of the wound rotor motor are more effective than those for the squirrel-cage machine.

Example. In Fig. 7.3 (a) an induction motor M is connected to the three-phase mains through the switch QF and the contactor KM1B or KM2B. Contactors KM5B, KM6B and the relay KV1 give an opportunity to exclude gradually the steps R21 and R22 of the accelerating rheostat from the rotor circuit. The contactor KM4Q, the resistor RQ and the voltage relay KV2 form the counter-force circuit. The contactor KM3Q provides injection of dc for braking.

The button Forward switches on the contactor KM1B, which connects its main contacts in the stator circuit, shunts the button Forward by the blocking contacts, and supplies the relay KV1. The contact of this relay supplies the contactor KM4Q to exclude the counter-force step from the rotor circuit. The motor runs along the rheostat speed-torque characteristic of the first running step. As soon as the first time delay is completed, the KM4Q contact in the KM5B circuit is closed. The contactor KM5B shunts the step R21 of the accelerating rheostat resulting in motor running along the rheostat curve of the second starting step. As the second time delay is completed, the motor moves up to the natural characteristic thanks to the R22 exclusion by KM6B. Here the motor completes its acceleration to the steady-state speed ω_L of the appropriate load torque T_L and the starting completes.

To reverse, the button Reverse is pressed. The contactor KM1B is switched off and the relay KV1 along with the contactors KM4Q, KM5B, KM6B lose their supply. Now, the resistors R21, R22, and RQ are introduced into the rotor circuit. In turn, the button Reverse switches on the contactor KM2B the main contacts of which connect the motor stator to the reverse voltage. The motor comes to the counter-force mode of operation. Herein the relay KV2 actuates unplugging the contact in the circuits KM4Q, KM5B, KM6B and providing an operation with the maximal rotor resistance. While braking, as given by (6.7), $E_2 \approx E_{20}S$, and the voltage of the relay KV2 drops. At $S \approx 1$ this relay will proceed to the off state and the contactor KM4Q will receive the supply. The motor runs backward along the starting rheostat characteristic. Being pressed again, the button Forward initialises the repeated reverse.

The button Stop disconnects the contactor KM1B (or KM2B) and adds the resistors to the rotor circuit. The closing contact of the button Stop loops the circuit of KM3Q the main contacts of which connect two stator phases to the dc circuit. The motor comes to the dc injection braking. As the time delay is completed, the contactor KM3Q is switched off.

7.3   Double-phase operation

Asymmetrical supply. Sometimes the motor supply is asymmetrical, with unequal phase voltages. The asymmetrical supply system may be simulated by the pair of forward and inverse phases. Here, forward voltage consecution U_{1f} creates the appropriate current I_{1f} and the forward field in the air gap whereas inverse voltage consecution U_{1i} creates the appropriate current I_{1i} and the inverse air gap field. Accordingly, the resulting torque may be presented by the algebraic sum

$$T \approx T_f + T_i$$

where, following (6.6), $T_f = \dfrac{m_1 I_{2d}^2 R_2}{\omega_0 S_f}$ is the torque of the forward phase consecution and $T_i = \dfrac{m_1 I_{2i}^2 R_2}{\omega_0 S_i}$ is the torque of the inverse phase consecution. The resulting torque curve depends on the asymmetry distortion degree (Fig. 7.4). The rotor slip in respect to the field of the forward phase consecution is $S_f = \dfrac{\omega_0 - \omega}{\omega_0}$ whereas the rotor slip relatively the field of the inverse phase consecution is $S_i = \dfrac{\omega_i + \omega}{\omega_i}$ that is $S_i = 2 - S_f$.
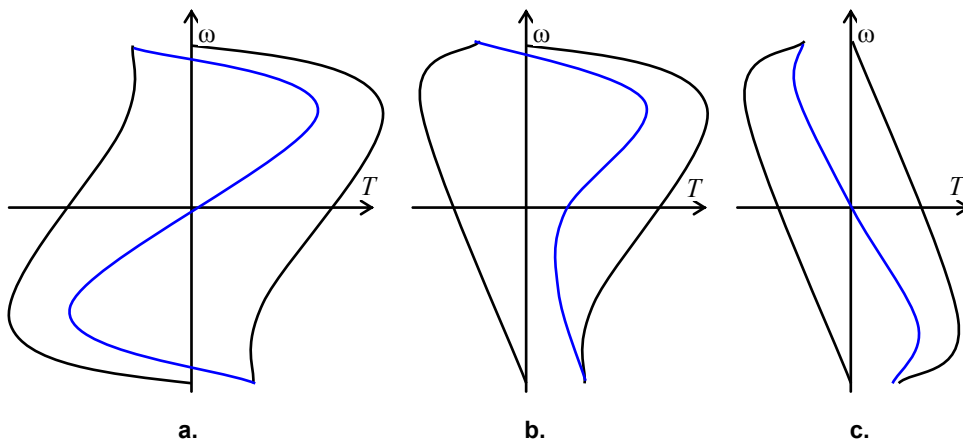

Fig. 7.4 Speed-toque curves of three-phase motor at two-phase supply

The motor replacement circuit at the inverse phase consecution is similar to the above discussed in Fig. 6.2 motor replacement circuit though the currents I_1, I_2 and voltage U_1 are replaced here by the currents I_{1i}, I_{2i} and voltage U_{1i} .

Double-phasing mode. The particular case of the asymmetrical motor supply is the event of a phase disconnection or break. In this *single-phasing mode* the stator voltage system is again resolved upon the two components, forward and inverse. It is assumed two identical MMF in the motor which try to rotate the rotor in opposed directions. Each MMF creates its own magnetic flux that induces the EMF in the rotor winding with corresponding current system. The forward magnetic flux interacts with the rotor currents of the forward phase consecution thus creating the forward torque. Reciprocally, the inverse magnetic flux and corresponding rotor current system create the inverse torque.

The resulting torque is defined as an algebraic sum of the above mentioned torques. Interaction of the magnetic fluxes and currents of the counteractive phase systems results in pulsing torques. The torque of the forward currents is as follows:

$$T_f = \frac{2T_{bf}(1+\varepsilon)}{\dfrac{S}{S_b} + \dfrac{S_b}{S} + 2\varepsilon}$$

and the torque of the inverse currents is as follows:

$$T_i = -\frac{2T_{bi}(1+\varepsilon)}{\dfrac{2-S}{S_b} + \dfrac{S_b}{2-S} + 2\varepsilon} \cdot$$

The resulting motor torque is as follows:

$$T = \frac{2T_{bf}(1+\varepsilon)}{\dfrac{S}{S_b} + \dfrac{S_b}{S} + 2\varepsilon} - \frac{2T_{bi}(1+\varepsilon)}{\dfrac{2-S}{S_b} + \dfrac{S_b}{2-S} + 2\varepsilon} \cdot$$

As in this case the run-up torque may be equal zero (Fig. 7.4 (a)), the special equipment can be demanded to start.

Introducing of enough high resistance to the rotor circuit, resulting in $S_b \gg 1$,, deforms significantly the speed-torque characteristic (Fig. 7.4 (b)) being suitable for the low speed operation and braking (Fig. 7.4 (c)).

High losses in the motor copper and steel heat the windings thus restricting an application of the single-phasing mode by the low power systems.

Capacitor-run motors. As well, in the low power systems the *capacitor-run motor* circuits are broadly used to connect the three-phase motors to the single-phase circuit (Fig. 7.5). As a rule, these circuits include the work capacitor C and the running capacitor C0. For reverse, the running winding changes the polarity. The rated voltage and current of the capacitor circuit are their phase values. For example, if the motor is counted on 127/220 V and 7.3/4.2 A, its ratings are assumed as 127 V and 4.2 A. The required work capacitor for the circuit in Fig. 7.5 (a) is equal $2800\dfrac{I_M}{U_1}$ μF, in Fig. 7.5 (b) $4800\dfrac{I_M}{U_1}$, in Fig. 7.5 (c) $1600\dfrac{I_M}{U_1}$, in Fig. 7.5 (d) $2740\dfrac{I_M}{U_1}$ whereas the running capacitance is selected as $C_0 \approx (2...3)C$. The capacitor sizes are proportional to the motor power. Thus, for the motor series 4A the capacitor cost at $P_M \approx 1$ kW approximately corresponds to the motor price and for 1.5 kW it is 1.5 times above the machine cost. At high powers these circuits are not used. The capacitor for the former two circuits is counted to the network voltage, for the third circuit the twofold voltage is required, and for the latter one is 15 % above the mains supply. This circuit is considered the most preferable. At low loading the voltage raises whereas idling is not recommended at all.
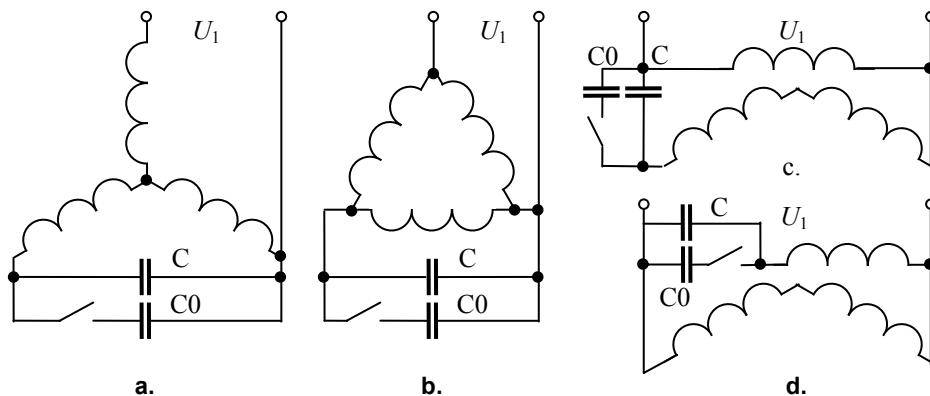
Fig. 7.5 Run-up circuits of capacitor-run motor

Double-phase motors. To operate in the single-phase circuits, the specific *double-phase motors* are manufactured which have two windings, the field winding L1 and the control winding L2 (Fig. 7.6 (a)). To adjust the motor, the control winding is affected whereas the field winding is supplied permanently. As far as the control is executed, the winding MMF asymmetry may result in the elliptical field shape instead of the circular one. Herewith, along with the forward voltage and currents needed for motoring, the inverse voltage and currents appear thus causing the braking.

The control voltage magnitude and phase as well as the space angle between the windings define the angular frequency and the power of these motors. Due to the rotor high resistance, the breakdown slip reaches 3…4 and the speed-torque characteristics of such machines are soft and non-linear (Fig. 7.6 (b)). The equation of the speed-torque characteristic of the double-phase motor is similar to the same equation of the three-phase motor at the asymmetrical supply.
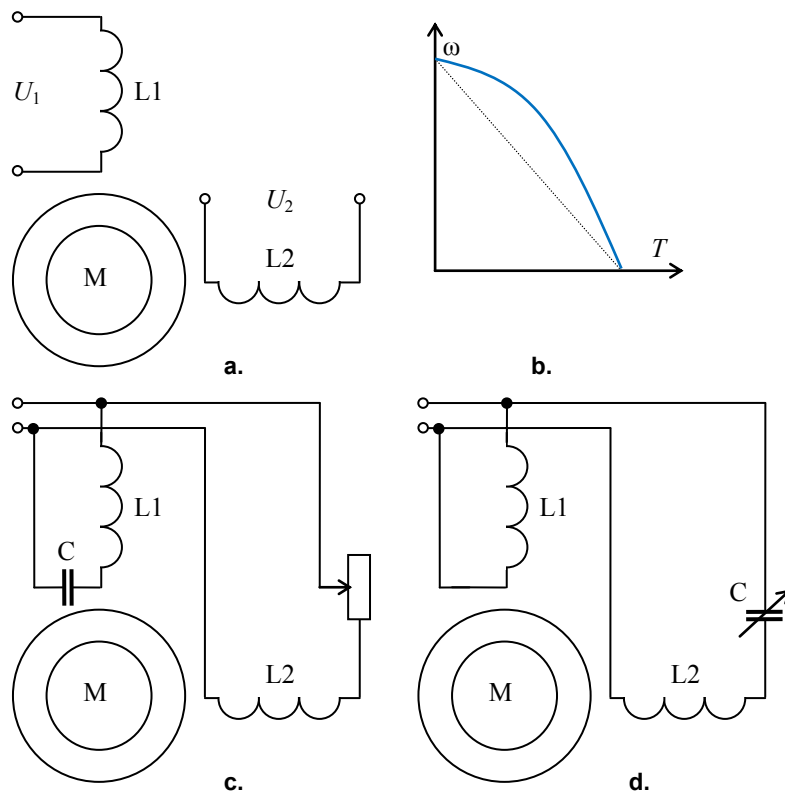
Fig. 7.6 Double-phase motors

The amplitude and phase methods are distinguished in the double-phase motor supply. In the first case (Fig. 7.6 (c))

$$U_1 = U_{1\max} \sin(\omega_1 t) \quad U_2 = U_{2\max} \sin\left(\omega_1 t - \frac{\pi}{2}\right)$$.

Here, the resistor changes the voltage $U_{2\max}$ at the constant phase shift. In the second case, the phase is adjusted at the constant voltage (Fig. 7.6 (d)). For reverse, the control winding changes the polarity.

The double-phase motor operation is accompanied with high energy losses which, in turn, heat the windings. Therefore these motors are rear used above 200 W. Their typical application area includes the refrigerator compressors and some domestic devices.

8   Scalar Control of Induction Motors

8.1   Voltage-frequency control

Frequency control. At the scalar control, the control variables are the dc quantities those magnitudes are adjusted. There are several scalar methods of the induction motor speed adjustment.

Accordingly (4.5), to adjust the speed of an ac motor the supply frequency must be changed. Thus, in the simplest case the speed adjustment is made by varying the inverter frequency, thereby affecting the synchronous speed of the machine. There will be a small variation of the speed under the loaded conditions because of the slip which may be corrected if necessary. However, the sole control of the inverter frequency is unsatisfactory and rarely used for the following reasons.

As (4.1) shows, along with the frequency drop at the fixed EMF, the flux will rise and it may bring the magnetic circuit to saturation. Herewith, after (1.3), (6.7) and (6.9), the torque, including the breakdown torque and the run-up torque, will increase (Fig. 8.1 (a)). While the flux rises, the magnetizing current given by (6.4) will increase as well, resulting in additional motor heating. And conversely, if the frequency increases, the flux will decrease. The weakened flux will adversely affect the ability of the machine to develop the torque.
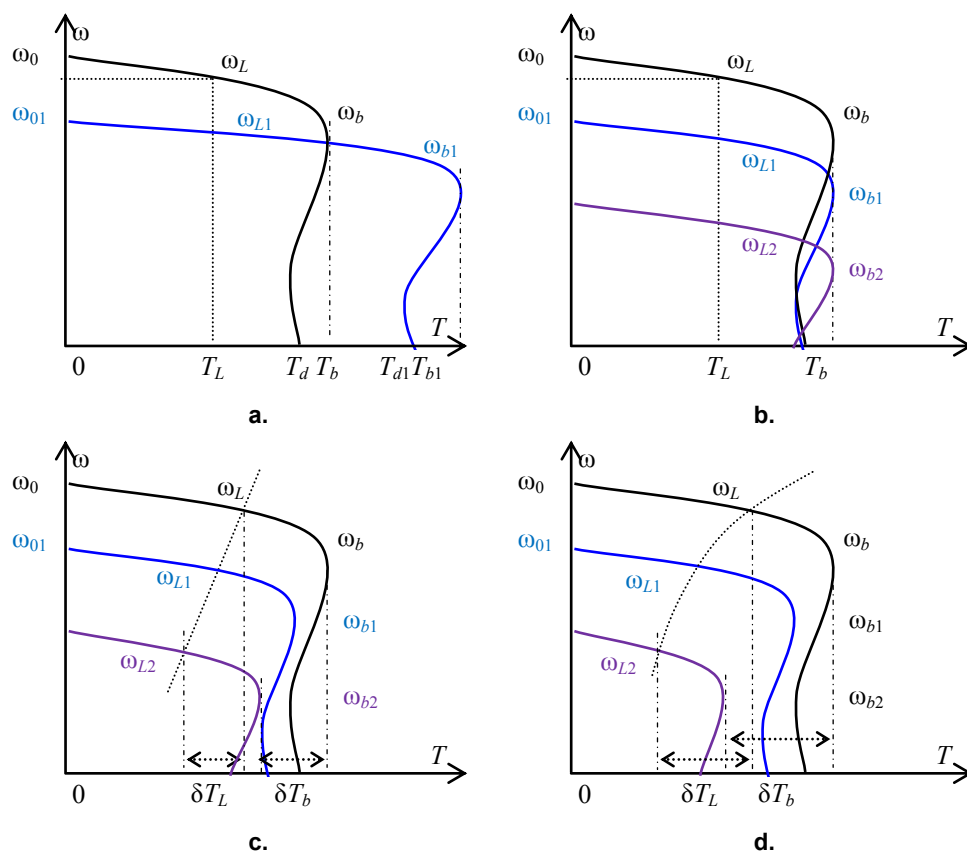

Fig. 8.1 Mechanical characteristics of VFC

Kostenko's rule. An alternative is to operate the motor within the definite voltage-frequency ratio, so that the maximum voltage is reached only at the maximum frequency. The simple *voltage-frequency control* (VFC) method which keeps quasi-constant overload capacity $\lambda = \dfrac{T_b}{T_L}$ is known as the Kostenko's rule. Assuming $R_1 = 0$ in (6.11), this implies the following control:

$$\frac{U_1}{\omega_1 \sqrt{T_L}} = \text{const}$$

where the stator voltage magnitude U_1 is changed along with the frequency ω_1 and the load counter-torque T_1. It is assumed also that the inverter used has the facility for separate adjustment of both the output voltage and the frequency.

At constant loading, $\dfrac{U_1}{\omega_1} = \text{const}$ (Fig. 8.1 (b)), the *constant voltage-frequency ratio* is supported. The *linear voltage-frequency ratio* meets the law $\dfrac{U_1}{\sqrt{\omega_1^3}} = \text{const}$ (Fig. 8.1 (c)). The machine flux here is reduced by the smaller voltage-frequency ratio, and the motor is operated with a gradually weakened field at a reduced torque. At the square counter-torque dependence, the control law also becomes *square*, $\dfrac{U_1}{\omega_1^2} = \text{const}$ (Fig. 8.1 (d)). In this operating mode the motor has a quadratically reduced pull-out torque throughout the entire speed range. The advantage of this *setting* is, that in the region below 50 Hz the motor can be excited to a higher degree by increasing the voltage without any danger of over-excitation of the

motor, until the rated torque is reached. In this way, to provide the start-up and overload operations the torque above the steady-state value is available. This is suitable for the centrifugal pumps, compressors, and fans those losses pull down proportionally to the speed cube. As Siemens Company calculated, at the 10 % speed drop this method saves up to 35 % of the consumed power. Therefore some vendors embed the frequency converters directly into the motor-gear units.

Operation above the rated voltage and frequency. As follows from $X_1 = \omega_1 L_{1\sigma}$, an increase of the applied frequency results in the stator reactance growing. In order to compensate for this, the drive must simultaneously increase the voltage. Otherwise, the stator current, flux, and torque would decrease. Nevertheless, the voltage level above the rated value is usually prohibited because the motor magnetic circuit is saturated in the rated mode. Thence, when the voltage reaches the maximum value and the frequency is increased further, the flux and thus also the torque should be dropped in inverse proportion. In this range, the breakdown torque decreases quadratically below the rated torque.

Meanwhile, some applications require the motor to be operated above the rated speed. As the applied voltage may not exceed the rated voltage, the torque drops along with the speed rise. This is referred to as the constant power range or the field-weakening mode because any change in torque is compensated by the opposite change in speed. Therefore, to cover both the constant torque region and the constant power region, the VFC is maintained only below 50 Hz. Above this frequency, the voltage-frequency ratio decreases, with a corresponding decrease in torque.

As a further alternative, the drive must be dimensioning larger to operate with the voltage and frequency above the rated values, for example, the motor of 230 V/50 Hz may be supplied by the inverter of 400 V at 400/230·50 = 87 Hz. The motor would develop $\sqrt{3}$ times the rated power by increasing the frequency. As opposed to the operation with a non-weakened field, the breakdown torque in this mode of operation remains at the same level as in the mains operation. The inverter must be also dimensioned for the higher output.

A prerequisite for the constant torque is a steady uniform cooling of the motor, also in the lower speed range. However, this is impossible with *fan-cooled motors* since the ventilation also decreases with the decreasing speed. Thus the forced ventilation cooling is required. *Forced cooling* can be omitted at constant torque if the motor is over-dimensioned as the torque must therefore be reduced.

Implementation of VFC. A variable ac voltage can be readily realized using the direct frequency converters or the dc link ac/ac converters, which operate in the voltage source inverting (VSI) mode and produce the required motor voltage waveform at all speeds. In all types of ac/ac converters, as the frequency is changed, the voltage amplitude is proportionally modified as Fig. 8.2 (a) shows. The corresponding circuit diagram is presented in Fig. 8.2 (b). Among the two control "handles", frequency and voltage, the frequency control is by far the most critical, as small variations in frequency produce large changes of slip frequency and, hence, significant changes in current and torque. Thus, it is customary to slave the frequency to the voltage to prevent the motor from receiving an inappropriate value of the voltage-frequency ratio. The standard way is to place the front-end limiter (particularly a first-order filter) shown in Fig. 8.2 (b), which restricts the frequency change to a value which the motor can respond without drawing an excessive current or without regenerating.
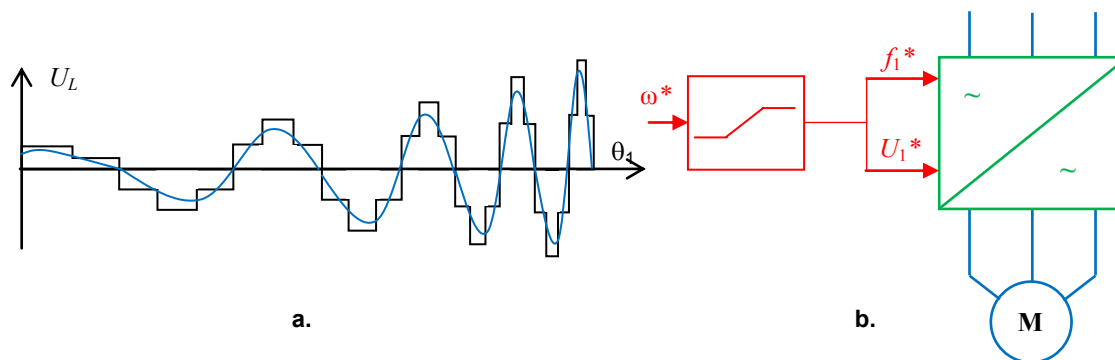
Fig. 8.2 Timing and circuit diagrams of VFC

Soft starters. The important application area of the open ended scalar control concerns the *soft starting*. Recall that when a motor is started at full voltage, it develops approximately 150 % starting torque and 600 % starting current. Using the *soft starters*, the motor can be started at the reduced voltage and frequency. For example, the motor may start with approximately 150 % torque, but only 150 % of full load current. As the motor is brought up to speed, the voltage and frequency are increased, and this has the effect of shifting the motor speed-torque curve. The soft starters accelerate the motor smoothly as the frequency and the voltage are gradually increased to the desired speed.

Examples are the multifunction microprocessor soft starters ALTISTART and TESYS from Schneider Electric which decrease the run-up current and prevent the shock loading by the accurate tuning of the starting torque. This equipment provides the adjusted starting *ramps* with smooth voltage rise at the S-shape and U-shape curves. To prevent the starting oscillation, many of them implement the duple run-up thanks to the preliminary dc excitation of the induction machine. Since the stator flux linkage approaches the rated level, the power inverter will switch to the normal mode.

Soft starters protect machines and cables from over-temperature at the lingering running. They prohibit the running even if the separate supply phase is broken or has a voltage drop. Often, they also execute the motor restart at the short-term supply dips and winding drying in the case of the isolation resistance decrease, etc.

Some applications need the starting torque above 150 % of the rated value. A conveyor, for example, may require 200 % of the rated torque for starting. To provide it, both the soft starter and the motor are to be appropriately dimensioned.

In electric drive on the basis of power converters *the "start on the fly"* may be applied. To this aim, the motor preliminary raced to some speed is smoothly accelerated by a control system to the demanded speed. In particular, electric drives from Omron provide automatic *search* the speed with a minimum current derivative corresponding to coincidence of the converter and stator frequencies. Some Siemens electric drives "start on the fly" even if the shaft rotates in opposite direction that is very effective for the fan control.

8.2　　Flux-frequency control

Stabilization of stator flux. According to (4.1), the motors running on an ac line operate with a constant flux because voltage and frequency are keeping constant. Motors operated at the constant flux are said to have the constant torque.

Following (1.3), as long as a constant voltage-frequency ratio is maintained, the motor will expect constant torque characteristics. An actual torque produced, however, is dependent upon the speed and load.

At the VFC, the resistance R_1 was ignored whereas actually $R_1 > 0$. Such voltage-frequency regulation has the benefits only above 5…10 Hz (lines U_1 in Fig. 8.3 (a, b)). At low speeds as well as in the small motors and at large loads, the ohmic voltage drop $I_1 R_1$ notably affects the control quality by lowering the motor magnetic flux and overload capacity as the frequency decreases. As the input voltage falls, the flux and torque reduce also. In the generator mode the product $I_1 R_1$ changes the sign thus increasing the flux.
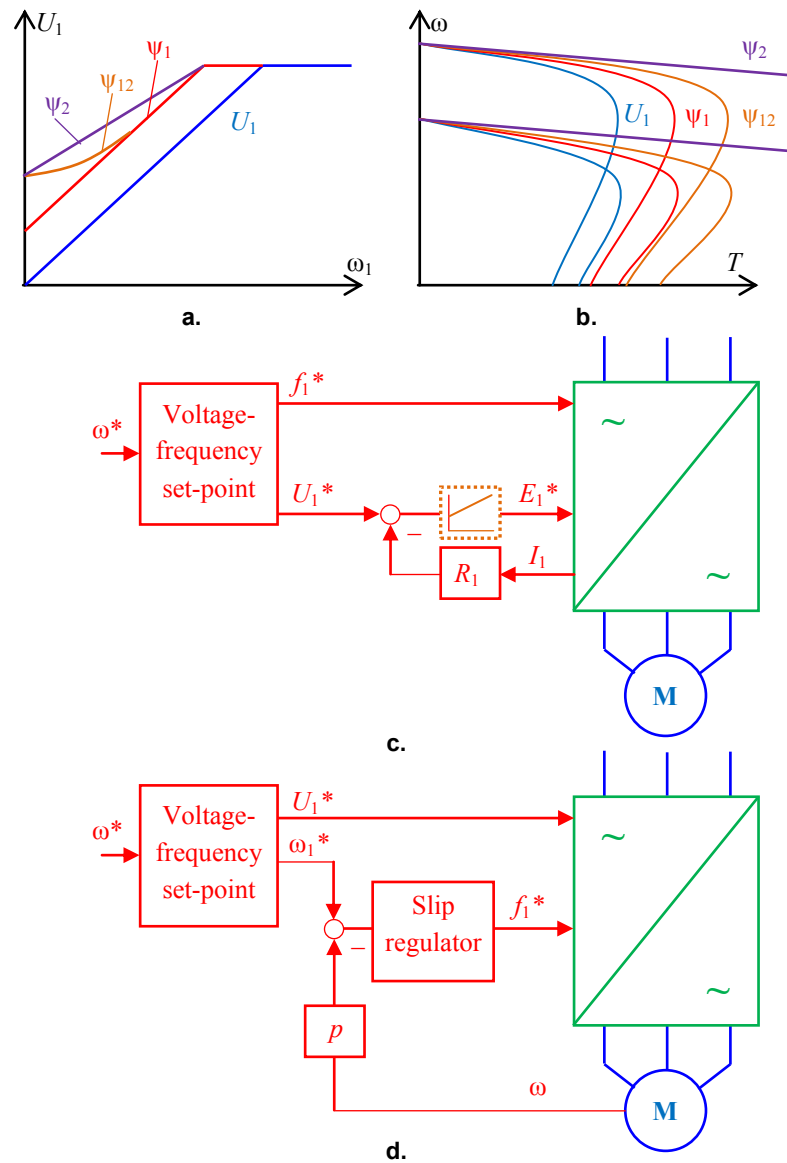
Fig. 8.3 Control and mechanical characteristics and circuit diagrams of the flux-frequency control

Strictly speaking, to keep the stable overload capacity it is required to adjust the stator EMF E_1 instead of the voltage U_1 aiming to fix the ratio (4.1),

$$\psi_1 = \frac{E_1}{\omega_1} = \text{const}$$
.

This mode of the variable-speed control is called a *stator flux-frequency control* or an *IR-compensation* (lines ψ_1 in (Fig. 8.3 (a, b))). To obtain the accurate EMF control, the stator EMF $E_1 = U_1 - I_1 R_1$ is calculated by sensing the current I_1 and subtracting the $I_1 R_1$ value from the voltage reference U_1^* (Fig. 8.3 (c)).

Actually, the EMF calculation is rather complicated because of the R_1 dependence on the temperature. In electric drives of some manufacturers the specific mode is introduced for the actual R_1 measuring and recalculation along with the wires heating therefore E_1 is counting quite accurately. Particularly, in ALTIVAR of Schneider Electric and VLT from Danfoss, the range of the IR-compensation reaches 30…80 V.

The discussed stator flux-frequency control supports the demanded overload capacity though at this control the induction motor keeps the usual drooping mechanical characteristic therefore the speed range remains moderate, $D = 50…100$.

Stabilization of effective flux. To compensate the stator resistance drop and the magnetization reluctance, stabilization of the effective flux, $\psi_{12} = $ const, is to be employed. This approach is known as an *effective flux-frequency control* or boost *compensation*, *boosting*. Herewith, the additional voltage enters the system at low speeds and in the starting position. Thanks to the boosting unit plotted by the dotted lines in Fig. 8.3 (c), the voltage reference has a zero-frequency bias starting from some additional non-zero value. Particularly, the boosting voltage of MOVITRAC may reach up to 70 V at $\omega_1 = 0$. In the converters MICROMASTER from Siemens, boosting follows all the run-up and braking modes. The lines ψ_{12} in Fig. 8.3 (a, b) illustrate the boosting mode.

Slip compensation. *Slip compensation* yields further dynamics improvement. This method is adopted in high performance induction motor drives where speed regulation is of concern. Better adjustment is obtained here by changing the frequency as a function of the loading level, thereby controlling the slip frequency while keeping the rotor speed roughly constant. The angular frequency of the rotor EMF ω_2 is defined from (4.5) and (6.1). Also, the slip frequency may be controlled directly by a speed sensor fitted to the motor shaft. The inverter frequency can then be generated by the digital summing of the shaft speed and the slip frequency signals as Fig. 8.3 (d) shows. Thus, the slip-control loop here is actually the torque control loop because the torque is practically proportional to the slip in the control range involved as follows from the motor speed-torque characteristic in Fig. 6.4 (b).

As the slip compensation is based on the positive feedback (increasing load increases the output frequency), an addition of too much compensation may cause the drive instability.

Though the slip compensation does not provide the strong constancy of the effective flux linkage, its benefit is the linear control. Particularly in the drives MOVITRAC the slip compensation range reaches of 10 Hz. In the Siemens electric drives the same compensation provides the slip stabilizing up to 1 %. In the ALTIVAR systems the non-linear slip compensation known as the *profile mode* is implemented.

8.3   Current-frequency control

Principle of CFC. According to (1.3), a suitable method to affect the induction motor torque and speed is to adjust the stator current at the stabilized rotor flux or the rotor current at the stabilized effective flux. An adjustment of the induction motor by changing the supply frequency along with the current control is called a *current-frequency control* (CFC). Unlike VFC, this approach requires an implementation of the current source inverter (CSI) instead of the VSI. The use of CSI excludes the overcurrents, even if the motor is stalled owing to the excessive load torque because the current is automatically limited by the inverter.

Circuit diagram of CFC. Figure 8.4 explains the method of the CFC. The circuit diagram is based on the cascade principle presented above in Fig. 2.4 (b). The outer loop stabilizes the speed ω measured by the speed sensor and compared with the set-point $\omega_0{}^\star$. The output of the speed regulator is proportional to the speed error ω_2 and, accordingly (6.1), to the slip fraction $S\omega_0{}^\star$. As follows from (4.5), the sum of ω_2 and $p\omega$ represents the set-point stator frequency $\omega_1{}^\star$ therefore the CSI will set the required speed.

Since the slip is stabilized by the speed regulator ($\omega_2 \equiv S$), the rotor flux linkage ψ_2 which is inversely proportional to the slip can also be considered as stabilized and independent of the supply frequency. The stator current is readily accessible as compared to the rotor current, therefore the torque after (6.6) at I_{12} = const may be suitably adjusted proportionally to the quadrant of the stator current I_1,

$$T_{12} = \frac{m_1 (I_{12} - I_1)^2 R_2}{\omega_0 S} \, .$$

Download free eBooks at bookboon.com

To control the stator current, the circuit includes an inner loop which follows the quadratic *function generator* $I_1^*(\omega_2)$ and involves a current regulator, a feedback, and a comparator. The function generator derives the demanded stator current I_1^* dependently of the slip frequency. The current control system compares the set-point current I_1^* with the actual sensed current I_1 to find the set-point δI_1^* of the CSI.

At the fixed effective flux linkage, the linear relation appears between the rotor speed ω and current I_2:

$$\omega = \frac{\omega_1 - \omega_2}{p} = \omega_0 - \frac{I_2 R_2}{p \psi_2}$$

that is quite similar to the dc motor characteristic (4.18). The same concerns the mechanical characteristic (lines ψ_2 in Fig. 8.3 (a, b)), which is quite similar to (4.17),

$$\omega = \omega_0 - \frac{T_L R_2}{2 m_1 p^2 \psi_2^2}$$
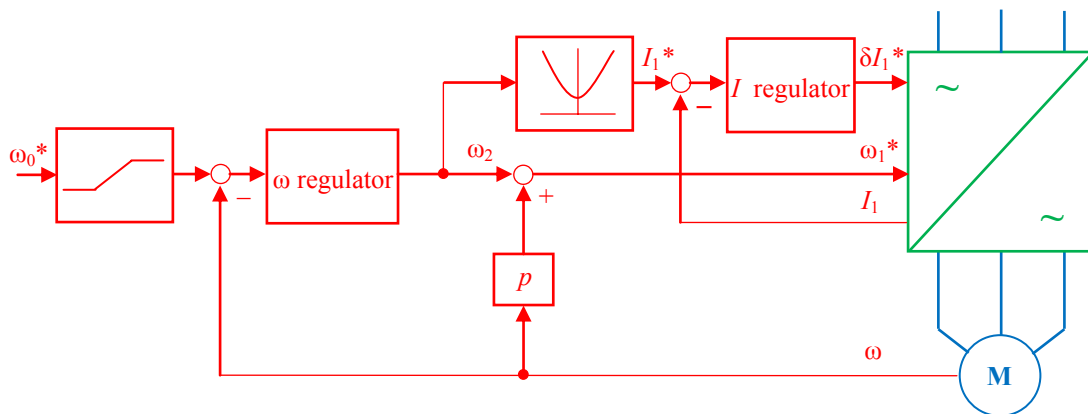
Fig. 8.4 Circuit diagram of the current-frequency control

The CSI are intended for such electrical equipment that needs the control of the current value, particularly in controlled-torque drives. Usually, these inverters are less sensitive to the parameter instability than the VSI. As compared with the VSI, they are not so popular because of the large input inductor and the requirement in a resistive-capacitive load. The switching frequency of CSI is lower, so the load current waveform is distorted, leading to larger derating of the load motor to avoid overheating. Thereat, this inverter is replaced usually by the traditional dc link VSI with the current feedback shown above in Fig. 5.2 (a). Whereas the three regulators perform independently, the transition of each leg affects both other phases. This may cause unnecessary switching combinations and, as a result, oscillations in the load as well as low-order harmonics. To increase accuracy, the non-linear function generators shown in Fig. 8.4 are usually introduced into the CFC circuits, which compensate the quadratic current-frequency relation (6.6). This results in the stabilizing of ψ_1, ψ_{12}, or ψ_2 similarly to VFC.

9   Vector Control of Induction Motors

9.1   Field-oriented control

Vector control vs. scalar control. The above discussed control methods refer to the scalar class because they are based on the rms (static) motor models. Nevertheless, when the currents, voltages and flux linkages of the induction motor change frequently, their scalar control keeps out the high dynamics. This is the reason why the accurate and quick-acting systems require the vector control. The primary objective of the vector control is to achieve good performance when speed and torque conditions change periodically or randomly. The underlying principle of the vector control is to separate out the component of the motor current responsible for the torque producing and the component responsible for the flux producing in such a way that they are magnetically decoupled, and then to control each independently. This principle is implemented by orientation of the arbitrary orthogonal reference frame (x, y) along one of the vectors defined the electromagnetic torque in (1.3) − ψ_1, ψ_2, ψ_{12}, I_1 or I_2. Hence, the projection of this vector on the other axis equals zero. In this way, both the magnitude and the phase of the drive variables are controlled like in the dc motor. The chosen adjusted vector defines the method of the vector control.

According (1.3), accurate spatial positioning either the stator current with respect to the rotor flux linkage or the rotor current with respect to the effective flux linkage provides precise torque regulation. The first approach to make it is a *field-oriented control* (*FOC*) called also a *trans-vector control*. FOC is the vector method of the separate torque and flux linkage management in the inverter-fed electric drive systems. So far as the current is the regulation object, the CSI is required for this purpose. As discussed above, in practice the CSI is usually replaced by the VSI enveloped by the deep current feedbacks.

To comply the vector principle, the FOC method does not affect the actual machine variables in the phase axes (L_1, L_2, L_3) but the orthogonal (x, y) variables one of which is oriented along the flux linkage vector wherefore the actual signals are converted and delivered to the (x, y) motor model by the forward Park's transformer. Thanks to this approach, all the model variables are considered as the dc signals suitable for the control. After the calculation, the obtained control signals are again converted to the phase axes by the reverse Park's transformer to supply the inverter.

Vector diagram of FOC. Figure 9.1 shows the vector diagram of the FOC which aligns the stator current I_1 with respect to the rotor flux linkage ψ_2. The first function of the control system is to turn the reference frame (x, y) at the field frequency ω_1. By rotation I_1 relatively ψ_2, the control system at all times keeps the constant projection I_{1x} thus providing the constancy of ψ_2 and, at the same time, adjusts the projection I_{1y} according to the demanded torque value. As $\omega_k = \omega_1$, (4.2) transforms as follows:
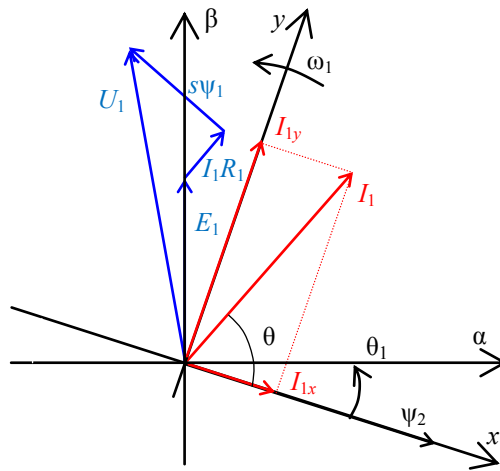
Fig. 9.1 Vector diagrams of FOC

$$U_{1x} = R_1 I_{1x} + \frac{d\psi_{1x}}{dt} - \omega_1 \psi_{1y},$$

$$U_{1y} = R_1 I_{1y} + \frac{d\psi_{1y}}{dt} + \omega_1 \psi_{1x},$$

(9.1)

$$0 = R_2 I_{2x} + \frac{d\psi_{2x}}{dt} - \omega_2 \psi_{2y},$$

$$0 = R_2 I_{2y} + \frac{d\psi_{2y}}{dt} + \omega_2 \psi_{2x}.$$

Current projections in (9.1) are kept constant because they do not depend on the supply frequency ω_1. As the reference frame (x, y) rotates at ω_1, an angle θ_1 of the immovable reference frame (α, β) with respect to (x, y) at any instant is given by

$$\theta_1 = \frac{\omega_1}{s} = \int_0^t \omega_1 dt$$

(9.2)

Circuit diagram of FOC. The appropriate circuit diagram is shown in Fig. 9.2. Here, the forward Park's transformer converts the motor phase current signals I_{L1}, I_{L2}, I_{L3} obtained by the sensors from the natural coordinate frame (L_1, L_2, L_3) to the immovable reference frame (α, β) using (4.7) and then to the rotation reference frame (x, y) using (4.9). Basing on I_{1x}, the motor model unit calculates the ψ_2 modulus using (4.3), (4.4) and (9.1) as follows:

$$|\psi_2| = \psi_{2x} = I_{1x} \frac{L_{12}}{1 + s\tau_e}$$

(9.3)

where $\tau_e = \dfrac{L_2}{R_2}$ is the rotor electromagnetic time constant from (3.2), L_{12} is the mutual inductance from (4.3), L_2 and R_2 are the rotor inductance and resistance. Hence, the x-projection of the stator current and I_{1x} with the time delay τ_e defines the effective rotor flux linkage $|\psi_2|$. Yet, the method is called also as the *rotor flux control*.
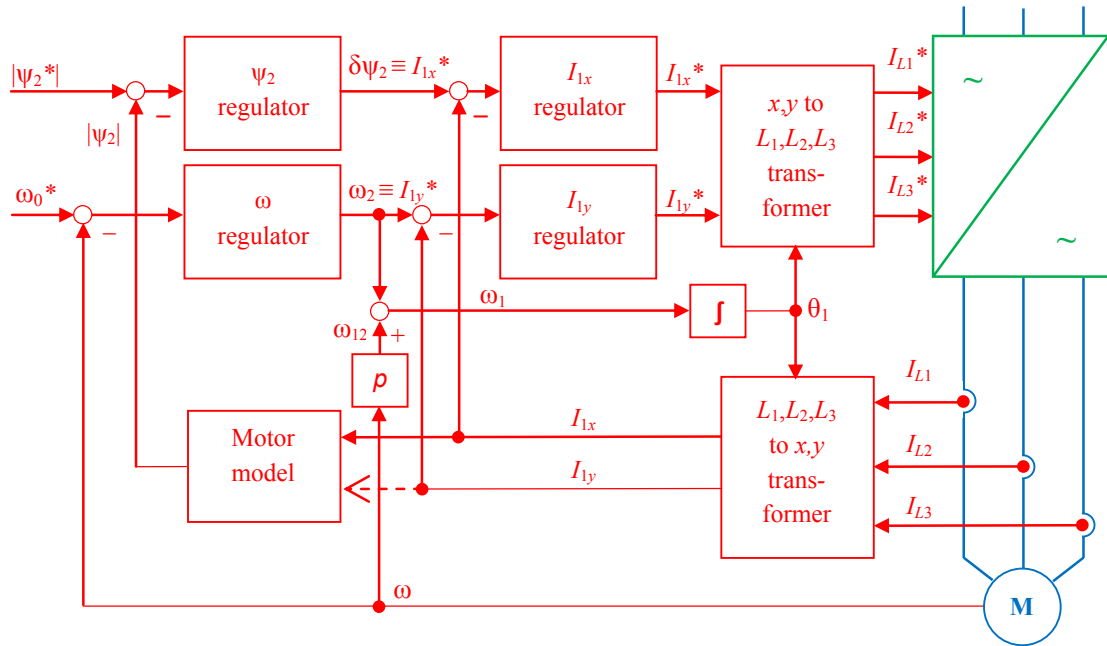
Fig. 9.2 Functional circuit of the field oriented control

Further, $|\psi_2|$ is compared with the required flux linkage $|\psi_2^*|$ and their difference enters the flux regulator. Thus, the rotor flux is stabilized by the close loop system. Next, the fixed flux generates the commanded flux-producing component of the stator current I_{1x}^*. This component is compared with the actual value of I_{1x} and the error enters the appropriate current regulator. After the scaling by the current regulator, the signal enters the reverse Park's transformer.

According to (4.3), (4.4) and (9.1), $\omega_2 = I_{1y} \dfrac{L_{12}}{\tau_e |\psi_2|}$ thus the rotor frequency can be controlled through the y-projection of the stator current. To this aim, another reference signal ω_0^* is compared with the actual motor angular frequency ω and their difference supplies the speed regulator. As follows from (6.1), the output of the speed regulator is proportional to the speed error ω_2, i.e. the slip fraction $S\omega_0^*$ and appropriate torque-producing component of the stator current I_{1y}^*. This component is compared with the actual value of I_{1y} and the error enters the appropriate current regulator. After the scaling in the current regulator, the signal also reaches the reverse Park's transformer. To get ω_1 for θ_1 calculation in (9.2), the sum of ω_2 and $p\omega$ is derived and integrated.

The reverse Park's transformer converts the amplitudes of the reference currents I_{1x}^*, I_{1y}^* from the (x, y) coordinate frame to the (α, β) frame using (4.9) and (9.2), and then to the (L_1, L_2, L_3) reference frame using (4.8). The resulting set-point currents I_{L1}^*, I_{L2}^*, I_{L3}^* specify the frequency and the amplitude of the inverter output. Here, both the CSI and the current controlled VSI shown above in Fig. 5.2 (a) can be applied.

As the system provides the constancy of $|\psi_2|$ and ω_2, the resulting motor torque is also constant and does not depend on ω. That is, the stator frequency changes along with the alternating ω according (4.1) thus providing

$$\omega_2 = \omega_1 - \omega p = \text{const}$$

that is quite similar to the dc motor models (1.4) and (4.12).

Sensorless control. During the last decades, a variety of *sensorless control* systems have been investigated aiming to replace the speed and position sensors. For the equipment with the modest speed regulation requirements (1...2 % or more), costly tachometers and associated hardware can be removed from the drive. Different sensorless control systems are successfully used in industry. In the drives where the tachometers are omitted, the motor model unit shown in Fig. 9.2 calculates the angular frequency in addition to the flux linkages referring to (4.3), (4.4), and (4.6) as follows:

$$T = m_1 p k_2 \psi_{2x} I_{1y}$$

$$\omega = \int_0^t \frac{T - T_L}{J} \, dt \qquad (9.4)$$

At the low-speed operation or standstill, however, the limitations of speed and position measurement can be found. Due to the drive system nonlinearity and difficulties in proper parameter identification, linear control theory is not always helpful. Besides, the drive dynamics usually changes with the operating point and some parameters drift in a wide range, depending on the system performance mode. For electric drives this problem arises especially when the rotor inertia changes significantly during operation. Therefore, the FOC performance, design, and implementation depend strongly on the accuracy of the motor parameter estimation as well as on the load, frequency, temperature variations, etc.

9.2   Direct torque control

DTC vs. FOC. In the systems built using the FOC principle, the frequency converter has the CSI properties thus the consumed current is defined only by the current control signals independently of the motor mode of operation and supply voltage U_1. Such PWM-based close loop systems control the torque indirectly through the instant stator currents. Oppositely, the *direct torque control* (*DTC*) implies the VSI for which the control system processes directly the stator flux and torque signals without having the need for inner loops with current regulators.

In order to realize the DTC, the motor model has to provide the flux and torque estimations, quite similar to FOC. The motor model of DTC aims to derive the flux using available measured signals, currents and voltages in this case. Following the flux determination, also the motor torque and speed are computed in the motor model. Additionally, the DTC system includes a voltage switching unit, which implements the SVM instead of the sinusoidal PWM used in FOC. The important point of SVM is the proper selection of the stator voltage vector in order to maintain the flux and torque within the limits of two hysteresis bands. For this purpose, the control system should be able to generate the set-point voltage space vector treated directly at fixed sample frequency.

Circuit diagram of DTC. The scheme of induction motor DTC shown in Fig. 9.3 aligns the stator current I_1 with respect to the stator flux linkage ψ_1. Here, the Park's transformer converts the motor currents I_{L1}, I_{L2}, I_{L3} and voltages U_{L1}, U_{L2}, U_{L3} obtained by sensors from the natural coordinate frame (L_1, L_2, L_3) to the immovable orthogonal frame (α, β) using (4.7) and (4.10). An equivalent model of the standard induction motor (4.2)…(4.6) can be used to calculate the machine variables in the stationary (α, β) frame at $\omega_k = 0$ as follows:

$$U_{1\alpha} = R_1 I_{1\alpha} + s\psi_{1\alpha}$$
$$U_{1\beta} = R_1 I_{1\beta} + s\psi_{1\beta}$$
$$\psi_{1\alpha} = L_1 I_{1\alpha} + L_{12} I_{2\alpha}$$
$$\psi_{1\beta} = L_1 I_{1\beta} + L_{12} I_{2\beta}$$

(9.5)

Fig. 9.3 Functional circuit of the direct torque control

Meaning enough high rotor time constant of the induction motor as compared to the calculation time of the DTC motor model, consider $\psi_2 = const$ within the calculation interval. Therefore, skipping the rotor parameters, the torque can be adjusted by the only control of ψ_1 through the stator voltage. Using this assumption, the motor model unit performs the following online computing:

$$\psi_{1\alpha} = \int\limits_0^t \left(U_{1\alpha} - R_1 I_{1\alpha}\right) dt, \;\; \psi_{1\beta} = \int\limits_0^t \left(U_{1\beta} - R_1 I_{1\beta}\right) dt$$

$$\psi_1 = \sqrt{\psi_{1\alpha}^2 + \psi_{1\beta}^2}$$

$$T = m_1 p \left(\psi_{1\alpha} I_{1\beta} - \psi_{1\beta} I_{1\alpha}\right)$$

$$\omega = \int\limits_0^t \frac{T - T_L}{J} dt, \;\; \omega_{12} = p\omega$$

(9.6)

The output magnitude $|\psi_1|$ is compared with the required flux linkage $|\psi_1^*|$ and their difference enters the flux hysteresis regulator. The output of the flux regulator takes one of the two values, 1 or 0. If the flux linkage ψ_1 is less than the reference flux linkage ψ_1^*, the flux will be stepped up that corresponds to the regulator output 1. If the flux linkage ψ_1 exceeds the reference flux ψ_1^*, the flux that corresponds to the regulator output 0 will be stepped down.

The speed regulator generates the slip frequency proportional to the electromagnetic torque. An electromagnetic torque error $T_{12} \equiv \omega_2$ comes to the torque hysteresis regulator. The output of the torque regulator takes one of the three values, 1, –1, or 0. The first value steps up the frequency, the second value steps it down, and zero never changes.

Switching unit for DTC. To describe the voltage switching unit, a switching model of the three-phase inverter shown earlier in Fig. 5.2 (a) is presented in Fig. 9.4 (a). Here, each load terminal assumes a potential defined by the control. The leg short-circuiting is avoided since the terminals are connected to either the positive or negative supply bus. In other words, the state of the single switch in a leg is off while another is conductive, except for the short protective intervals, when both of switch contacts are broken.
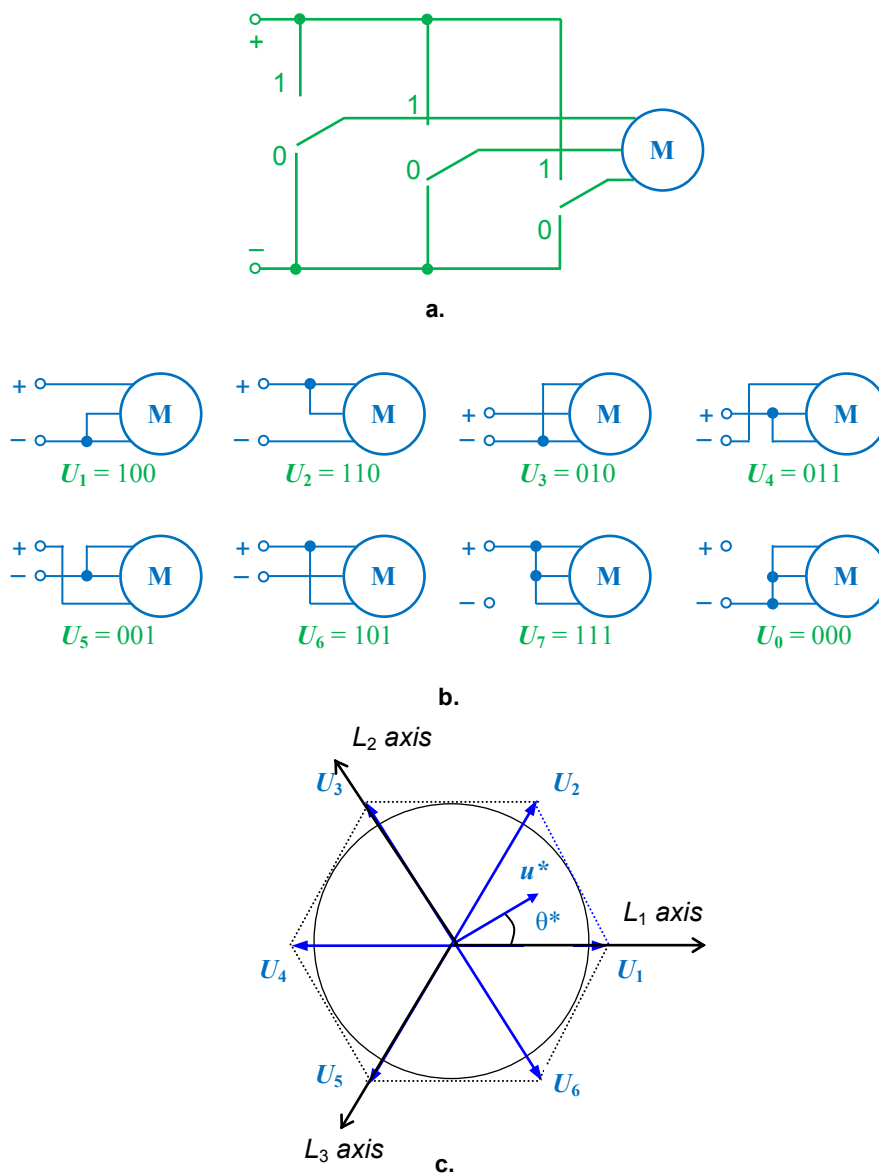
Fig. 9.4 Switching model of the three-phase VSI

Designate the switches by the binary variables, which indicate whether the switch is in the top (1) or bottom (0) position. Accordingly, a three-bit binary word with eight different codes defines all possible switching states of the converter, 100, 110, 010, 011, 001, 101, 111, and 000. These states are shown in Fig. 9.4 (b).

To proceed from the switching model to SVM, associate each binary word of Fig. 9.4 (b) with a particular space vector and describe the switching states of the converter by eight space vectors $\mathbf{U}_0...\mathbf{U}_7$.

This vector set includes six *active voltage space vectors* $\mathbf{U}_1$ to $\mathbf{U}_6$ corresponding to the switching states 100, 110, 010, 011, 001, 101, and two *zero voltage space vectors* $\mathbf{U}_0$, $\mathbf{U}_7$ keeping with 111 and 000. On the plane shown in Fig. 9.4 (c) (known also as the Concordia graph), six active space vectors are situated 60° apart, segmenting the plane by equal sectors. Voltage vectors $\mathbf{U}_1$, $\mathbf{U}_3$, $\mathbf{U}_5$ are oriented along the axes of L_1, L_2, and L_3 phases. Supply dc voltage U_d specifies the amplitudes of the space vectors. The demanded reference vector is determined by its module u^* and phase θ^*. Allowable magnitude of the reference vector for each of an angle is

$$u^* \leq u^*_{max} = \frac{U_d}{\sqrt{3}}.$$

Since u^* is normally not coinciding with one of the available space vectors, its allowable phase is

$$\theta^* \leq \theta^*_{max} = \frac{\pi}{3}.$$

The switching unit aims to approximate the line-modulated signal with one of the eight space vectors available in VSI thus providing high drive performance in terms of minimizing unwanted harmonics and reducing the switching frequency. For this purpose, the switching unit, as the SVM modulator implies, has two integer entries, the reference voltage signal u^* and the reference frequency signal f^*. The first signal changes the time duration of the zero space vectors in the full modulation period, which decreases if $u^* = 1$ and increases in the case of $u^* = 0$. The second signal defines the number of carrier periods in each modulation period of the generated voltage. It decreases if $f^* = 1$, increases in the case of $f^* = -1$, and keeps the state if $f^* = 0$. The additional input θ_1 indicates the sector of the current space vector.

Table 9.1 implements a possible commutation DTC algorithm. It shows how, dependently of u^* and f^*, the positions of the voltage vectors are selected. Among the two allowable zero vectors, that is selected which requires the minimum switching number.

u^*	f^*	Commutations					
1	1	$U_1 \to U_2$	$U_2 \to U_3$	$U_3 \to U_4$	$U_4 \to U_5$	$U_5 \to U_6$	$U_6 \to U_1$
	0	$U_1 \to U_0$	$U_2 \to U_7$	$U_3 \to U_0$	$U_4 \to U_7$	$U_5 \to U_0$	$U_6 \to U_7$
	−1	$U_1 \to U_6$	$U_2 \to U_1$	$U_3 \to U_2$	$U_4 \to U_3$	$U_5 \to U_4$	$U_6 \to U_5$
0	1	$U_1 \to U_3$	$U_2 \to U_4$	$U_3 \to U_5$	$U_4 \to U_6$	$U_5 \to U_1$	$U_6 \to U_2$
	0	$U_1 \to U_7$	$U_2 \to U_0$	$U_3 \to U_7$	$U_4 \to U_0$	$U_5 \to U_7$	$U_6 \to U_0$
	−1	$U_1 \to U_5$	$U_2 \to U_6$	$U_3 \to U_1$	$U_4 \to U_2$	$U_5 \to U_3$	$U_6 \to U_4$

Table 9.1 Switching table for selection of voltage space vectors

This scheme produces a fast torque response while keeping the stator flux and torque as decoupled as possible and providing less parameter dependency and complexity compared with FOC.

9.3   Tracking and positioning

Path control. Vector control is the compulsory operation of the electric drives provided the *path control* that ensures a match between the currently measured positions and a target position of the driven mechanism. Position data are usually obtained from position encoders and path regulators, which are used to perform the proper path control. The higher the number of pulses of the incremental position sensor, the better path jerk-free operation can be achieved, especially at low speeds. To generate the pulses, optical sensors and resolvers are mounted on the driven machine and adjusted by different ways. Typically, all path sensors distinguish between the rising and falling pulse edges.

The *tracking* and the *positioning path electric drives* are discerned. The former ones control the path all round the operation whereas the latter manage only the required final and intermediate positions of the mechanism route. The main feature of the tracking drive is a *tracking accuracy* measured by a *tracking error* which must be as low as possible at the highest permissible motion speed along the tracking contour. The major characteristic of the positioning drive is a *positioning accuracy* measured by a *position error* (called also a *droop*) in the demanded points which must again be minimal at the highest permissible motion speed between the target points.

Tracking. The main tracking modes are the *hold*, the *permanent speed*, the *permanent acceleration*, and the *harmonic oscillation* tracking.

In the first mode, at $\omega = 0$, the tracking error is caused by the load disturbance T_L. The hold error

$$\delta_\varphi = \frac{T_L}{k_{\delta\varphi}}$$

is defined by the *torque quality* factor $k_{\delta\varphi}$ which describes the ratio of the load torque to the induced error (Fig. 9.5 (a)). When the low inertial ratio (3.5) exists between the motor and the mechanism, the *slight vibration* arises at standstill. At some cases, an elasticity of the mechanical gears and improper lubrication cause *jerking* at standstill as well. To prevent these shortcomings, different *damping* measures are applied.
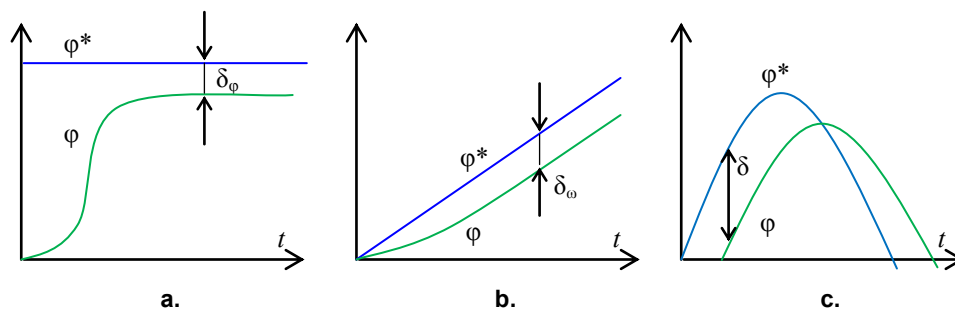

Fig. 9.5 Tracking errors

At the permanent speed motion, the speed error appears in the system,

$$\delta_\omega = \frac{\omega}{k_{\delta\omega}}$$

where $k_{\delta\omega}$ called a *speed quality* describes the ratio between the permanent speed and the induced error (Fig. 9.5 (b)).

At the permanent acceleration motion a following acceleration error exists in the system:

$$\delta_{s\omega} = \frac{d\omega}{dt}\frac{1}{k_{\delta s\omega}}.$$

In this case the ratio of the permanent acceleration to the induced error, $k_{\delta s\omega}$, is called an *acceleration quality*.

The total drive tracking error,

$$\delta > \delta_{s\omega} + \delta_\omega + \delta_\varphi,$$

is usually evaluated in the harmonic oscillation mode (Fig. 9.5 (c)). This error includes also the instrumental errors from the set-point devices and sensors, gear kinematic errors, their backlashes and gaps, control system errors, etc.

Positioning. Unlike the tracking, the *positioning mode* relates to the load moving from some fixed point to another one in a minimal time. Three kinds of this mode can be distinguished. At the small relocations, the regulators and converters operate within the linear zone of their characteristics. At the middle motions, the motor and converter currents are restricted.

On the long paths, the motor speed is also limited in addition to the current restriction. In any case, the load motion must be finished by the accurate stopping within the minimal *coasting* distance and the *position lock* in the demanded point. The electric drives from Omron and Mitsubishi, for example, are served with the special functions to provide the machine locking by automatic *gain changing* and *suppression of slight vibrations* within the separate step.

So called *homing* known also as a *home position return* represents the particular case of positioning. It is the process of the machine tool fitting in the starting working position. To make it, the working process begins usually with *zeroing* i.e. with the search of the coordinate zero point.

To perform positioning, the *stroke-end* and the *strokeless position systems* are used (Fig. 9.6) dependently of the presence of the mechanical path limiters. As well, the *incremental* and the *absolute position systems* are distinguished. The incremental system built on the basis of the pulse position sensors starts its operation by homing and calculates each pulse throughout the motion until the final position. Such system loses the path information in the case of the supply switching off. The absolute systems are built on the absolute encoders which memorize the starting base. At the supply disconnection they reproduce the home position and, thus, are able to continue operation. Usually they involve the *backup batteries* or the *uninterruptible power supply* (*UPS*).
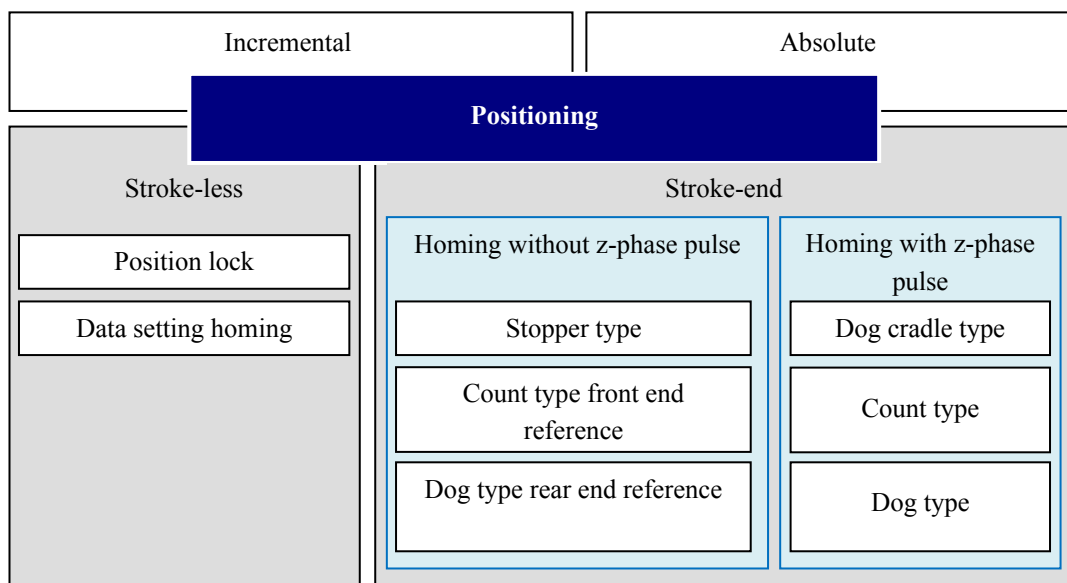

Fig. 9.6 Positioning systems and methods

Positioning accuracy at small relocations is defined mainly by the static error δ_φ, thus, the higher is the system torque quality factor, the more accurate will be the low-speed positioning. However, at the middle and large scale movement, the high quality factor results in transient deterioration. To process the middle-distance paths, the best is the triangular speed diagram which involves the linear acceleration following the linear deceleration. To perform the large-distance motion, the best is the trapezoidal speed diagram with the linear acceleration following the permanent speed motion and the linear deceleration at the end. One peculiarity of the positioning systems is the need in the quality factor variation during the operation therefore some manufacturers provide the specific *gain search function* for this purpose.

Homing. Multiple homing algorithms have been developed by different drive vendors.

The simplest is the situation in which the homing starts in the drive switching-on position with the *data setting homing* when the operator sets manually the zero of the count system. The *stopper type homing* expects the stopping upon the *collide* on the mechanical stopper mounted on the bench and assumes the definite machine durability.

Other homing methods apply the signals of the *proximity dogs* which are mounted in front of the *home position address*.

At the instant of the proximity dog collision, the electric drive begins to slow down its motion from the *fast feed* (*rapid freerate*) to the *creep speed*, known also as a *settling speed*. The acceleration and deceleration rates of the positioning electric drive are usually defined by the appropriate time constants τ_d and τ_q counted at the rated motor speed ω_M (Fig. 9.7 (a)). Due to the *up-to-speed* errors and smoothing near the demanded point $\omega*$, the actual run-up t_d and braking t_q times differ from the appropriate expected times t_d* and t_q*. The full *positioning cycle* includes the *running time* t_p, the *rapid freerate time* t_L, the *braking time* t_q, the *home position shift distance time* called the *settling time* t_s at the settling speed ω_s, and the *dwell time* t_0 of the *in-position range*.
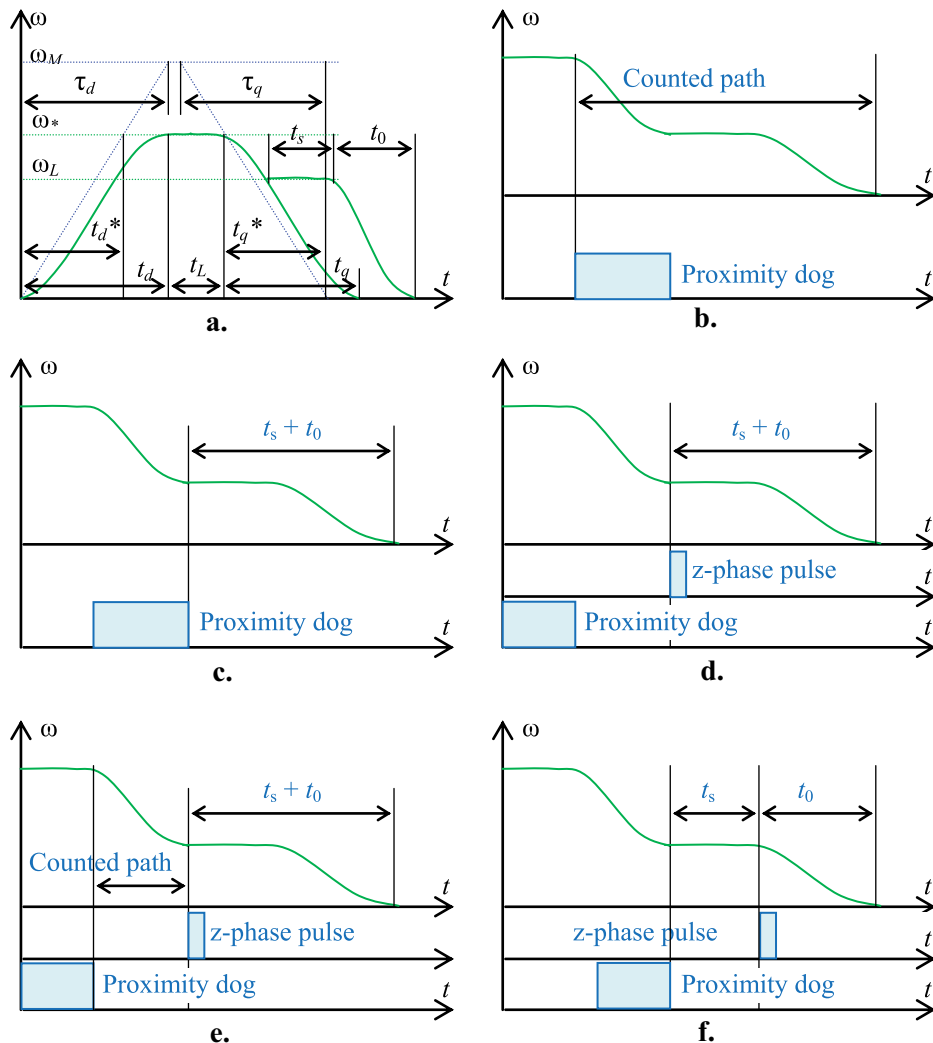

Fig. 9.7 Positioning methods

At the *count type front end reference homing*, after the acquiring of the front end of the proximity dog signal, the system calculates the required braking and settling paths before running to the home position address (Fig. 9.7 (b)).

At the *dog type rear end reference homing* , after the speed lowering to the settling level, the system "waits" the rear end of the proximity dog and then goes along the settling path to the home position (Fig. 9.7 (c)).

At the *dog cradle type homing*, after the acquiring the proximity dog signal, the system "waits" the z-phase pulse of the position encoder. The z-phase pulse generated once per the encoder turn provides the system to go along the settling path to the home position (Fig. 9.7 (d)).

At the *count type homing*, after the acquiring the proximity dog signal, the system goes along the counted braking path, then "waits" the z-phase pulse of the position encoder and then runs along the settling path to the home position (Fig. 9.7 (e)).

At the *dog type homing*, after the braking, the system "waits" the rear front of the proximity dog and the z-phase pulse of the position encoder, and then runs along the settling path to the home position (Fig. 9.7 (f)).

As the gear backlashes and gaps decrease the positioning quality, some accurate electric drives, particularly from Siemens, include additional function of the *backlash compensation* which corrects the positioning program at the reverse operations.